U.S. Department
of Transportation

**Federal Railroad Administration**

# Prediction of Fatigue Crack Growth in Rail Steels

D. Broek
R. C. Rice
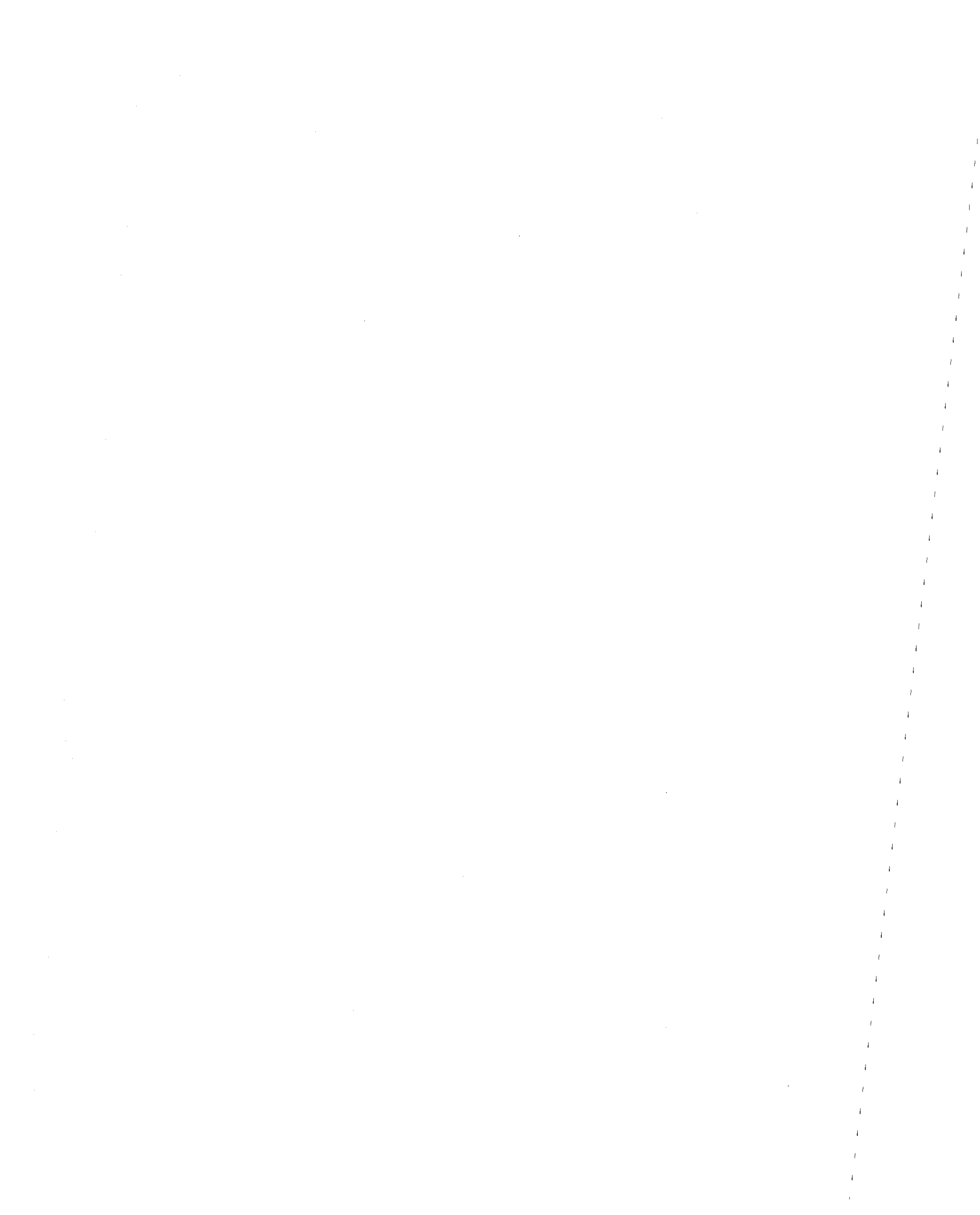
Battelle Columbus Laboratories
505 King Avenue
Columbus, OH 43201

This document is available to
the U.S. public through the
National Technical Information
Service, Springfield, Virginia
22161

| 1. Report No.  FRA/ORD-81/31 | 2. Government Accession No. | 3. Recipient's Catalog No.  PB82 1 2960 2 |
|---|---|---|
| 4. Title and Subtitle  PREDICTION OF FATIGUE CRACK GROWTH IN RAIL STEELS | | 5. Report Date  October 1981. |
| | | 6. Performing Organization Code  314009 |
| 7. Author(s)  D. Broek and R.C. Rice | | 8. Performing Organization Report No.  DOT-TSC-FRA-80-30 |
| 9. Performing Organization Name and Address  Battelle Columbus Laboratories *  505 King Avenue  Columbus OH 43201 | | 10. Work Unit No. (TRAIS)  RR119/R1329 |
| | | 11. Contract or Grant No.  DOT-TSC-1076-2 |
| 12. Sponsoring Agency Name and Address  U.S. Department of Transportation  Federal Railroad Administration  Office of Research and Development  Washington DC 20590 | | 13. Type of Report and Period Covered  Final Report  July 75 - July 77 |
| | | 14. Sponsoring Agency Code |

16. Abstract

Measures to prevent derailments due to fatigue failures of rails require adequate knowledge of the rate of propagation of fatigue cracks under service loading. The report presents a computational model for the prediction of crack growth in rails. The model was derived on the basis of experiments of crack growth under service simulation loading. The applications of the model are discussed. Material data on fatigue crack growth in rail steels are required for the execution of the predictive model. Such data were generated during the present program, but reported elsewhere (Ref. 1, 2, 3).

| 17. Key Words  Rail, Cracks, Fatigue Crack Propagation, Prediction Train Service Loading | 18. Distribution Statement  DOCUMENT IS AVAILABLE TO THE PUBLIC THROUGH THE NATIONAL TECHNICAL INFORMATION SERVICE, SPRINGFIELD, VIRGINIA 22161 |
|---|---|

| 19. Security Classif. (of this report)  Unclassified | 20. Security Classif. (of this page)  Unclassified | 21. No. of Pages  146 | 22. Price |
|---|---|---|---|

Form DOT F 1700.7 (8-72)      Reproduction of completed page authorized

# PREFACE

# METRIC CONVERSION FACTORS

## Approximate Conversions to Metric Measures

| Symbol | When You Know | Multiply by | To Find | Symbol |
|---|---|---|---|---|
| **LENGTH** | | | | |
| in | inches | *2.5 | centimeters | cm |
| ft | feet | 30 | centimeters | cm |
| yd | yards | 0.9 | meters | m |
| mi | miles | 1.6 | kilometers | km |
| **AREA** | | | | |
| in² | square inches | 6.5 | square centimeters | cm² |
| ft² | square feet | 0.09 | square meters | m² |
| yd² | square yards | 0.8 | square meters | m² |
| mi² | square miles | 2.6 | square kilometers | km² |
| | acres | 0.4 | hectares | ha |
| **MASS (weight)** | | | | |
| oz | ounces | 28 | grams | g |
| lb | pounds | 0.45 | kilograms | kg |
| | short tons (2000 lb) | 0.9 | tonnes | t |
| **VOLUME** | | | | |
| tsp | teaspoons | 5 | milliliters | ml |
| Tbsp | tablespoons | 15 | milliliters | ml |
| fl oz | fluid ounces | 30 | milliliters | ml |
| c | cups | 0.24 | liters | l |
| pt | pints | 0.47 | liters | l |
| qt | quarts | 0.95 | liters | l |
| gal | gallons | 3.8 | liters | l |
| ft³ | cubic feet | 0.03 | cubic meters | m³ |
| yd³ | cubic yards | 0.76 | cubic meters | m³ |
| **TEMPERATURE (exact)** | | | | |
| °F | Fahrenheit temperature | 5/9 (after subtracting 32) | Celsius temperature | °C |

*1 in. = 2.54 cm (exactly). For other exact conversions and more detail tables see NBS Misc. Publ. 286, Units of Weight and Measures. Price $2.25 SD Catalog No. C13 10 286.

## Approximate Conversions from Metric Measures

| Symbol | When You Know | Multiply by | To Find | Symbol |
|---|---|---|---|---|
| **LENGTH** | | | | |
| mm | millimeters | 0.04 | inches | in |
| cm | centimeters | 0.4 | inches | in |
| m | meters | 3.3 | feet | ft |
| m | meters | 1.1 | yards | yd |
| km | kilometers | 0.6 | miles | mi |
| **AREA** | | | | |
| cm² | square centimeters | 0.16 | square inches | in² |
| m² | square meters | 1.2 | square yards | yd² |
| km² | square kilometers | 0.4 | square miles | mi² |
| ha | hectares (10,000 m²) | 2.5 | acres | |
| **MASS (weight)** | | | | |
| g | grams | 0.035 | ounces | oz |
| kg | kilograms | 2.2 | pounds | lb |
| t | tonnes (1000 kg) | 1.1 | short tons | |
| **VOLUME** | | | | |
| ml | milliliters | 0.03 | fluid ounces | fl oz |
| l | liters | 2.1 | pints | pt |
| l | liters | 1.06 | quarts | qt |
| l | liters | 0.26 | gallons | gal |
| m³ | cubic meters | 36 | cubic feet | ft³ |
| m³ | cubic meters | 1.3 | cubic yards | yd³ |
| **TEMPERATURE (exact)** | | | | |
| °C | Celsius temperature | 9/5 (then add 32) | Fahrenheit temperature | °F |

°F  -40    0    32   80   98.6   120   160   212
°C  -40   -20   0    20   37     40    60    100

## LIST OF ILLUSTRATIONS

## LIST OF TABLES

EXECUTIVE SUMMARY

This report presents part of the results of a study on rail material
failure properties to better define fatigue crack growth mechanisms in rail
steel. This work was conducted as part of the Improved Track Structures
Research Program sponsored by the Federal Railroad Administration. The results
are presented in five volumes entitled:

Fatigue Crack Propagation In Rail Steels - DOT-TSC-FRA-77-3/FRA/ORD-77/14

Fatigue Crack Growth Properties of Rail Steels - Final Report - DOT-TSC-
FRA-80-29/FRA/ORD-81/30

Prediction of Fatigue Crack Growth in Rail Steels - Final Report -
DOT-TSC-FRA-80-30/FRA/ORD-81/31

Cyclic Inelastic Deformation and Fatigue Resistance of a Rail Steel:
Experimental Results and Mathematical Models - Interim Report DOT-TSC-
FRA-80-28/FRA/ORD-81/29

Fracture and Crack Growth Behavior of Rail Steels Under Mixed Mode
Loadings - Interim Report (in preparation).

The objective of the work described in this report was the development
of a computational failure model for the prediction of flaw growth in rail
steel under actual service loading. The predictive methodology addresses
three types of rail flaws: transverse fissure, horizontal split head and
vertical split head. These defects have a high frequency of occurrence and
rail failure resulting from such defects accounts for a significant number of
railroad accidents.

A computational model was established for the prediction of fatigue crack
growth in rail steels under service loading. Fatigue crack propagation tests
were performed to establish the fatigue crack propagation behavior under vari-
able amplitude loading to determine the significant parameters of the service
load history. Using constant amplitude fatigue crack growth data developed
previously and reported in the DOT-TSC-FRA-80-29, the service simulation
test data were predicted using a linear crack growth integration model. Since
load interaction effects are very small because most load cycles have the
same maximum in tension, the linear integration model is adequate for service
crack growth prediction. A rail is subjected to a complex load sequence

during the passage of a single truck. Experimental data verified that small
variations in this load sequence are insignificant. Thus, the passage of a
truck can be simulated by two load cycles of approximately equal amplitude.
Actual (measured) wheel-rail load spectra were used to establish a hypothetical
service load history representing one million gross tons of traffic. Limita-
tions in the model are due to the unknown magnitude of the residual stress,
the variability in material behavior, and the large inherent scatter of crack
growth properties of rail steel.

# 1. INTRODUCTION

Fatigue failure of railroad rails is a common cause of derailment accidents. The reduction of fatigue failures may be achieved by more intensive track maintenance, reduction of traffic or loads, or replacement of rail. In addition, timely detection of fatigue cracks may prevent most cracks from causing failures.

The measures to reduce fatigue failure can be effectively selected only if adequate methods exist to predict the time to crack initiation and the subsequent rate of crack growth. Such predictions require a rather accurate knowledge of service loads, rail stresses, and fatigue and crack-growth properties of rail material. Moreover, a computational scheme is required that can use the information to predict the behavior under service circumstances.

One portion of the Federal Railroad Administration's (FRA) Improved Track Structures Research Program is the development of a predictive rail failure model that enables a determination of optimal inspection periods through a prediction of crack growth. The research reported here concerns a program to develop such a model.

The laboratory fatigue crack growth data used as an input to the predictive model were obtained from 66 rail samples taken from track all over the United States. These data were generated during Phase I of the present program. They are compiled in a separate report[1], but a summary is given herein.

Actual cracks in rails are subjected to stress cycles with varying mean stress of combined tension and shear; they can have different orientations and have a complex shape. Moreover, the rail experiences varying temperatures which may affect the behavior of cracks. Data on the influence of these parameters were generated in Phase II of the program and compiled in a separate report[2], but the most important results are presented here as well.

The primary objective of the program was the establishment of a computational failure model, which can predict the growth of a flaw in a rail under actual service loading. Flaw growth in a rail is a complex problem of a quasi-elliptical embedded flaw in a nonuniform stress field growing under a variable amplitude load history of mixed modes. Probably, the most difficult

1

aspect of the problem is the prediction of flaw growth under variable ampli-
tude loading. In the variable amplitude load tests, this problem was singled
out, disregarding the additional complexities of the elliptical flaw shape,
the nonuniform stress field, and the mixed mode loading which were investi-
gated earlier in the program. Thus, the problem addressed was that of a
through-the-thickness crack with a straight front growing under simulated
service loading of the mode I type. Once crack growth under these circum-
stances can be properly predicted, the failure model can be generalized to
include the other complexities. The development of the failure model is
described in this report.

The experimental techniques employed in this program are discussed
in Section 2. Since the stress-intensity factor is used for crack growth
correlation, a brief introduction of this subject is presented in Section 3.
Fatigue crack propagation under variable amplitude loading is often complicated
by load interaction effects. This problem is addressed first in Section 4.

During the passage of one wheel, the rail is subjected to a large
stress cycle and some smaller ones. The small load variations were shown to
have a negligible effect on crack propagation, which permits certain simpli-
fications of the simulated service stress history. These are discussed in
Section 5.

Simulated service stress histories for crack growth predictions and
experiments were derived on the basis of measured wheel-rail load spectra.
These spectra are presented in Section 6, together with the derivation of the
service stress histories used in the experiments. Since crack growth predic-
tions have to be based on the simplest possible representation of service
loading while still retaining characteristics of the service stress history,
several possible simplifications are discussed also in Section 6. The
results of service simulation tests are presented at the end of Section 6.

The crack growth prediction model is developed in Section 7. The
final sections of the report are concerned with the generalization and appli-
cation of the failure model.

## 2. EXPERIMENTAL DETAILS

### 2.1. Rail Materials

A detailed description of the sample sources was presented in Reference 1. The 66 samples were identified by numbers 001 through 066. A summary of the information relevant to this phase of the program is presented in Table 1. All rail samples used for the present experiments are listed in Table 2 in ascending order of crack propagation life as determined in Phase 1. The crack propagation life is defined as the number of cycles required to extend a crack in a compact tension specimen from 1 inch to failure.

Tables 1 and 2 present the most important details of the materials, such as the weight and the year of production and the carbon, manganese, sulfur, and oxygen content. Also, the primary processing variables are indicated, i.e., control cooled (CC) and vacuum degassed (Vac. Deg.). Finally, the most important mechanical properties are given, viz, tensile ultimate strength (TUS), tensile yield strength (TYS), and the elongation for a 1-inch gage length.

### 2.2. Specimens

Several specimens used in this phase of the program were of the compact tension (CT) type. Their dimensions are shown in Figure 1. The specimens were provided with a 1.650-inch-deep chevron notch (0.900 inch from the load line). These specimens were precracked in a Krause fatigue machine until a crack of about 0.1 inch had formed. At this point, the specimens contained a simulated fatigue crack of about 1 inch (as measured from the load line, see Figure 1).

CT specimens are not suitable for experiments where the minimum load in a cycle is compressive, since the stress distribution in a CT specimen in compression bears no straightforward relation to compressive stress distributions in cracked rail. Therefore, the service simulation experiments were performed on single edge notch (SEN) specimens, illustrated in Figure 2. A basis of comparison between SEN specimens and CT specimens was established earlier in the program[2]. The SEN specimens were precracked in the same fatigue machine they were subsequently tested in.

TABLE 1. STATISTICS OF 66 RAIL SAMPLES

| Variable | Low Value | High Value | Mean | Standard Deviation | Standard Deviation in Percent of Mean |
|---|---|---|---|---|---|
| % C | .57 | .85 | .76 | .06 | 8 |
| % Mn | .61 | 1.48 | .88 | .17 | 20 |
| % S | .014 | .052 | .029 | .010 | 34 |
| Grain Diameter, mm | .066 | .120 | .087 | .021 | 25 |
| Pearlite Interlamellar Spacing, $\overset{o}{A}$ | 2,470 | 4,160 | 3,211 | 632 | 20 |
| TUS, ksi | 111 | 142 | 133 | 5.5 | 4 |
| TYS, ksi | 60 | 82 | 73 | 5 | 7 |
| Crack Growth Life,[a] log cycles | 5.18 | 6.22 | 5.68 | .30 | 5 |

(a) Constant amplitude crack growth life at R = 0 from 1 inch to failure.

TABLE 2.  CHARACTERISTICS OF RAIL SAMPLES USED FOR EXPERIMENTS

| Sample | Crack Growth Life 1-in. to Failure, kc | Weight, lbs/yd | Year | Chemical Composition | | | | | | Processing | | Mechanical Properties | | |
|---|---|---|---|---|---|---|---|---|---|---|---|---|---|---|
| | | | | C weight percent | Mn weight percent | Si weight percent | S weight percent | O ppm | H ppm | CC + Yes - No | Vac Deg + Yes - No | TUS, ksi | TYS, ksi | Elongation, percent in 1 inch |
| 016 | 150 | 133 | 1957 | 0.81 | 0.93 | 0.17 | 0.044 | 42 | 0.7 | + | - | 138.6 | 75.6 | 9.5 |
| 025 | 153 | 133 | 1966 | 0.80 | 0.91 | 0.23 | 0.016 | 28 | 0.7 | + | - | 141.1 | 75.7 | 9.5 |
| 023 | 155 | 133 | 1957 | 0.79 | 0.92 | 0.21 | 0.040 | 40 | 0.7 | + | - | 135.1 | 77.3 | 10.5 |
| 030 | 197 | 119 | 1958 | 0.80 | 0.90 | 0.16 | 0.028 | 53 | 0.6 | | - | | 76.8 | |
| 013 | 216 | 127 | 1954 | 0.74 | 0.89 | 0.24 | 0.028 | 49 | 0.9 | + | - | 129.3 | 72.8 | 12.5 |
| 014 | 269 | 133 | 1955 | 0.78 | 0.74 | 0.17 | 0.014 | 85 | 0.8 | - | - | 135.4 | 75.9 | 12.0 |
| 010 | 277 | 85 | 1919 | 0.63 | 0.74 | 0.14 | 0.028 | 135 | 1.0 | - | - | 111.5 | 58.7 | 17.0 |
| 009 | 381 | 130 | 1929 | 0.61 | 1.46 | 0.29 | 0.039 | 58 | 0.7 | + | - | 139.8 | 81.8 | 14.0 |
| 032 | 404 | 133 | 1953 | 0.80 | 0.94 | 0.18 | 0.035 | 62 | 0.5 | + | - | 139.5 | 80.0 | 12.0 |
| 021 | 419 | 133 | 1955 | 0.79 | 0.90 | 0.11 | 0.024 | 43 | 0.7 | | - | 132.3 | 77.2 | 12.0 |
| 006 | 490 | 115 | 1974 | 0.72 | 0.97 | 0.10 | 0.028 | 24 | 0.4 | | + | 135.0 | 71.2 | 11.0 |
| 031 | 596 | 133 | 1956 | 0.79 | 0.76 | 0.15 | 0.022 | 51 | 0.5 | - | - | 133.4 | 75.6 | 11.0 |
| 001 | 736 | 130 | 1929 | 0.63 | 1.48 | 0.21 | 0.022 | 98 | 0.9 | + | - | 136.4 | 76.5 | 13.5 |
| 022 | 803 | 133 | 1956 | 0.78 | 0.87 | 0.20 | 0.028 | 47 | 0.5 | - | - | 130.7 | 76.0 | 13.0 |
| 038 | 1047 | 112 | 1930 | 0.57 | 1.48 | 0.16 | 0.029 | 80 | 0.3 | - | - | 124.2 | 74.9 | 17.0 |
| 051 | 1047 | 130 | 1931 | 0.84 | 0.72 | 0.19 | 0.016 | 49 | 0.6 | | - | 141.5 | 81.2 | 9.5 |
| 065 | 1118 | 124 | 1975 | 0.82 | 0.90 | 0.17 | 0.016 | 42 | 0.3 | + | | 131.3 | 73.3 | 11.0 |
| 029 | 1256 | 119 | 1958 | 0.72 | 0.89 | 0.19 | 0.046 | 44 | 0.6 | | - | 125.5 | 61.7 | 12.0 |
| 020 | 1302 | 119 | 1957 | 0.75 | 0.83 | 0.15 | 0.033 | 33 | 0.8 | | | 131.4 | 72.0 | 11.0 |

5
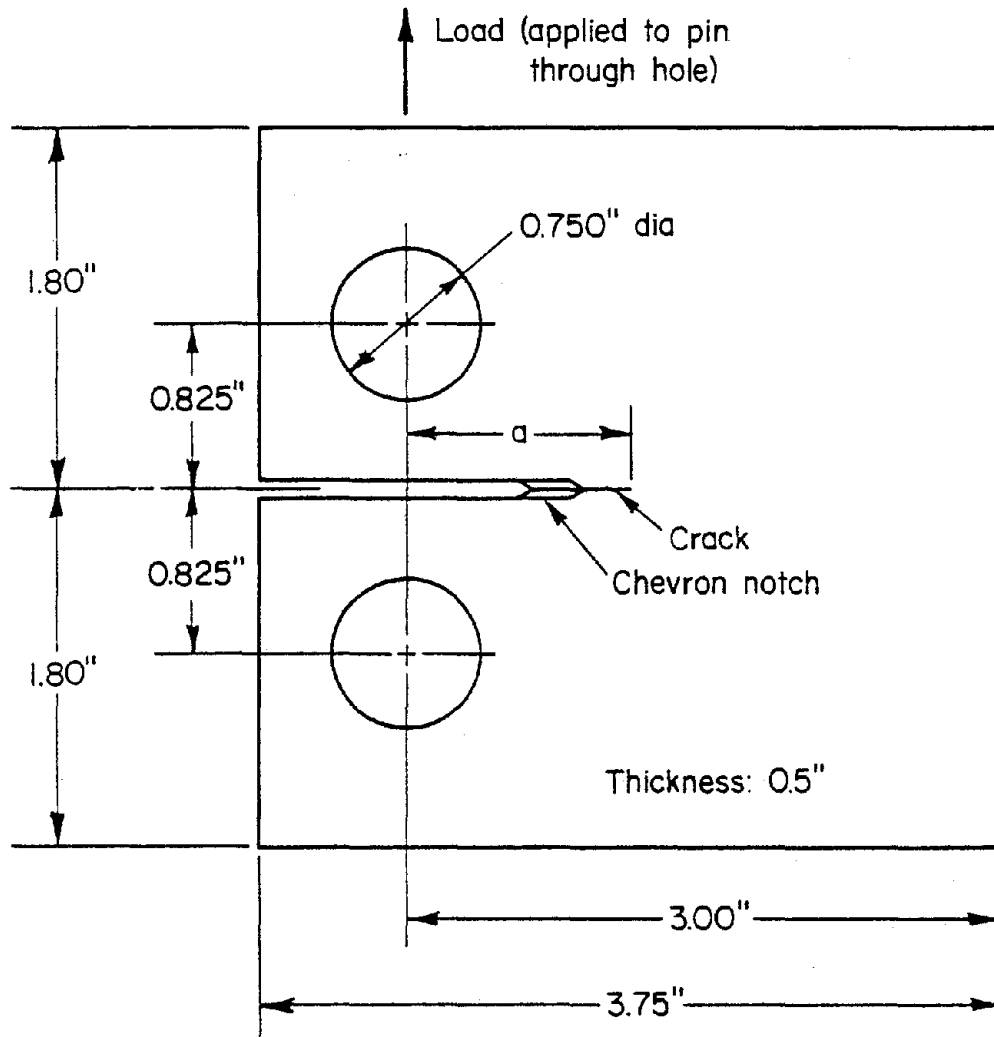
FIGURE 1. COMPACT TENSION FATIGUE CRACK GROWTH SPECIMEN
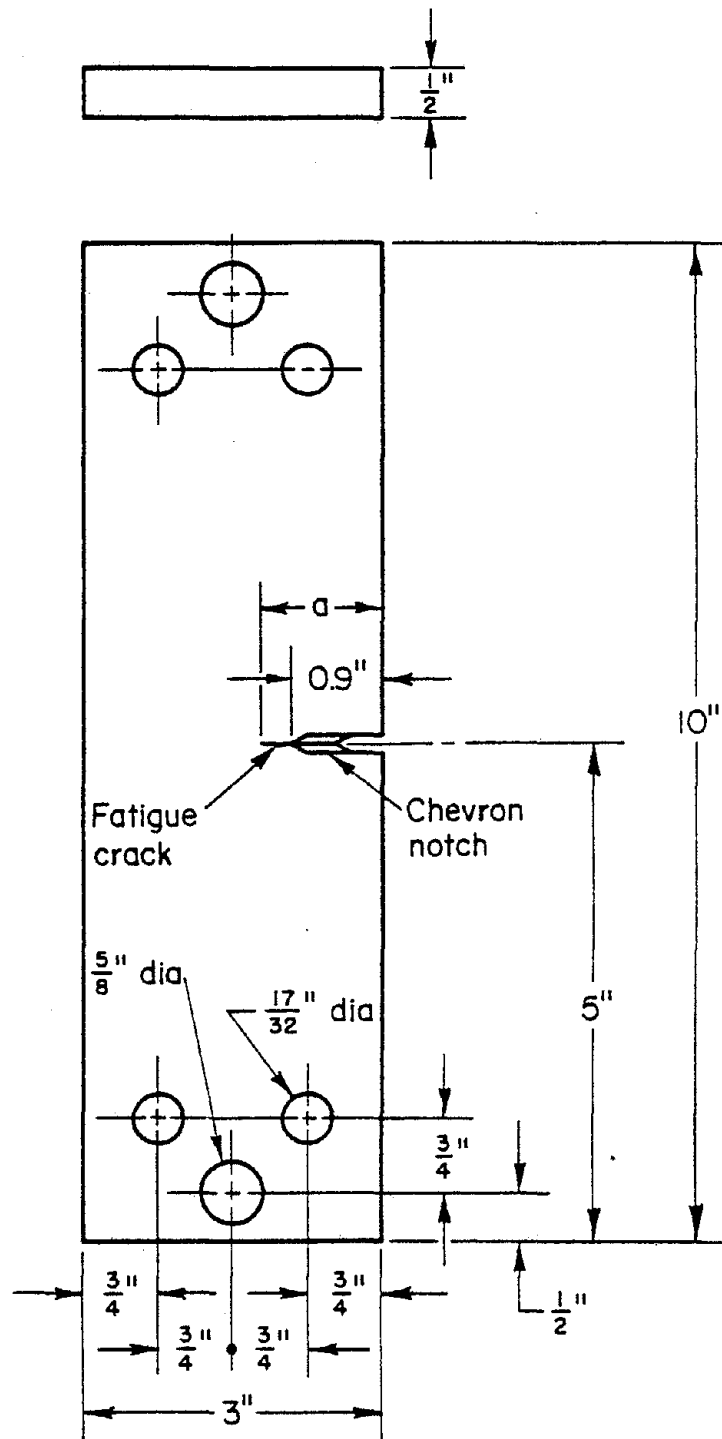
FIGURE 2. SINGLE-EDGE NOTCH CRACK GROWTH SPECIMEN

The orientation of the specimen within the rail is shown in Figure 3. Two orientations were used for the CT specimens, namely, LT and TL. All SEN specimens were of the LT orientation. The first letter in the designation gives the direction of loading with respect to the rail; i.e., longitudinal (L), transverse(T), and short transverse (S). The second letter is the direction of crack growth, also with respect to the rail. (Note that crack growth in LT specimens is representative of a transverse fissure in a rail; crack growth in TL specimens is representative of a horizontal split head; whereas, crack growth in the SL specimens is representative of a vertical split head).

## 2.3. Testing Procedures

Crack growth experiments were conducted in a 25-kip capacity electrohydraulic servocontrolled fatigue machine. All tests were conducted in laboratory air at 68 F and 50 percent relative humidity.

Two methods of crack length measurements were used. In some experiments, crack growth was measured visually using a 30 power traveling microscope. The cracks were allowed to grow in increments of approximately 0.05 inch after which the test was stopped for an accurate crack size measurement. Crack size was recorded as a function of the number of load cycles.

In the other experiments, crack size was recorded automatically by means of a crack growth gage consisting of 20 parallel strands of copper foil adhesively bonded to the specimen as illustrated in Figure 4. The strands ran perpendicular to the crack at a spacing of 0.05 inch. When the crack tip reached a strand, failure of the strand occurred so that the successive breakage of strands was a measure of crack growth.

Electric current through the gage was affected by the failure of a strand which was detected by an electronic decoder and stored in the process computer in line with the fatigue machines. At the end of the test, the growth data could be retrieved from the computer for processing and analysis. On several occasions, the automatic crack growth records were compared with visual crack size measurements and found satisfactory. Use of the crack gage permitted continuation of experiments during off-work hours.

Service simulation load histories were put on magnetic tape which monitored the fatigue machine through the on-line computer.
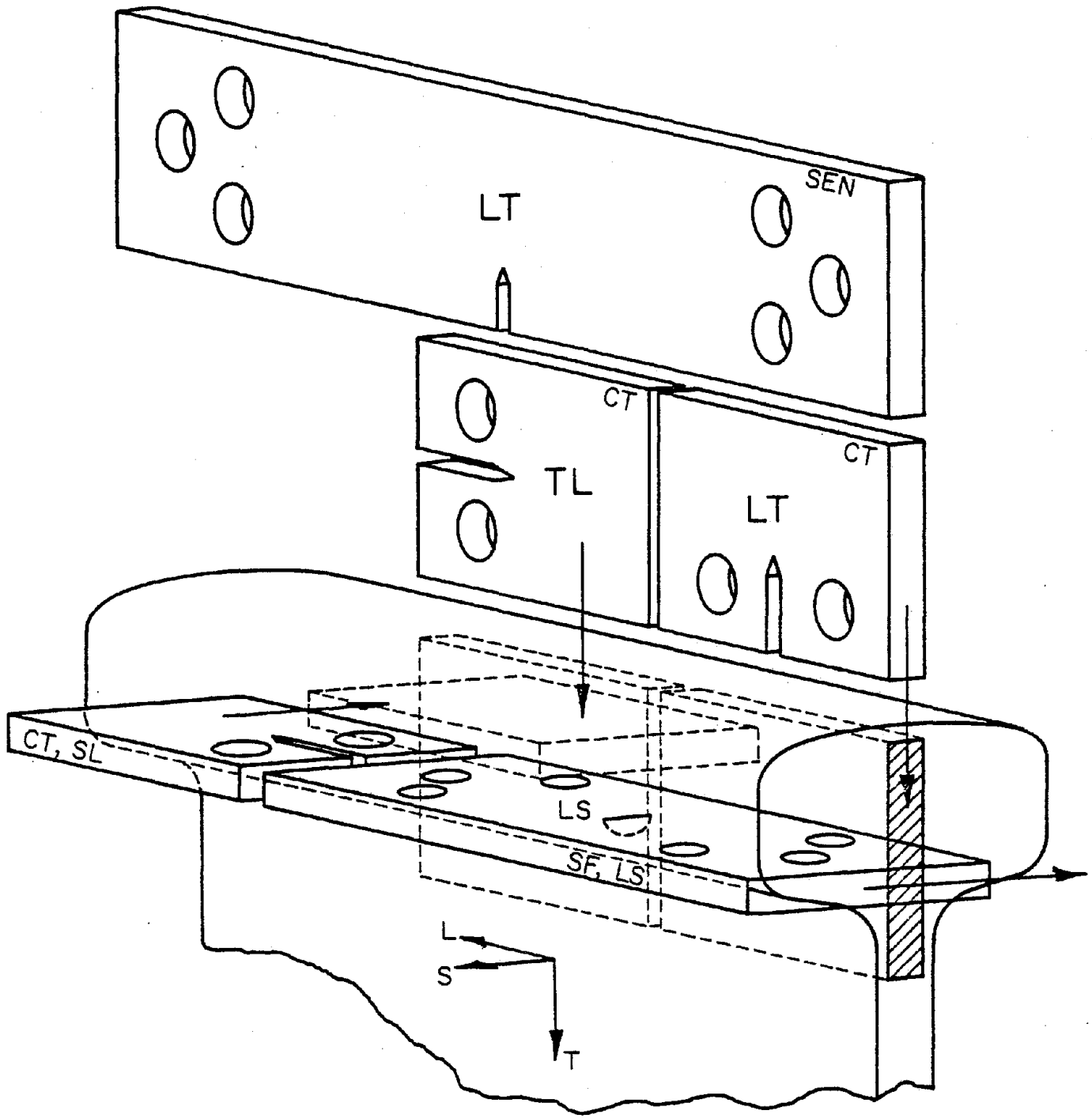
FIGURE 3.  ORIENTATION OF SPECIMENS
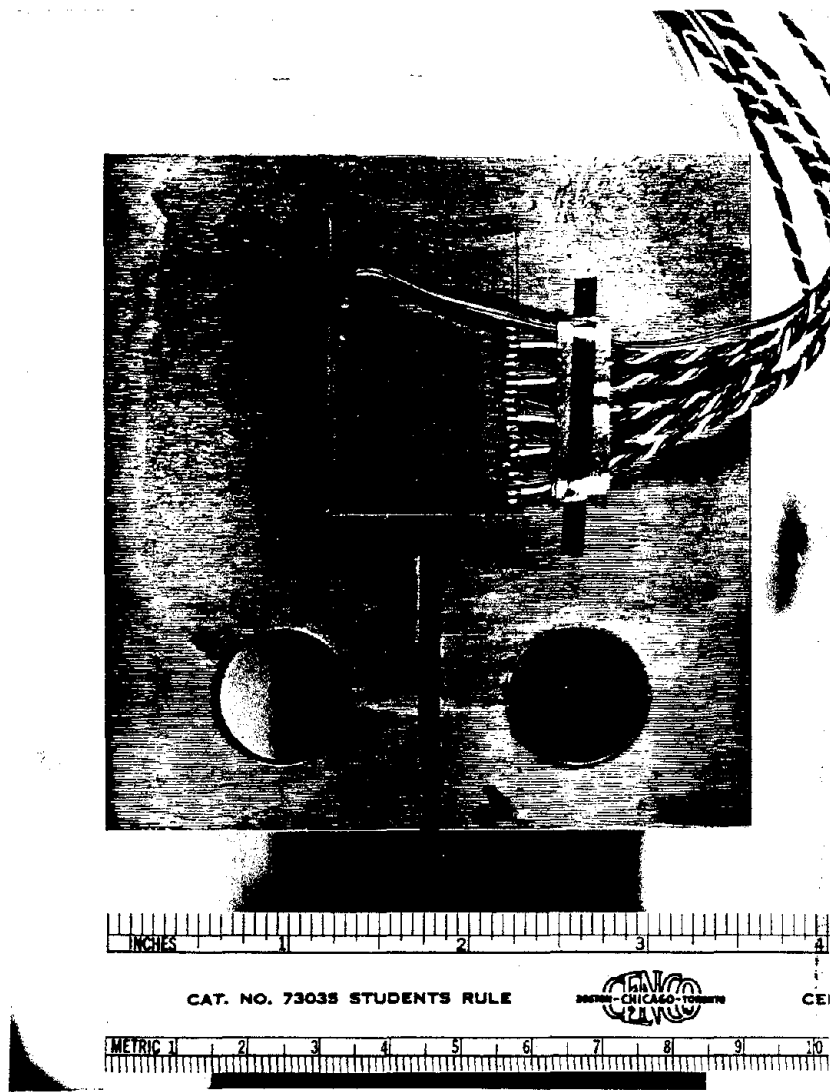
FIGURE 4.  CRACK PROPAGATION GAUGE MOUNTED ON CT SPECIMEN

## 3. DATA PROCESSING AND DATA PRESENTATION

### 3.1. Crack Growth Rates

The crack growth records of CT and SEN specimens are not directly comparable nor are they directly applicable to the case of a crack in a rail. The correlation between cracks of different types can be made only if crack growth data can be expressed in a unique way independent of the crack size, the geometry, and the loading system. This can be done on the basis of the stress-intensity factor, K.[3]

The stresses at the tip of a crack can always be described as

$$\sigma_{ij} = \frac{K}{\sqrt{2\pi r}} \, f_{ij}(\theta) \quad , \tag{3.1}$$

where $\sigma_{ij}$ (i = x,y,z; j = x,y,z) represents the stress in any direction and r and $\theta$ are polar coordinates originating at the crack tip. The functions $f_{ij}(\theta)$ are known functions. Thus, Equation (3.1) shows that the stress field at the tip is completely described by the stress-intensity factor, K.

A crack can be subjected to three different loading cases (modes). Tension loading is denoted as Mode I, in-plane shear is Mode II, and out-of-plane shear is Mode III. Equation (3.1) is valid for all three modes, except that the functions $f_{ij}(\theta)$ are different for each mode, but apart from that they are independent of geometry. Naturally, the stress-intensity factors for the three modes are different.

Stress-intensity factors can be calculated for various types of cracks. The general form for the expression of K is

$$K = \beta\sigma\sqrt{\pi a} \quad , \tag{3.2}$$

where a is the crack size, $\sigma$ is the remote stress, and $\beta$ is a geometry function.

Since the stress-intensity factor describes the whole stress field by Equation (3.1), the stress distribution at the tips of two different cracks will be equal if the stress intensities have the same value. In that case, the cracks also behave in the same way, i.e., show the same rate of growth. As a consequence, fatigue crack growth rates associated with different geometries

can be compared on the basis of the stress-intensity factor: equal K means equal growth rates within the range of variability of crack growth rates of a given material.

The rate of crack growth per cycle is denoted by the derivative da/dN, which is related to K by

$$\frac{da}{dN} = f(\Delta K) \quad . \tag{3.3}$$

In this equation, $\Delta K$ is the range of the stress-intensity factor obtained by substituting $\Delta \sigma$ in Equation (3.2). In turn, $\Delta \sigma$ is the range over which the remote stress varies during a load cycle.

If da/dN data are plotted as a function of $\Delta K$ on double-logarithmic graph paper, the result is often a straight line. This suggests that

$$\frac{da}{dN} = C\Delta K^n \quad , \tag{3.4}$$

a commonly used expression in which C and n are constants. Figure 5 presents an illustration of this equation, using the data of 66 rail steel samples tested at R = 0* in the first phase of this program.[1]

It is generally recognized that da/dN is dependent not only on the range of stress but also on the maximum stress in a cycle or the stress ratio R (which is equivalent). Also, there is generally an upswing of the rate of crack growth towards the end of the test because the failure conditions are approached. Failure occurs when the stress-intensity factor approaches a critical value, $K_{Ic}$. It was shown in this program[2] that a general equation for crack growth in rail steels is

$$\frac{da}{dN} = C(1-R)^2 \left( K_{max}^2 - K_{th}^2 \right) \frac{K_{max}^m}{K_{Ic} - K_{max}} \tag{3.5}$$

Equation (3.5) accounts for the effect of R-ratio and shows that da/dN becomes infinite when the stress intensity at maximum load becomes equal to $K_{Ic}$, the critical stress intensity for fracture. It also reflects that crack growth rates approach zero when the stress intensity approaches a certain threshold level, $K_{th}$. Figure 6 shows the representation of crack growth data according to Equation (3.5) for rail steels. These are the average properties of the steels tested in this program at room temperature.[2] In phase II

---

* R is the ratio of minimum to maximum stress in a cycle.
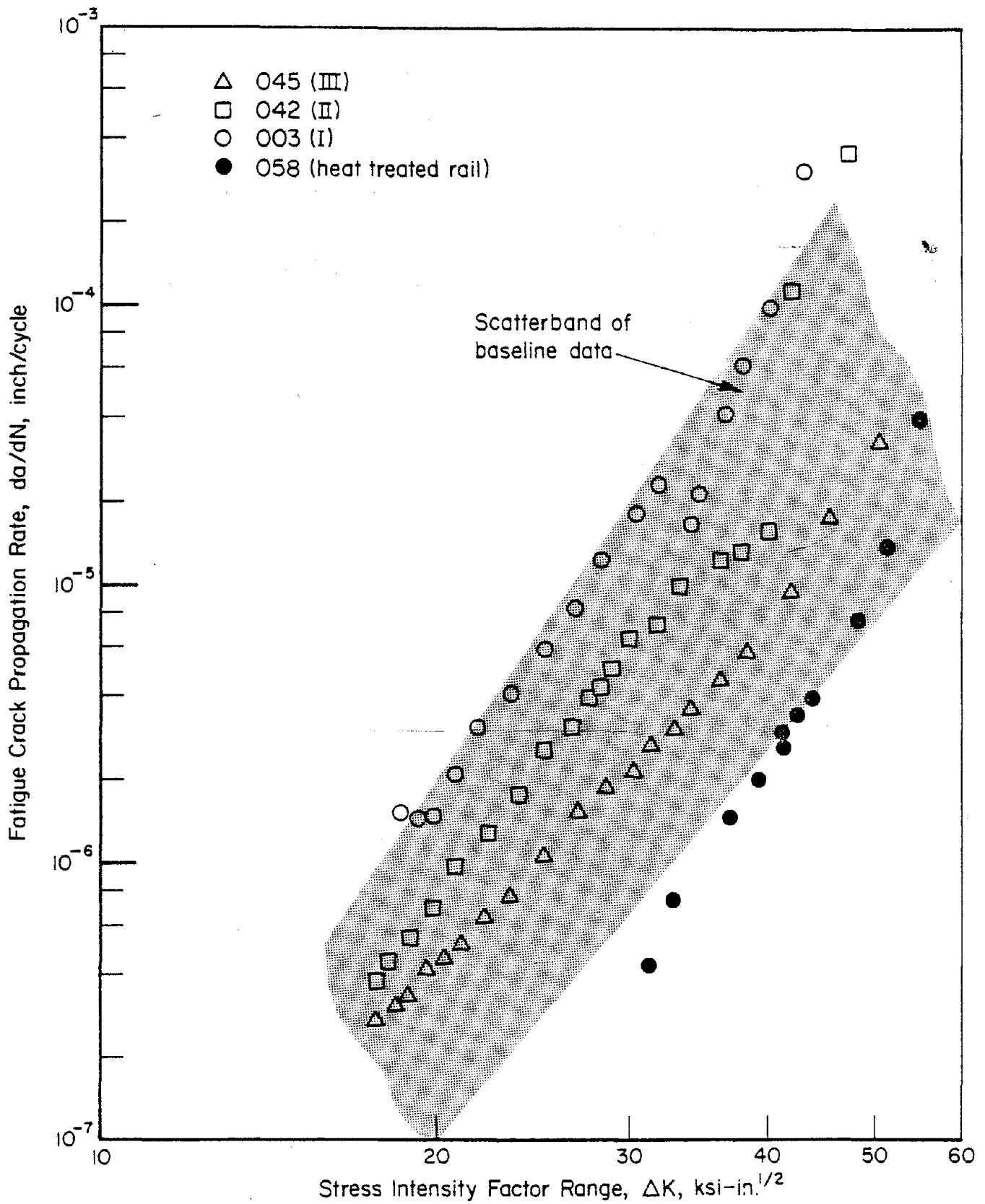
FIGURE 5. FATIGUE CRACK PROPAGATION RATE BEHAVIOR OF 66 RAIL
SAMPLES TESTED AT R = 0 IN THE FIRST PHASE OF
THE PRESENT PROGRAM[1]
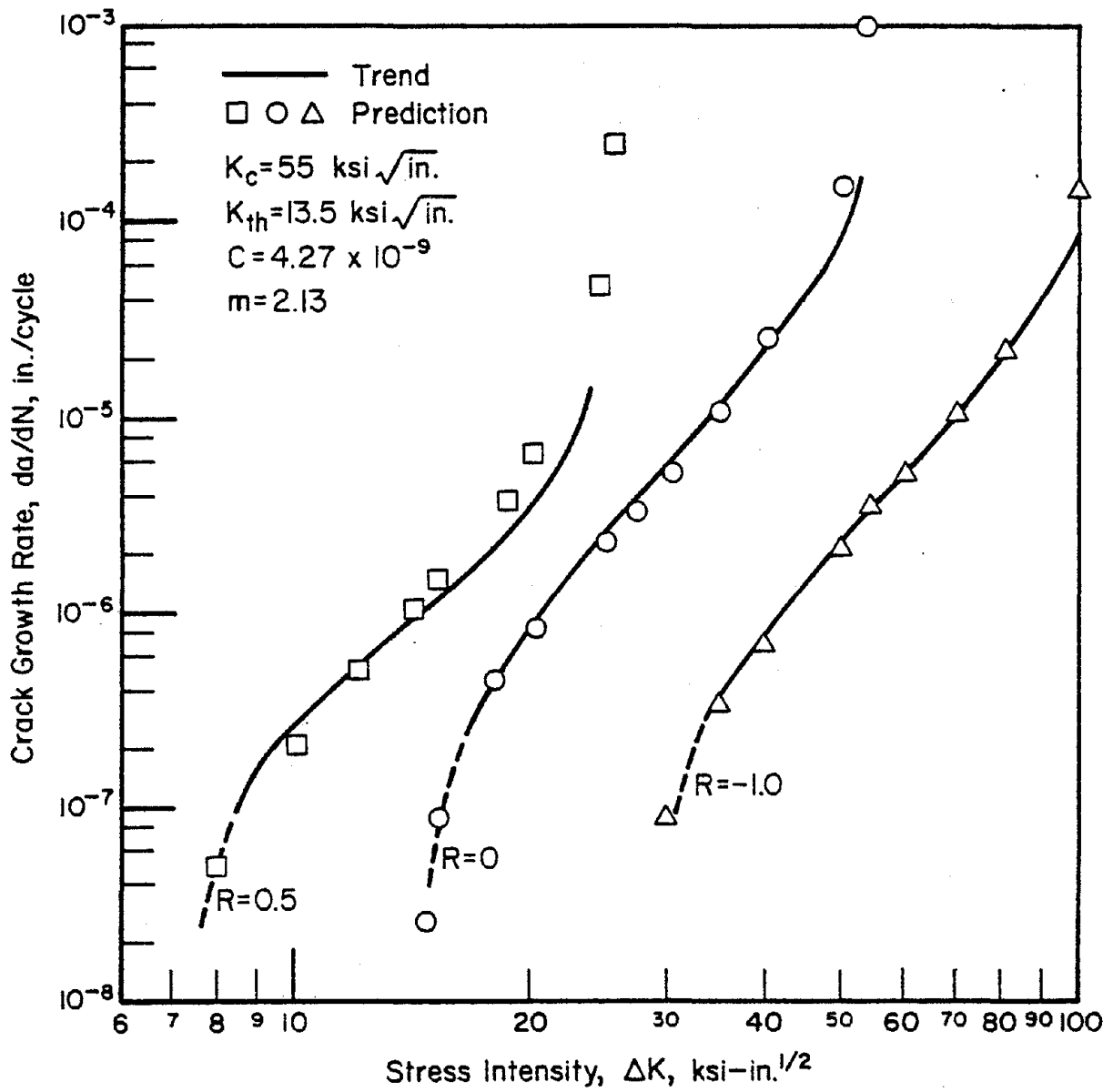
FIGURE 6. APPLICABILITY OF CRACK GROWTH EQUATIONS,
ORIENTATION LT, ROOM TEMPERATURE

14

of this program, data were generated for crack growth in rail steels as affected by a variety of factors (i.e., crack orientation, temperature, R-ratio), so that the constants in Equation (3.5) can be evaluated for different circumstances.

## 3.2. Stress-Intensity Factors

The stress-intensity factor for the CT specimen used in this investigation is given as

$$K = \frac{P}{2BW^{\frac{1}{2}}} \left(1 + \frac{a}{W}\right) \left(1 - \frac{a}{W}\right)^{-3/2} \left\{7.000 - 7.050 \frac{a}{W} + 4.275 \left(\frac{a}{W}\right)^2\right\} , \qquad (3.6)$$

in which P is the applied load, a is as defined in Figure 1, B is the thickness, and W is the width.

It is not immediately clear that Equation (3.6) has the character of Equation (3.2). This is more evident in the stress-intensity factor for the SEN specimen, which is given as

$$K = \frac{P}{BW}\sqrt{a} \left\{1.99 - 0.41 \frac{a}{W} + 18.7 \left(\frac{a}{W}\right)^2 - 38.48 \left(\frac{a}{W}\right)^3 + 53.85 \left(\frac{a}{W}\right)^4\right\} , \qquad (3.7)$$

with a as defined in Figure 2, B is the thickness, and W is the width. Obviously, P/BW is the remote stress.

## 4. LOAD INTERACTION EFFECTS

### 4.1. Background

The prediction of crack growth under variable amplitude loading may be highly complicated by retardation caused by load interaction. If a high load (stress) is inserted in a sequence of low amplitude cycles, the rate of growth during subsequent low amplitude cycles may be drastically reduced.[3] The high stresses associated with the overload introduce a large plastic zone at the tip of the crack. Upon unloading, the surrounding elastic material will contract, but the material within the plastic zone will not because it is permanently deformed. Thus, the surrounding elastic material will compress

15

the material in the plastic zone, introducing residual compressive stresses at the crack tip. These compressive stresses and consequent crack closure reduce the effect of subsequent low stress cycles — causing lower crack growth rates than would have been observed if no overload had occurred.

The retardation effect in certain materials (particularly aluminum alloys) may be so large that the crack can become completely dormant for thousands of cycles subsequent to a sufficiently high overload.[4] As a consequence, high loads may be beneficial for crack growth. If retardation occurs, it has to be accounted for in a predictive failure model by using a retardation factor which depends upon the plastic properties of the material and can only be determined experimentally. In general, steels do not show large retardation effects.

Some overload tests were performed on CT specimens of TL orientation to characterize the rail steel behavior. The specimens were subjected to constant amplitude cycling to the same load level (2500 pounds) used in the baseline experiments.[1] Overloads were applied periodically at crack growth intervals of about 0.1 inch. Various tests were performed with overloads of 3000, 3500, and 5000 pounds at R = 0 and R = 0.5.


## 4.2. Results


The numerical results of the overload tests are given in Table 3 and are plotted in Figure 7 for R = 0 and in Figure 8 for R = 0.5. In two cases, data for crack growth without overloads were available[2] for the same rail samples. These data are also shown in Figures 7 and 8. In addition, some comparative data for other rail samples[2] are given.

The overload ratio, $\rho$, is defined as the overload divided by the maximum load of the constant amplitude loading. Obviously, no retardation occurred for $\rho$ = 1.2 and 1.4, but $\rho$ = 2 does have a modest retarding effect. This is shown more clearly in Figures 9 and 10 where the crack growth rates are plotted as a function of $\Delta K$. Figure 9 presents the rate data for cases with and without overloads. Irregularities in crack growth are equally prominent in both cases. Figure 10 shows the data for $\rho$ = 2. Since no baseline data were available for the same rail sample, the trend line of all TL data at R = 0[2] is shown for comparison. A delayed retardation can be observed;

## TABLE 3. RESULTS OF OVERLOAD TESTS

### Maximum Load in All Tests 2500 Pounds, CT-TL Specimens

| OC1 - 2 R = 0.5 $P_o$ = 3500 Pounds | | 006 - 2 R = 0 $P_o$ = 3500 Pounds | | 013 - 2 R = 0 $P_o$ = 5000 Pounds | | 023 - 3 R = 0 $P_o$ = 3000 Pounds | |
|---|---|---|---|---|---|---|---|
| a, in. | N, kc | a, in. | N, kc | a, in. | N, kc | a, in. | N, kc |
| 1.057 | 370 | 0.987 | 310 | 0.913 | 155 | 0.926 | 400 |
| 1.089 | 535 | 1.076 | 446 | 0.947 | 195 | 0.959 | 523 |
| 1.117 | 615 | 1.088 | 460 | 0.958 | 210 | 1.011 | 638 |
| 1.130 | 660 | 1.105 | 475 | 0.978 | 245 | 1.047 | 693 |
| 1.150 | 720 | 1.129 | 493 | 1.014 | 275 | 1.054 | 703 |
| 1.172 | 780 | 1.175 | 524 | 1.055 | 300 | 1.061 | 716 |
| 1.212 | 870 | 1.215 | 546 | 1.064 | 310 | 1.070 | 730 |
| 1.265 | 970 | 1.233 | 554 | 1.072 | 325 | 1.091 | 756 |
| 1.277 | 1000 | 1.249 | 562 | 1.084 | 345 | 1.115 | 790 |
| 1.301 | 1032 | 1.268 | 570 | 1.111 | 365 | 1.166 | 845 |
| 1.330 | 1066 | 1.306 | 585 | 1.141 | 385 | 1.209 | 890 |
| 1.361 | 1100 | 1.350 | 600 | 1.165 | 400 | 1.227 | 900 |
| 1.387 | 1130 | 1.380 | 605 | 1.188 | 405 | 1.241 | 910 |
| 1.407 | 1145 | 1.411 | 615 | 1.204 | 425 | 1.255 | 920 |
| 1.428 | 1160 | 1.451 | 625 | 1.217 | 445 | 1.305 | 950 |
| 1.509 | 1205 | 1.497 | 635 | 1.244 | 475 | 1.326 | 960 |
| 1.538 | 1220 | 1.519 | 640 | 1.270 | 495 | 1.354 | 970 |
| 1.563 | 1235 | 1.550 | 645 | 1.299 | 530 | 1.406 | 988 |
| 1.599 | 1250 | 1.598 | 652 | 1.318 | 545 | 1.448 | 1000 |
| | | | | 1.355 | 565 | 1.510 | 1015 |
| | | | | 1.372 | 570 | 1.511 | 1023 |
| | | | | 1.397 | 590 | 1.604 | 1030 |
| | | | | 1.425 | 605 | 1.623 | 1033 |
| | | | | 1.456 | 615 | 1.650 | 1036 |
| | | | | 1.521 | 618 | 1.691 | 1039 |
| | | | | 1.571 | 640 | 1.728 | 1042 |
| | | | | 1.605 | 651 | 1.761 | 1044 |
| | | | | 1.672 | 663 | 1.804 | 1045 |
| | | | | | | 1.902 | 1047 |
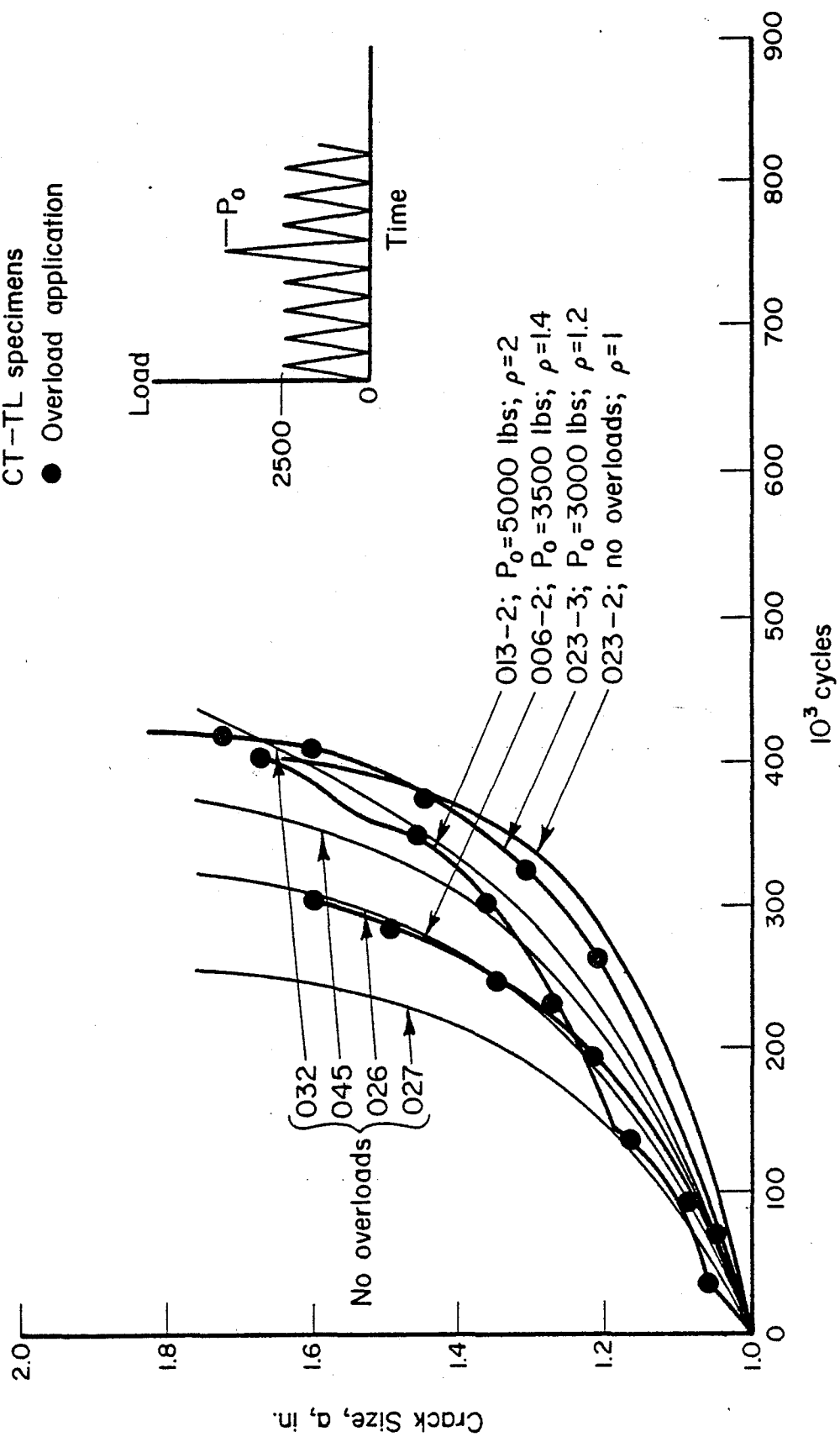
FIGURE 7. EFFECT OF OVERLOADS ON CRACK GROWTH AT R = 0
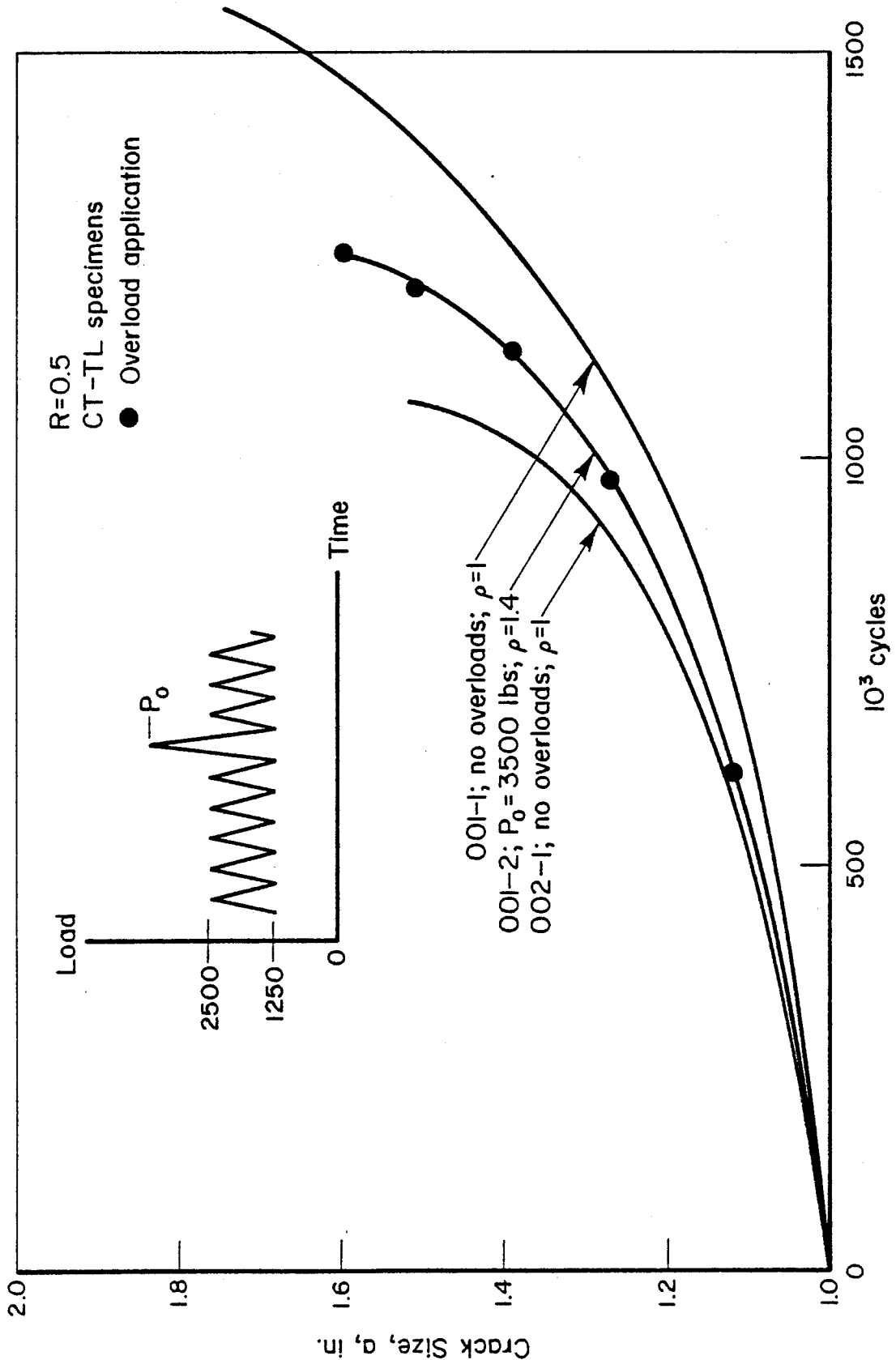
FIGURE 8. EFFECT OF OVERLOADS ON CRACK GROWTH AT R = 0.5

19
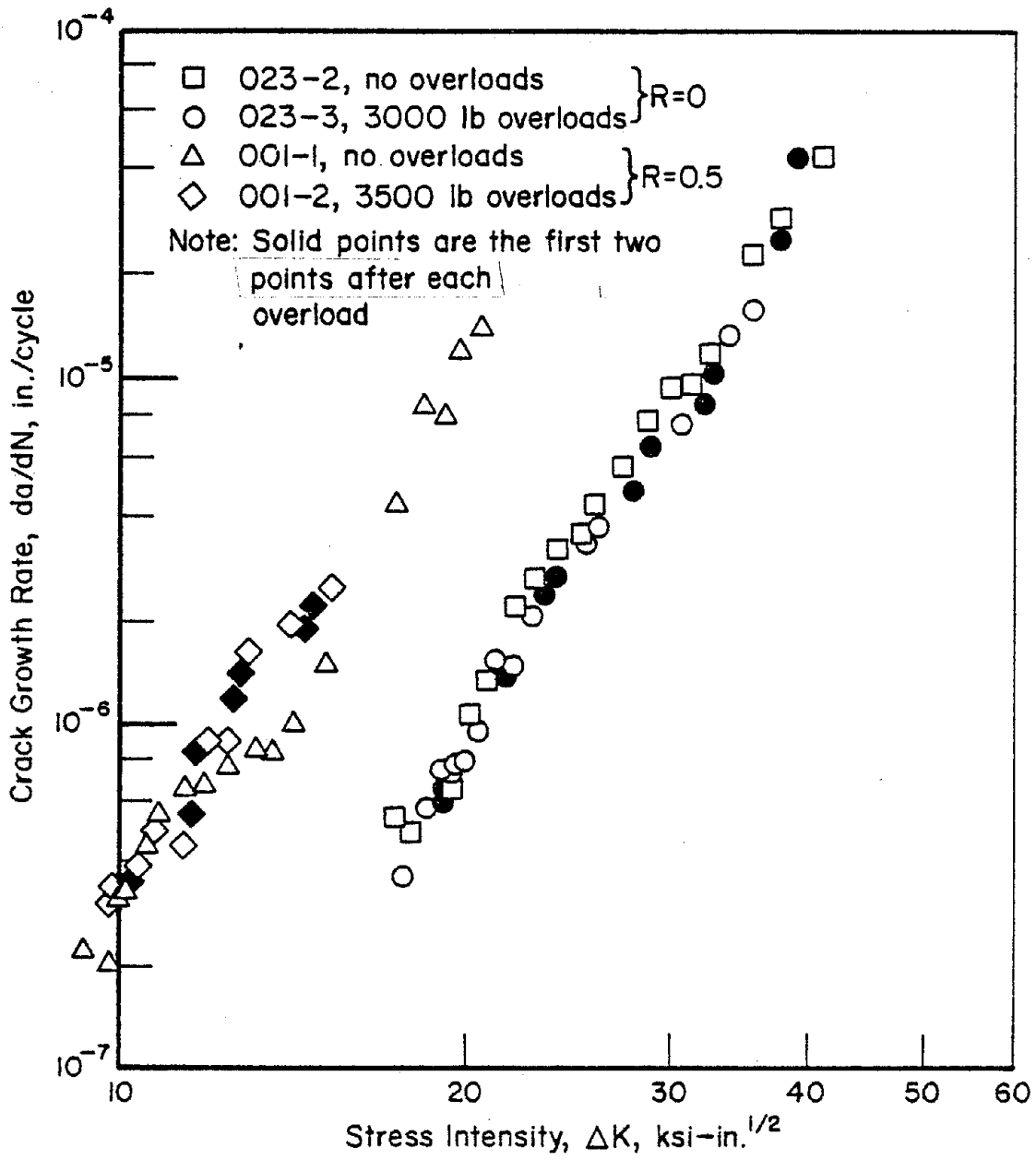
FIGURE 9. EFFECT OF OVERLOADS ON GROWTH RATES
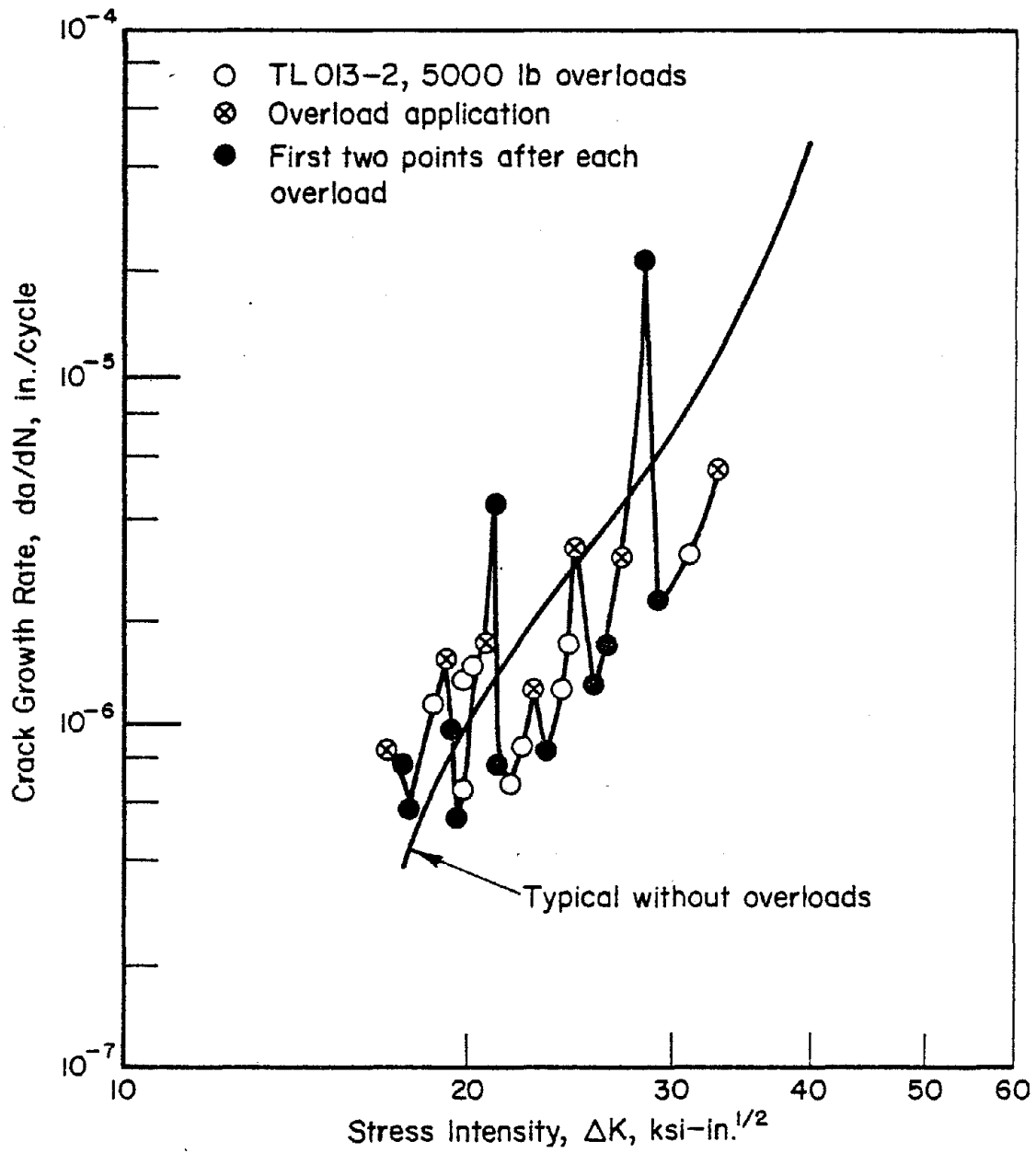
FIGURE 10. EFFECT OF HIGH OVERLOADS ON CRACK GROWTH RATE

immediately after the overload, the crack growth rate is higher than normal. Thereafter, it drops and becomes lower than normal for a period of time. From the crack growth curve in Figure 7, it appears that the net result is a slight increase in crack growth life.

A comparison with the retardation effect observed for other materials is difficult because different investigators use different measures for retardation and because the phenomenon depends upon so many factors that data for comparable circumstances are hard to find. An attempt to make a comparison resulted in Figure 11, which shows data from two different sources.[5,6] The data were analyzed to obtain approximate values for $N_r/N$, where $N_r$ is the number of cycles subsequent to the overload required to grow the crack over a distance large enough that normal constant amplitude behavior was restored, and N is the number of cycles in a test without overloads to grow the crack over the same distance, all other circumstances being equal.

Figure 11 shows that for R = 0, crack growth in 2024-T3 aluminum is virtually arrested for an overload ratio of $\rho \approx 2.5$. For $\rho = 2$ and R = 0, a retardation occurs of $N_r/N = 4.6$. From the data in Figure 7, it is estimated that for rail steel $N_r/N < 2$ under equal circumstances. (The rail steel data are also shown in Figure 11). Retardation data for steels[7,8] indicate similar trends for other steels.

According to Figure 11, the retardation effect is reduced for negative R-ratios, i.e., if the cyclic loading is partially compressive. Compressive overloads tend to accelerate crack growth ($N_r/N < 1$), which is also shown in Figure 11. Compressive loads give rise to reversed plastic flow in the crack tip plastic zone, which reduces the compressive residual stresses. Thus, if a tensile overload is preceded or followed by a compressive overload, the retardation effect due to the tensile overload can be significantly reduced (compression-tension) or annihilated[5] (tension-compression), as is illustrated in Figure 12.

The retardation effect in rail steels is smaller than in 2024-T3 aluminum (Figure 11). Moreover, rails under service loading experience many cycles of high compressive stress (in particular the rail head), which further reduces or annhilates retardation. Therefore, it is concluded that retardation will not be of great significance for cracks in rails under service loading. This conclusion will receive further consideration in later sections of this report.
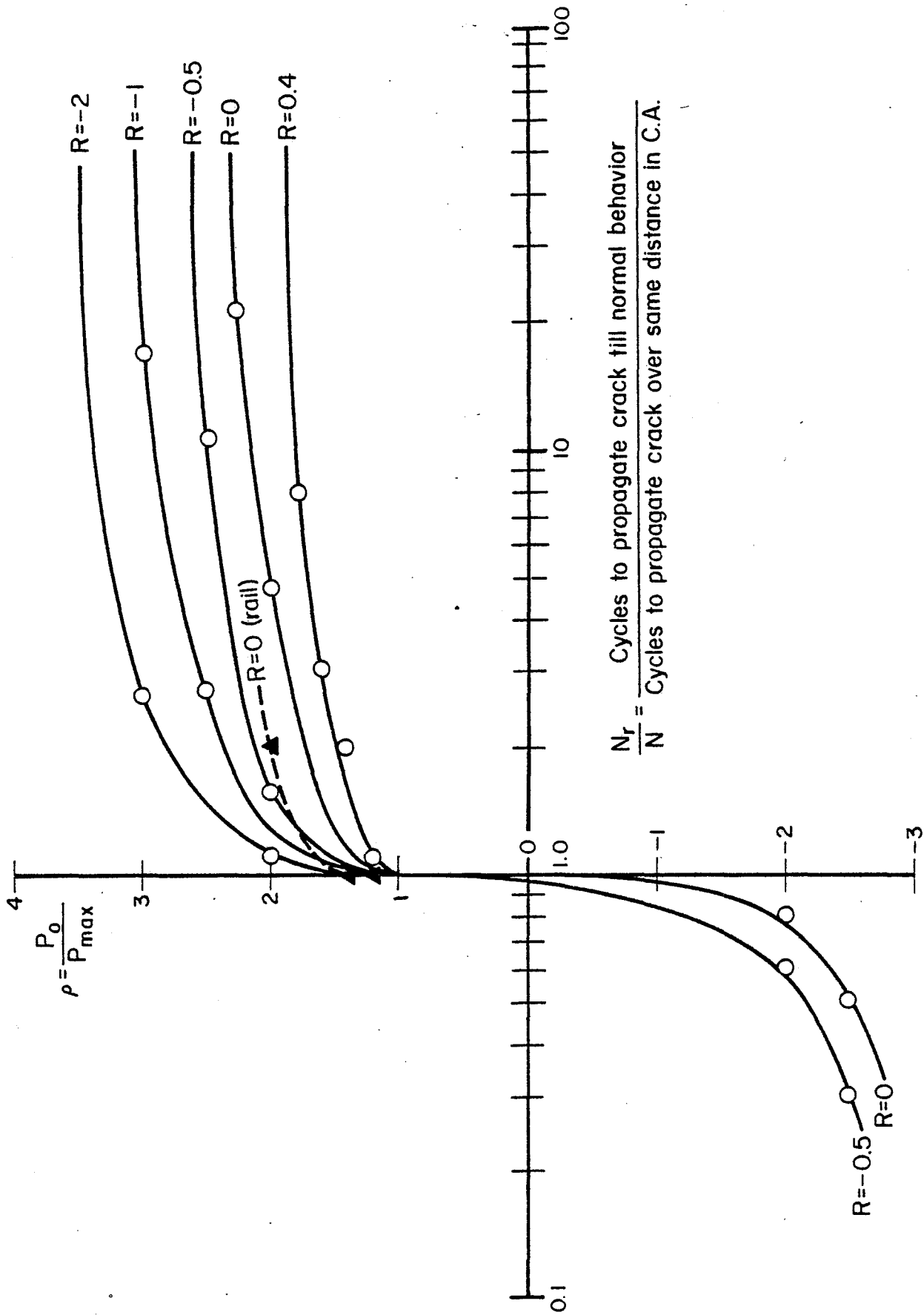
FIGURE 11. RETARDATION AS A FUNCTION OF OVERLOAD RATIO (Data from References 5 and 6 for 2024-T3 aluminum)

23
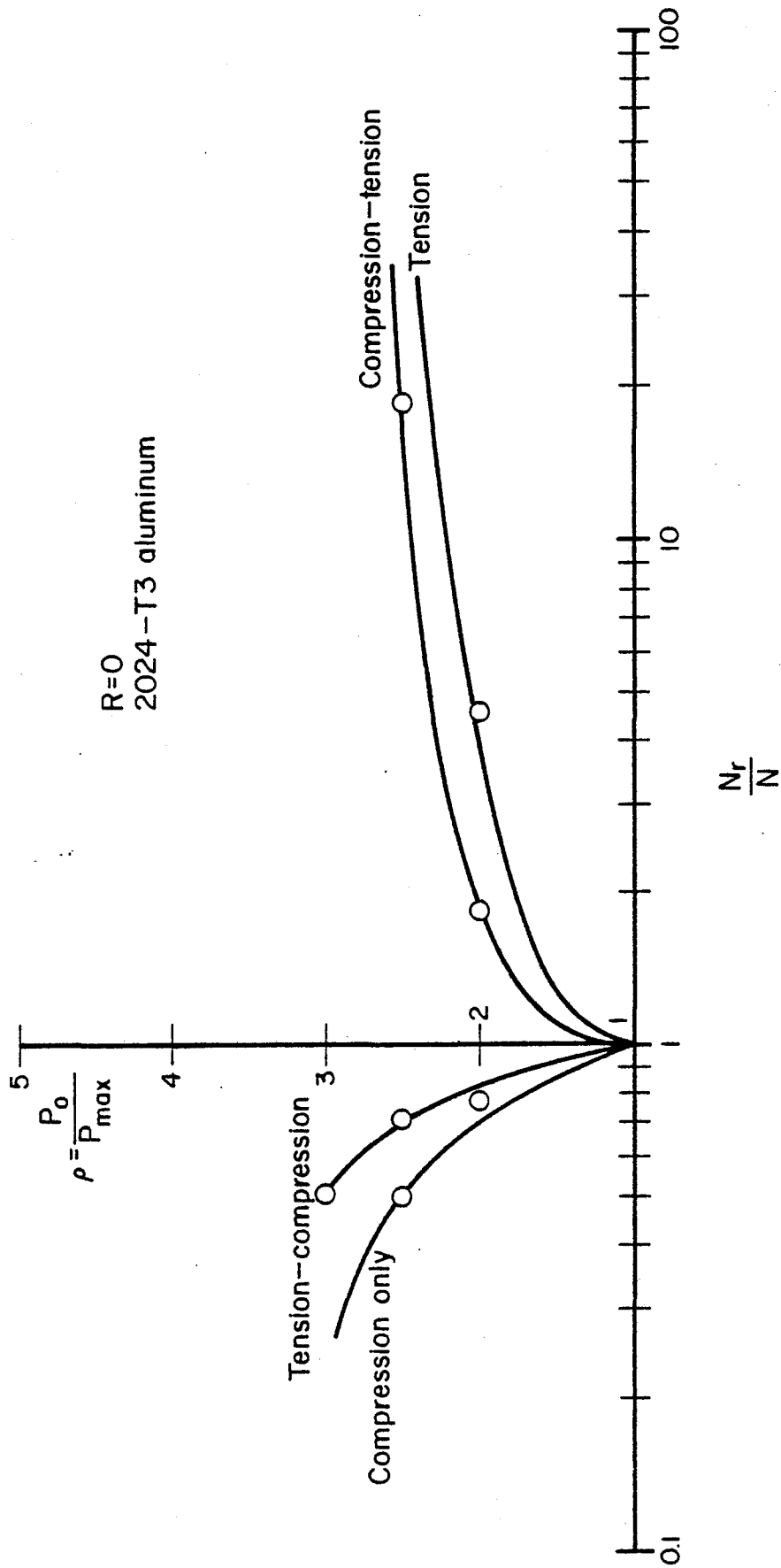
FIGURE 12. EFFECT OF COMPRESSIVE LOADS ON RETARDATION (Data from Reference 5, see previous figure for definition of $N_r/N$)

24

# 5. SIMPLE STRESS SEQUENCES IN RAIL

## 5.1. The Stress Intensity in Cracked Rail

In a parallel program, an engineering stress analysis was made of cracked rail.[9] At the time the variable amplitude tests were designed, stress analysis results were available for an elliptical transverse crack in the rail head. The minor axis was 0.75 inch (vertical). The crack was located approximately in the center of the rail head. The rail was subjected to the passage of a wheel load of 19,000 pounds. The variation of the mode I stress intensity, $K_I$, at the lower extremity of the crack is shown in Figure 13.

Consider (Figure 13) the case of a stiff roadbed. Disregarding for awhile the sign of the stress intensity, $K_I$ first increases due to upward bending of the rail when the wheel is still relatively far away. When the wheel comes closer, the rail is bent downward and as a result the stress intensity reverses and goes to a minimum when the wheel is nearby. There is another smaller reversal of $K_I$ when the wheel moves right over the location of the flaw[9]. Naturally, a symmetric pattern develops when the wheel moves away.

If only one wheel would pass, the increase of $K_I$ due to upward bending would occur again. However, this does not occur during passage of a truck because the second wheel approaches too soon. After passage of the second wheel of the truck, the increase of $K_I$ due to upward bending becomes effective again before $K_I$ returns to zero. The pattern is repeated when the second truck goes by. In the case of a soft roadbed, the pattern of variation is the same, but the magnitude of the successive reversals is different.

The largest excursions of $K_I$ are negative. This is of academic significance only, because a crack would simply close under compression and $K_I$ would be undefined. (The stress intensity has no physical significance in case of compressive loads.) However, if a residual tensile stress exists in the rail, the variations in stress are in the positive range. As indicated in Figure 13, a residual tensile stress of 20 ksi for this crack results in $K_I$ = 12 ksi$\sqrt{\text{in}}$. In that case, the passage of a wheel would cause $K_I$ to increase first from 12 ksi$\sqrt{\text{in}}$. to 13 ksi$\sqrt{\text{in}}$. due to upward bending. The downward bending would then decrease $K_I$ to 6 ksi$\sqrt{\text{in}}$. In other words, the variations of $K_I$ shown in Figure 13 would still be applicable. For the case

Due to residual stress of 20,000 psi there is a residual $K_I = 12$ ksi$\sqrt{\text{in}}$ for the given crack geometry and location.
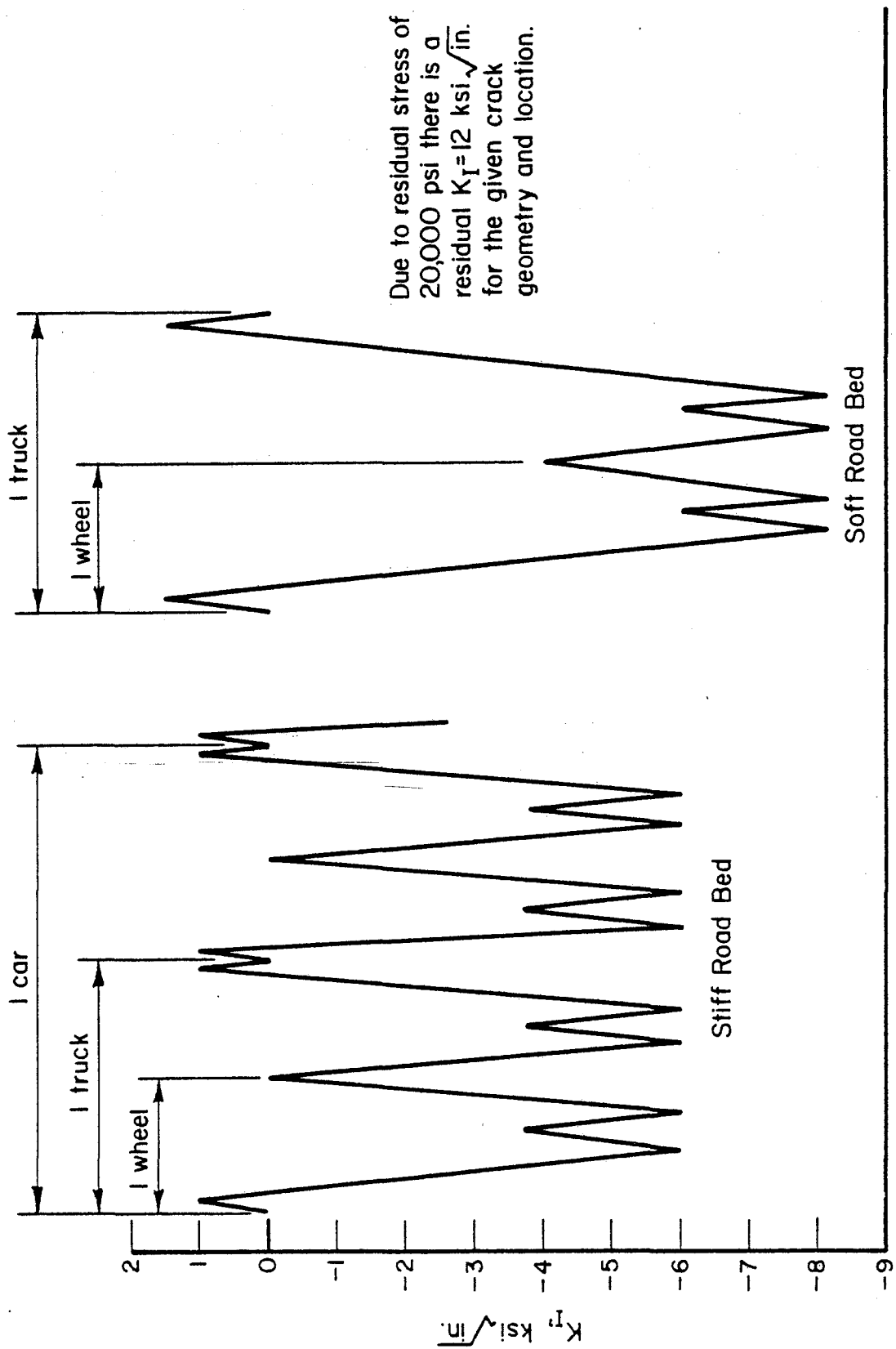
FIGURE 13. $K_I$ HISTORY FOR PASSAGE OF 19,000 POUND WHEEL LOADS ON STIFF AND SOFT ROAD BEDS FOR A PARTICULAR CRACK GEOMETRY AND LOCATION

26

under consideration, a previous computation had shown that there was indeed a residual tensile stress at the extremity of the crack of 20 ksi.

The computed $K_I$ is proportional to the wheel load. Thus, a wheel load of 9500 pounds would cause variations of half the magnitude shown in Figure 13; whereas, a 38,000-pound load would cause variations of twice that magnitude. In both cases, the residual stress level would still be the same. Thus, in the first case, $K_I$ would vary from 12 to 12.5 ksi$\sqrt{\text{in}}$. and from there to 9 ksi$\sqrt{\text{in}}$. In the second case, $K_I$ would go from 12 to 14 ksi$\sqrt{\text{in}}$. and from there to 0. Higher wheel loads would close the crack. All of the above examples assume a residual tensile stress of 20 ksi. If the residual stress is lower, compressive stresses will occur at lower wheel loads.

## 5.2. Rail Stress Sequence Tests

A number of load sequences were designed to evaluate the significance of the various reversals of $K_I$ when a wheel passes. These load sequences, denoted A, B, C, D, E, and F will be discussed below. All of these sequences were applied in tests on CT specimens.

Since for R = 0 baseline data were available for all individual rail samples, sequences A and B were taken at R = 0. They are shown in Figure 14. Since most previous testing of CT specimens was at a maximum load of 2500 pounds, this same maximum load was selected. On this basis, the variations of $K_I$ (shown in Figure 13) were changed proportionally as shown in the left part of Figure 14.

The small variations at the top of the cycle have a range which is 15 percent of the total range of the cycle. Since the rate of crack growth is proportional to the fourth or higher power of the range, these small variations will contribute 5 percent or less of the total crack growth. If they are smaller than the threshold, they will have no contribution. In order to evaluate the relative significance of these small load variations, sequences A and B in Figure 14 were designed. They were repeated continuously to simulate the passage of a succession of cars of the same weight.

Figure 15 shows the load variations for a car of half the weight of the previous cars, but the residual stress level is the same. Following the same arguments as in the previous paragraph, load sequence C was designed
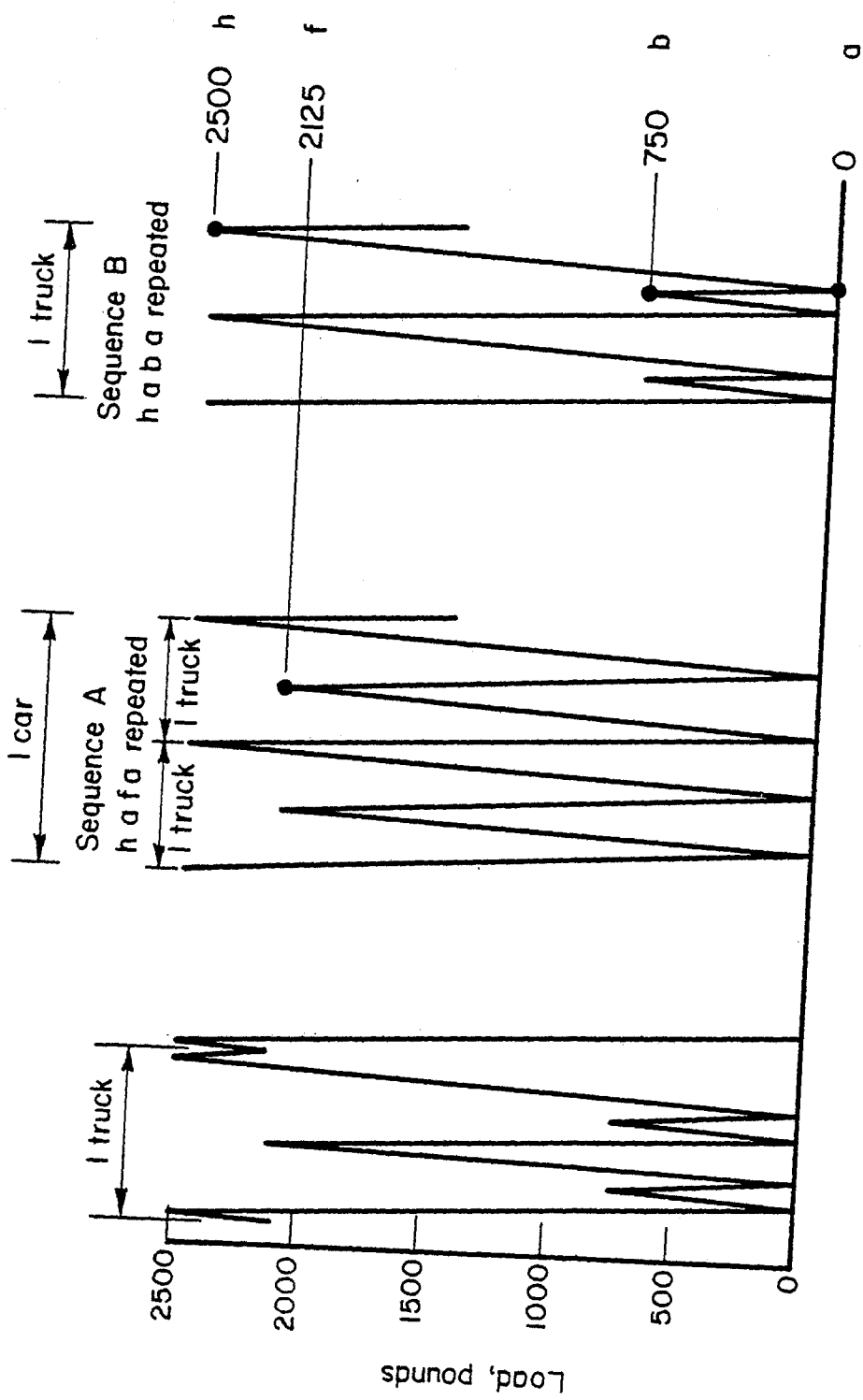
FIGURE 14. SEQUENCES A AND B TO EVALUATE RELATIVE SIGNIFICANCE OF LOAD VARIATIONS CAUSED BY PASSAGE OF ONE HEAVY CAR

28
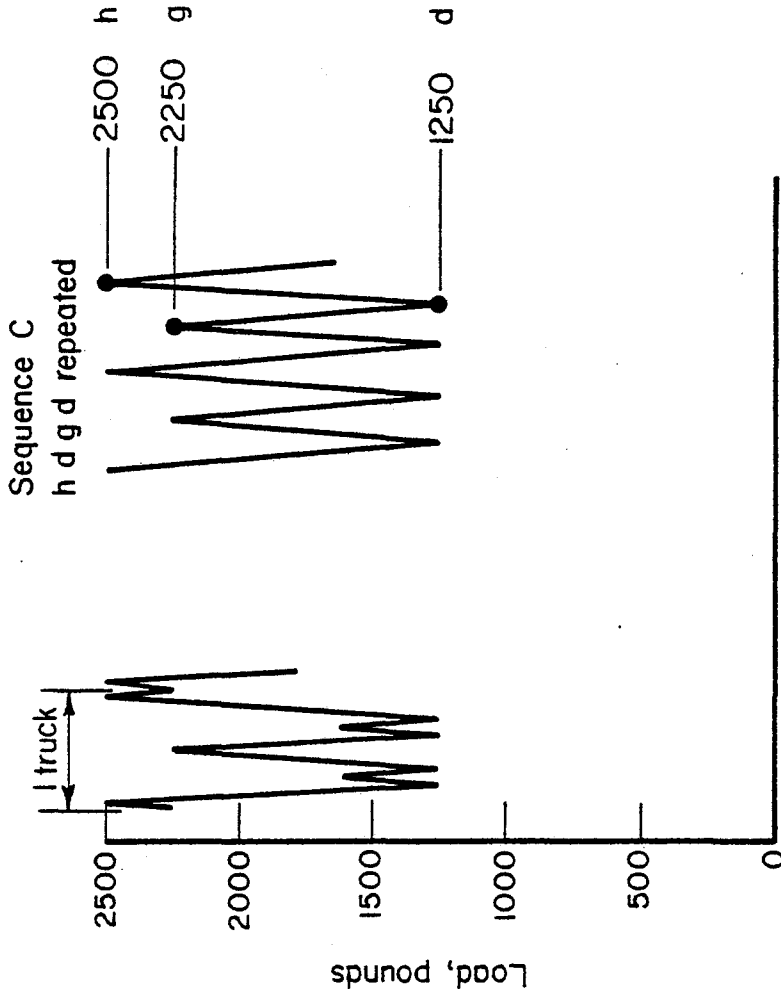
FIGURE 15. SEQUENCE C TO EVALUATE RELATIVE SIGNIFICANCE OF LOAD VARIATIONS CAUSED BY PASSAGE OF ONE LIGHT CAR

as shown in Figure 15. This sequence is basically $R = 0.5$ loading, with a maximum load of 2500 pounds.

Load sequences D, E, and F are a combination of the previous cases. Sequence D (Figure 16) is a succession of light and heavy cars (each car consisting of 2 trucks) with all the small load variations included. Sequence E is basically the same, but all small load variations were omitted (Figure 17). Finally, sequence F (Figure 18) is a sequence of blocks of 1000 heavy cars and 1000 light cars with the same wheel loads as in sequence E.

## 5.3. Results of Sequence Tests

The test data of the sequence tests are compiled in Table 4. A graphic display of the data is presented in Figures 19, 20, and 21. Also shown in these figures are predicted crack growth curves as discussed in the following. In order to avoid extrapolations due to different pre-crack sizes, all crack growth curves were started at a crack size of 1.07 inches.

Figure 19 shows the results of two tests employing sequence A on the same rail sample. The variability of the material is clearly exhibited by these two tests which show a difference of almost a factor 3 on life. Obviously, any predictions made cannot be more accurate than within a factor of 3; i.e., if the prediction was right for one test, it would be a factor of 3 off for the other.

The results for sequence B in Figure 19 are for a different rail sample, so that no direct comparison can be made between the two sequences. However, with the two largely different results for sequence A, such a comparison would not be too meaningful anyway. An indirect comparison of sequences A and B can be made on the basis of the predicted curves as explained below.

The simplest representation of the passage of a car (2 trucks) would be four cycles of the same amplitude. Sequences A and B were designed to show whether this is permissible or not. In sequence A, the small load variations associated with the passage of a truck were omitted (Figure 14), but the relative size of the two large cycles was maintained. In sequence B, on the other hand, the small load cycles at the low load side were maintained, but the two large cycles were made of the same magnitude. Of course, the

30

Sequence D — f h a b a f a b a h f h a b a f a b a h f g c e c f c e c g f g c e c f c e c g repeated

FIGURE 16. SEQUENCE D FOR INTERMITTENT PASSAGE OF HEAVY AND LIGHT CARS

31

FIGURE 17. RATIONALIZED SEQUENCE E FOR INTERMITTENT PASSAGE OF HEAVY AND LIGHT CARS
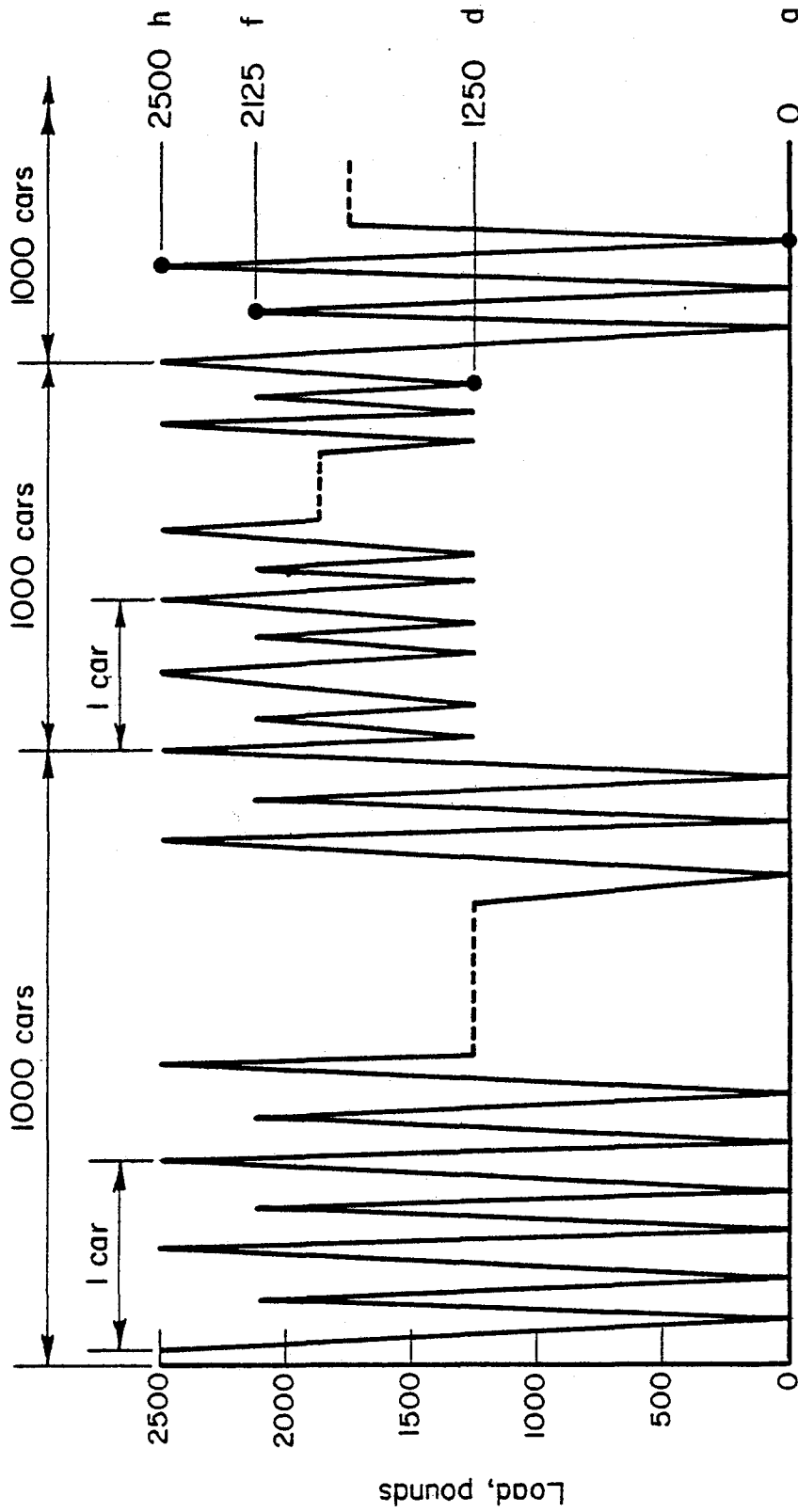
FIGURE 18. RATIONALIZED SEQUENCE F FOR BLOCKS OF 1000 HEAVY CARS AND 1000 LIGHT CARS

TABLE 4.   RESULTS OF SEQUENCE TESTS

| 065-1 Sequence A a, in. | 065-1 Sequence A N, 1000 cars | 065-3 Sequence A a, in. | 065-3 Sequence A N, 1000 cars | 021-1 Sequence B a, in. | 021-1 Sequence B N, 1000 cars | 065-2 Sequence C a, in. | 065-2 Sequence C N, 1000 cars | 025-1 Sequence D a, in. | 025-1 Sequence D N, 1000 cars | 025-2 Sequence E a, in. | 025-2 Sequence E N, 1000 cars | 025-4 Sequence E a, in. | 025-4 Sequence E N, 1000 cars | 025-3 Sequence F a, in. | 025-3 Sequence F N, 1000 cars |
|---|---|---|---|---|---|---|---|---|---|---|---|---|---|---|---|
| 1.07 | 0 | 1.07 | 0 | 1.07 | 0 | 1.07 | 0 | 1.07 | 0 | 1.07 | 0 | 1.07 | 0 | 1.07 | 0 |
| 1.09 | 3 | 1.11 | 21 | 1.10 | 10 | 1.12 | 40 | 1.12 | 9 | 1.10 | 10 | 1.08 | 2 | 1.12 | 14 |
| 1.13 | 11 | 1.13 | 43 | 1.11 | 13 | 1.15 | 81 | 1.17 | 20 | 1.15 | 24 | 1.13 | 13 | 1.17 | 37 |
| 1.19 | 20 | 1.23 | 78 | 1.16 | 22 | 1.17 | 89 | 1.22 | 28 | 1.20 | 37 | 1.18 | 22 | 1.22 | 45 |
| 1.26 | 27 | 1.32 | 98 | 1.21 | 35 | 1.22 | 127 | 1.27 | 36 | 1.25 | 48 | 1.23 | 30 | 1.27 | 53 |
| 1.30 | 31 | 1.39 | 106 | 1.26 | 40 | 1.27 | 162 | 1.32 | 44 | 1.30 | 57 | 1.28 | 38 | 1.32 | 60 |
| 1.33 | 37 | 1.43 | 111 | 1.31 | 44 | 1.32 | 189 | 1.37 | 50 | 1.35 | 65 | 1.33 | 44 | 1.37 | 66 |
| 1.37 | 40 | 1.48 | 115 | 1.36 | 48 | 1.35 | 207 | 1.42 | 56 | 1.40 | 72 | 1.38 | 50 | 1.47 | 76 |
| 1.42 | 44 | 1.51 | 118 | 1.41 | 53 | 1.39 | 224 | 1.47 | 62 | 1.45 | 79 | 1.43 | 55 | 1.52 | 80 |
| 1.46 | 46 | 1.57 | 121 | 1.46 | 55 | 1.42 | 235 | 1.52 | 66 | 1.50 | 84 | 1.48 | 60 | 1.57 | 84 |
| 1.50 | 48 | 1.62 | 123 | 1.51 | 57 | 1.47 | 255 | 1.57 | 70 | 1.55 | 90 | 1.53 | 64 | 1.82 | 94 |
| 1.54 | 50 | 1.66 | 125 | 1.57 | 59 | 1.57 | 285 | 1.62 | 74 | 1.60 | 95 | 1.58 | 67 | 1.87 | 95 |
| 1.58 | 51 | 1.72 | 127 | 1.62 | 60 | 1.62 | 298 | 1.67 | 77 | 1.65 | 99 | 1.63 | 71 | 1.92 | 96 |
| 1.62 | 53 | 1.82 | 129 | 1.66 | 61 | 1.67 | 308 | 1.72 | 80 | 1.70 | 103 | 1.68 | 73 | | |
| 1.68 | 54 | | | 1.73 | 63 | 1.72 | 315 | 1.77 | 82 | 1.75 | 106 | 1.73 | 76 | | |
| | | | | | | 1.77 | 323 | 1.87 | 85 | 1.80 | 108 | 1.78 | 77 | | |
| | | | | | | 1.82 | 329 | 1.92 | 86 | 1.85 | 109 | 1.83 | 79 | | |
| | | | | | | 1.92 | 33? | | | 1.90 | 110 | 1.88 | 80 | | |
| | | | | | | 2.00 | 342 | | | 1.95 | 112 | | | | |

Legend:

○   (O65) Sequence A (2 tests)
- - - Prediction (based on O65)
△   (O2l) Sequence B
——— Prediction (based on O2l)
—·—· Prediction (based on average)

Crack Size, a, in.

$10^3$ Cars
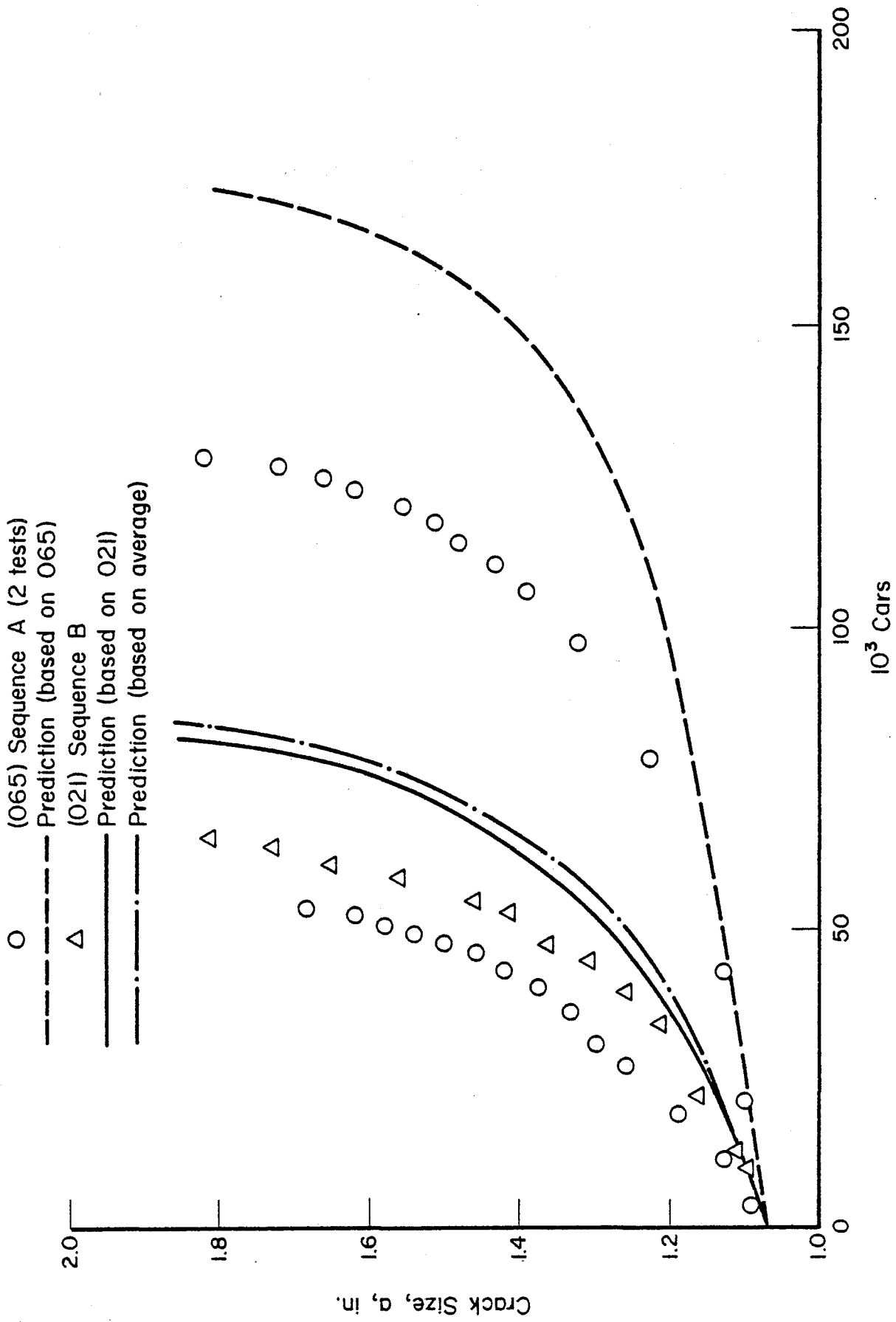
FIGURE 19.   RESULTS OF TESTS WITH SEQUENCE OF SIMILAR CARS

35
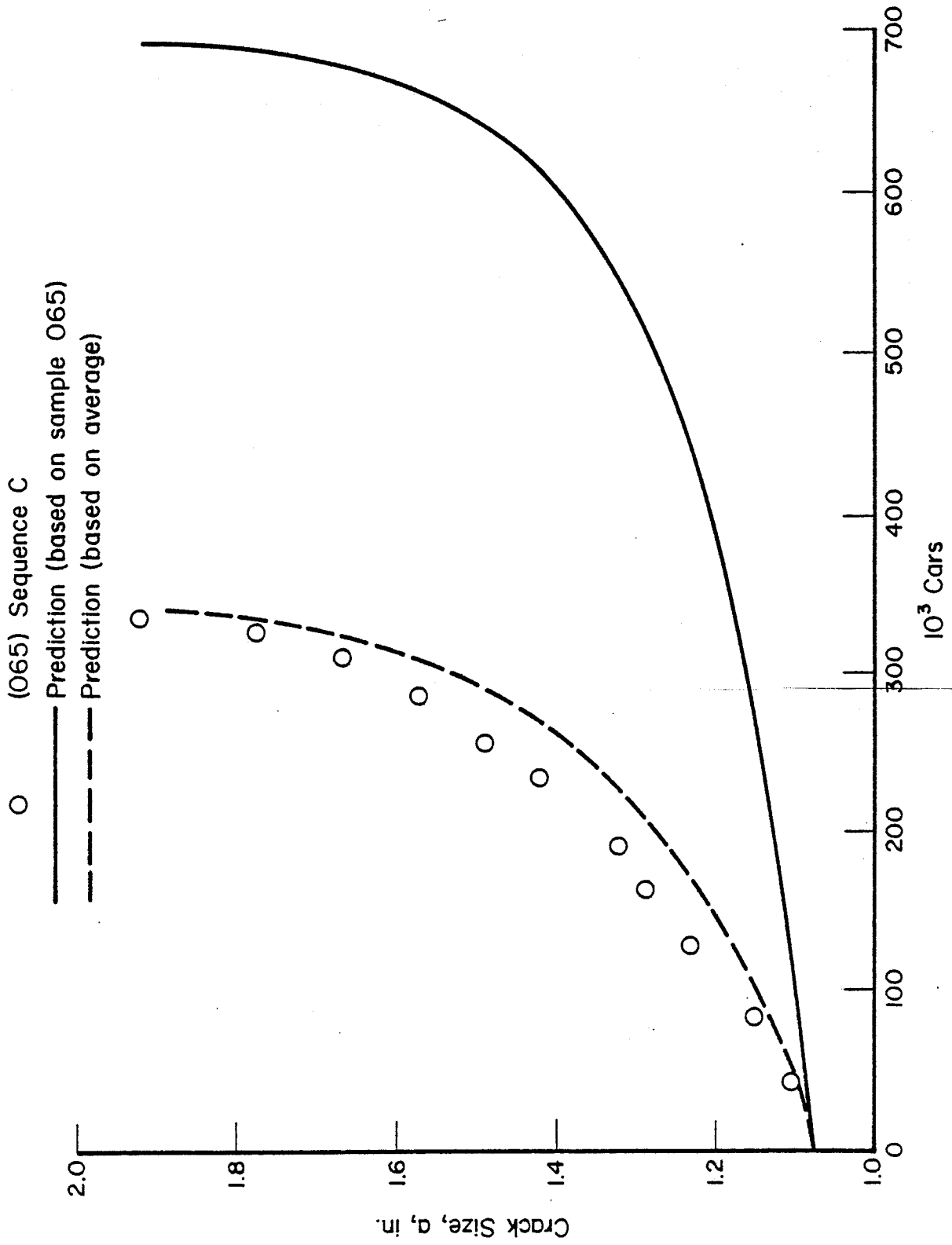
FIGURE 20. RESULTS OF TESTS WITH SEQUENCE OF LIGHT CARS

○       (065) Sequence C
——      Prediction (based on sample 065)
– – –   Prediction (based on average)

Crack Size, a, in.

$10^3$ Cars
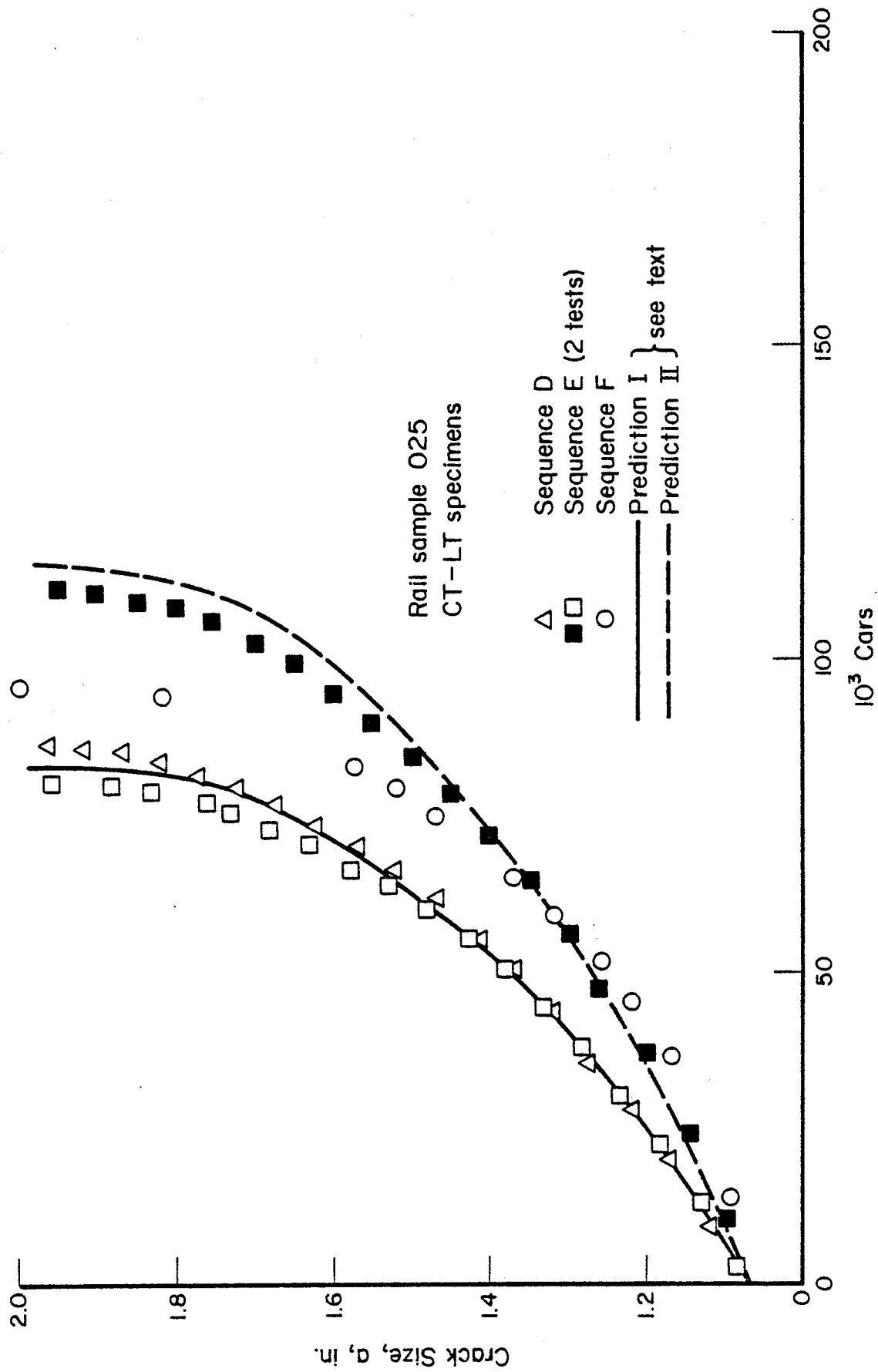
FIGURE 21. RESULTS OF TESTS WITH SEQUENCE OF DIFFERENT CARS

next step would be to omit the small cycles from sequence B, which would re-
duce the sequence to constant-amplitude cycling (for which the results were
already available) with 4 cycles per car. The small cycles in sequence B
are only 30 percent of the large cycles. Crack growth is proportional to the
fourth power (or higher) of the stress intensity (i.e., the load). Thus the
small cycles would contribute only $(0.3)^4$ x 100% = 0.8% of the crack growth,
which means that they should be negligible, even if there is no retardation.

Therefore, the predicted curves in Figure 19 are based on the
premise that the passage of a car can be represented by four cycles of con-
stant amplitude. One curve was calculated for each of the two rail samples
tested (i.e., 065 and 021) by using the baseline constant-amplitude data.[1]
The curve for Sample 021 is within about 20 percent of the test data over the
entire range. The curve for Sample 065 is considerably less accurate, which
is largely due to material variability as discussed above. A third curve
shows a prediction based on the average of all baseline data for 66 samples[1] ,
which under the assumptions made, should cover all three test records in
Figure 19. Similar procedures were followed for sequence C in Figure 20.

The results shown in Figure 21 are the most interesting. Sequence D
is for a succession of heavy and light cars (Figure 16) in which all the small
cycles were included. Sequence E is equivalent to D, but the small cycles
were omitted; whereas, sequence F is the same as E, but the cars were combined
in series of 1000 heavy and 1000 light cars.

Two tests on Sample 025 on sequence E showed reasonable agreement.
Tests with sequences D and F were conducted on the same rail sample.
Apparently, the small load cycles are of negligible effect (compare results
of D and E), whereas the 1000 - 1000 sequence gives essentially the same
results as the 1 - 1 sequence. Thus, for all practical purposes, D, E,
and F can be considered equivalent.

The predicted curves in Figure 21 are based on the constant-ampli-
tude data of Sample 025. Predicted Curve I was calculated by assuming four
constant-amplitude cycles per car, naturally accounting for a cycle ratio
R = 0 for the heavy cars and R = 0.5 for the light cars. Retardation effects
were not considered and the prediction of crack growth was based on a linear
integration of crack growth rates. Predicted Curve II made use of the same
baseline data; however, the calculation recognized that two of the four

cycles associated with one car are of somewhat lesser magnitude. As a result, the predicted crack growth is slower.

It can be concluded from Figure 21 that omission of the small load variations is permitted and that it is reasonable to consider a car equivalent to four cycles of equal magnitude. (Prediction II is just slightly unconservative.) The same conclusion is arrived at when considering all three Figures 19, 20, and 21. The accuracy of the predictions is hampered by the material variability. Therefore, a representation of the cyclic history by four cycles per car is no less accurate than a more complex sequence and definitely the most conservative. (Note that the predictions in Figures 19 and 20 are still unconservative.) Because of these results, it was decided to omit all small load variations in the service simulation tests, employing four cycles per car.

## 6.  SERVICE SIMULATION

### 6.1.  The Load Spectrum

Actual service-load spectra were obtained from a parallel program on wheel-rail load measurements.[10] Cumulative probability curves are given in Figure 22 for four different railroads, denoted as I, II, III, and IV. These were preliminary curves, since no others were available at the time. The spectra are peak counts of measured load histories. They show the probability that a certain wheel load is exceeded. As an example, for the Spectrum IV, there is a probability of 30 percent that a wheel load exceeds 17 kips. A combination of Spectra I and II was used as a basis for the service simulation tests. For this purpose, a normal load exceedance diagram for 1 million gross tons (1 MGT) of traffic was generated in the following way.

For estimating purposes, 3700 axle passes (peak load occurrences) per day represent an annual traffic of about 20 MGT. This means that 365 x 3700/20 = 67,000 axles represent 1 MGT. It was assumed that half the traffic was based on Spectrum I and half was based on Spectrum II, which is 33,500 axles each.

Table 5 lists a series of load levels and the probability that each level is exceeded for each of the two spectra. This information can be extracted from Figure 22. From these probabilities, the number of axles (total 33,500) which will exceed a given load level can be calculated. Adding these numbers for the two spectra gives the total number of exceedances for 1 MGT or 67,000 axles (Table 5). This results in the exceedance diagram for 1 MGT shown in Figure 23.

## 6.2. The Simulated Service History

The load exceedance diagram still has to be converted into a stress exceedance diagram. This will be discussed in a later section. At this point, it is sufficient to note that the stresses (stress ranges) will be proportional to the loads. A 60,000-pound wheel load was assumed to result in a stress range of 8.44 ksi. Thus with 1 kip wheel load resulting in a stress range of 0.14 ksi, the load exceedance spectrum can be converted into the stress exceedance diagram of Figure 24.

For the purpose of analysis and tests, it is necessary to approximate the spectrum by a number of discrete levels. It has been shown for aircraft load histories[11] that 8 to 12 discrete levels are generally adequate. A staircase approximation of the selected 12-level stress spectrum is shown in Figure 24. Rather than selecting the levels as a certain fraction of the maximum, they are an automatic result of building the staircase by intersecting the spectrum at selected numbers of exceedances; i.e., 1, 2, 10, 50, 200, etc. The advantage of this procedure will become apparent later.

Without considering the actual values of the stress, the discrete levels will be denoted by 1 through 12. as an example, Level 7 is exceeded 5000 times; Level 6 is exceeded 2000 times. This means that the stress history for 1 MGT should contain 3000 occurrences of Level 7. It should further contain 2 occurrences of Level 1, 8 of Level 2, 40 of Level 3, etc.

Note that the spectrum was clipped at Level 1, at two occurrences per MGT. Higher stress levels may occur; however, they will be rare. One cycle of that level will contribute practically no crack growth as compared to the other 67,000 cycles, Thus, it is impractical to include very high stress levels. (Of course, these high levels cannot be ignored if the

TABLE 5. COMBINED SPECTRA I AND II FOR 1 MGT

| Load Level, kips | Percent of Peaks Exceeding Load Level Spectrum I | Spectrum II | Number of Exceedances on 33,500 Axles I | II | Total Exceedances on 67,000 Axles or 1MGT |
|---|---|---|---|---|---|
| 5 | 99.9 | 87 | 33,500 | 29,145 | 62,645 |
| 6 | 99 | 81 | 33,165 | 27,135 | 60,300 |
| 7.5 | 90 | 72 | 30,150 | 24,120 | 54,270 |
| 11 | 70 | 55 | 23,450 | 18,425 | 41,875 |
| 13.5 | 60 | 50 | 20,100 | 16,750 | 36,850 |
| 16 | 50 | 40 | 16,750 | 13,400 | 28,150 |
| 21.5 | 30 | 29 | 10,050 | 9,715 | 19,765 |
| 25 | 20 | 20 | 6,700 | 6,700 | 13,400 |
| 31.5 | 8 | 10 | 2,680 | 3,350 | 6,030 |
| 36.5 | 2.6 | 5 | 871 | 1,675 | 2,546 |
| 44 | .22 | 1 | 74 | 335 | 409 |
| 51 | .01 | .1 | 3 | 34 | 37 |
| 58 | | .01 | | 3 | 3 |
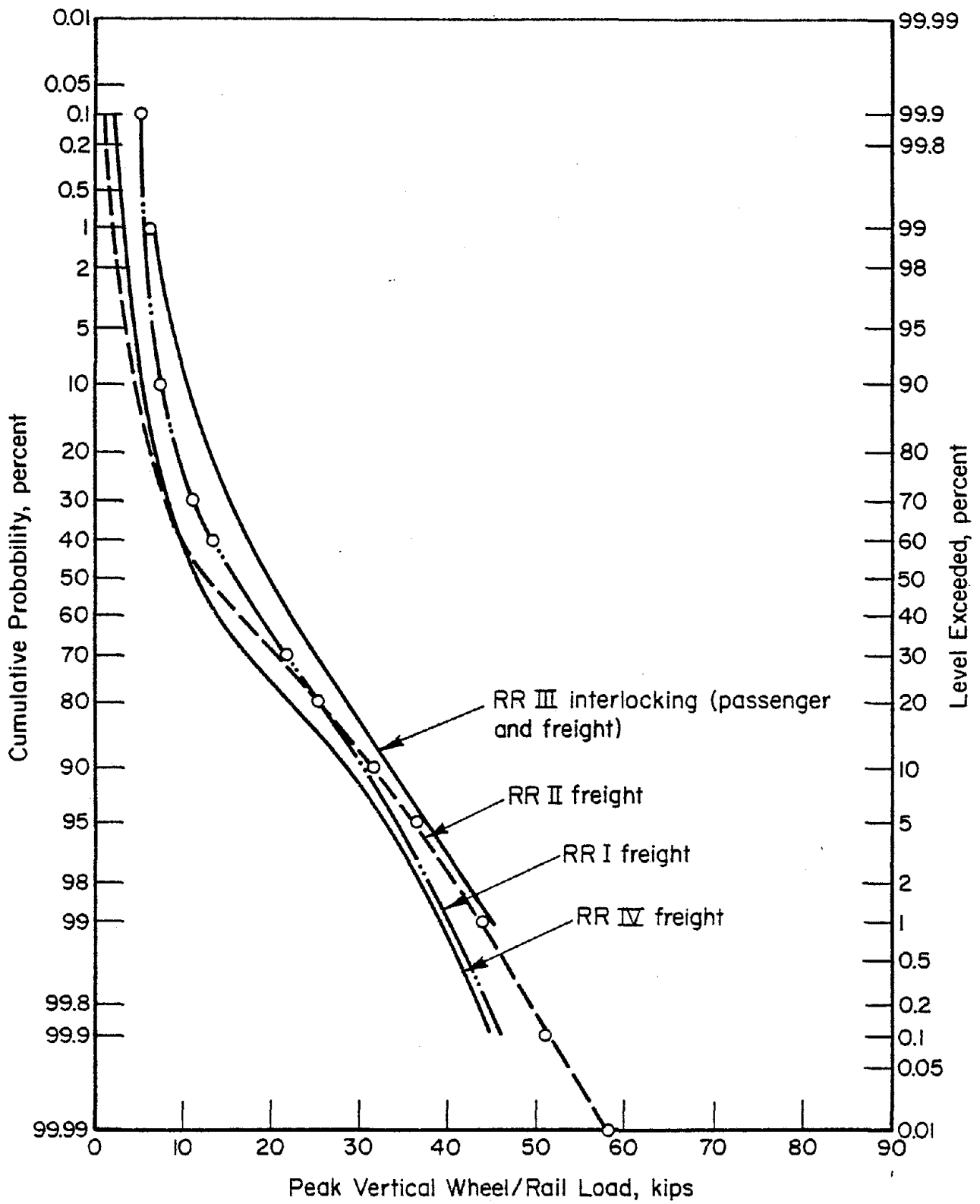
FIGURE 22. LOAD PROBABILITY DIAGRAM

42
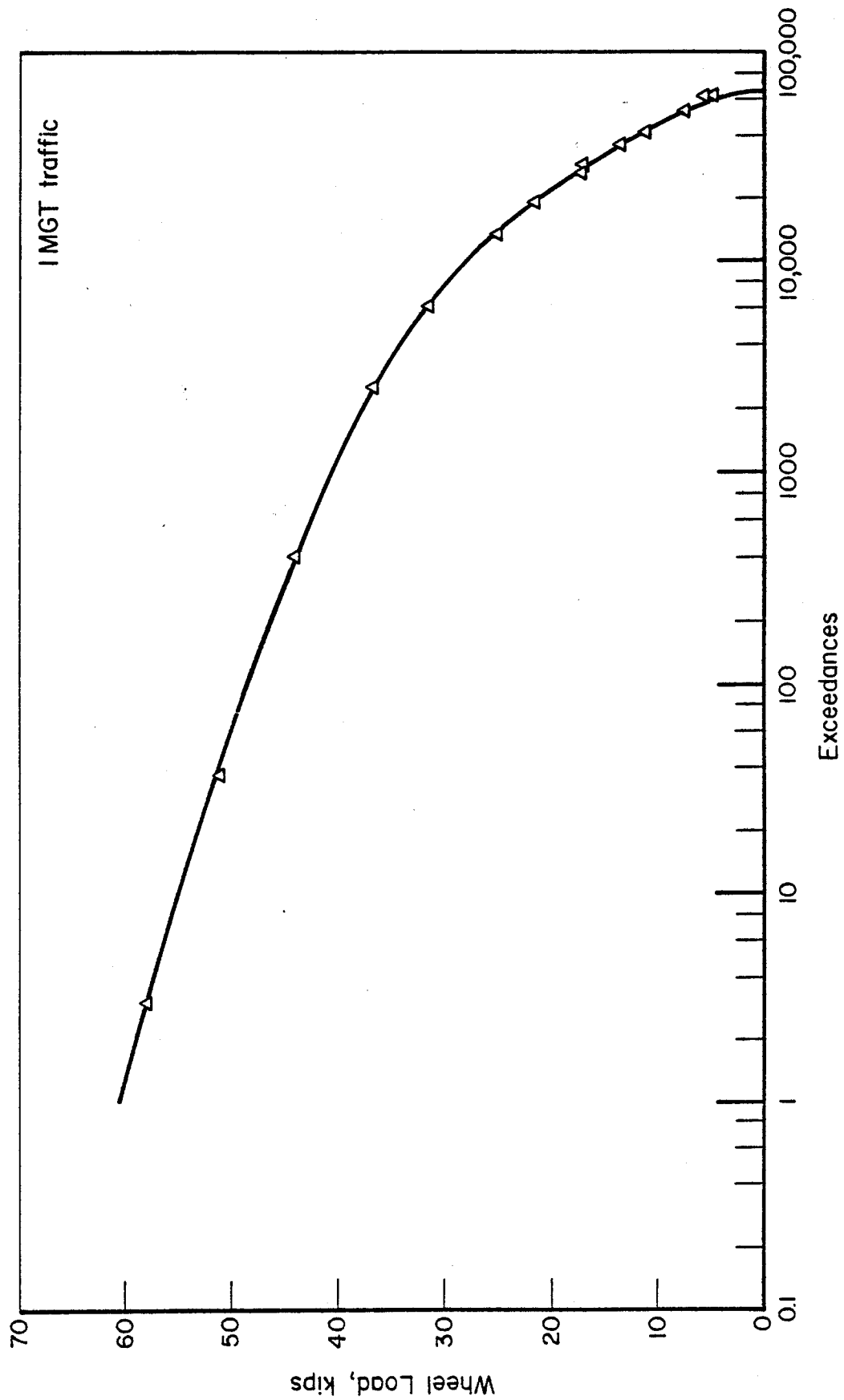
FIGURE 23. LOAD EXCEEDANCE SPECTRUM FOR 1 MGT
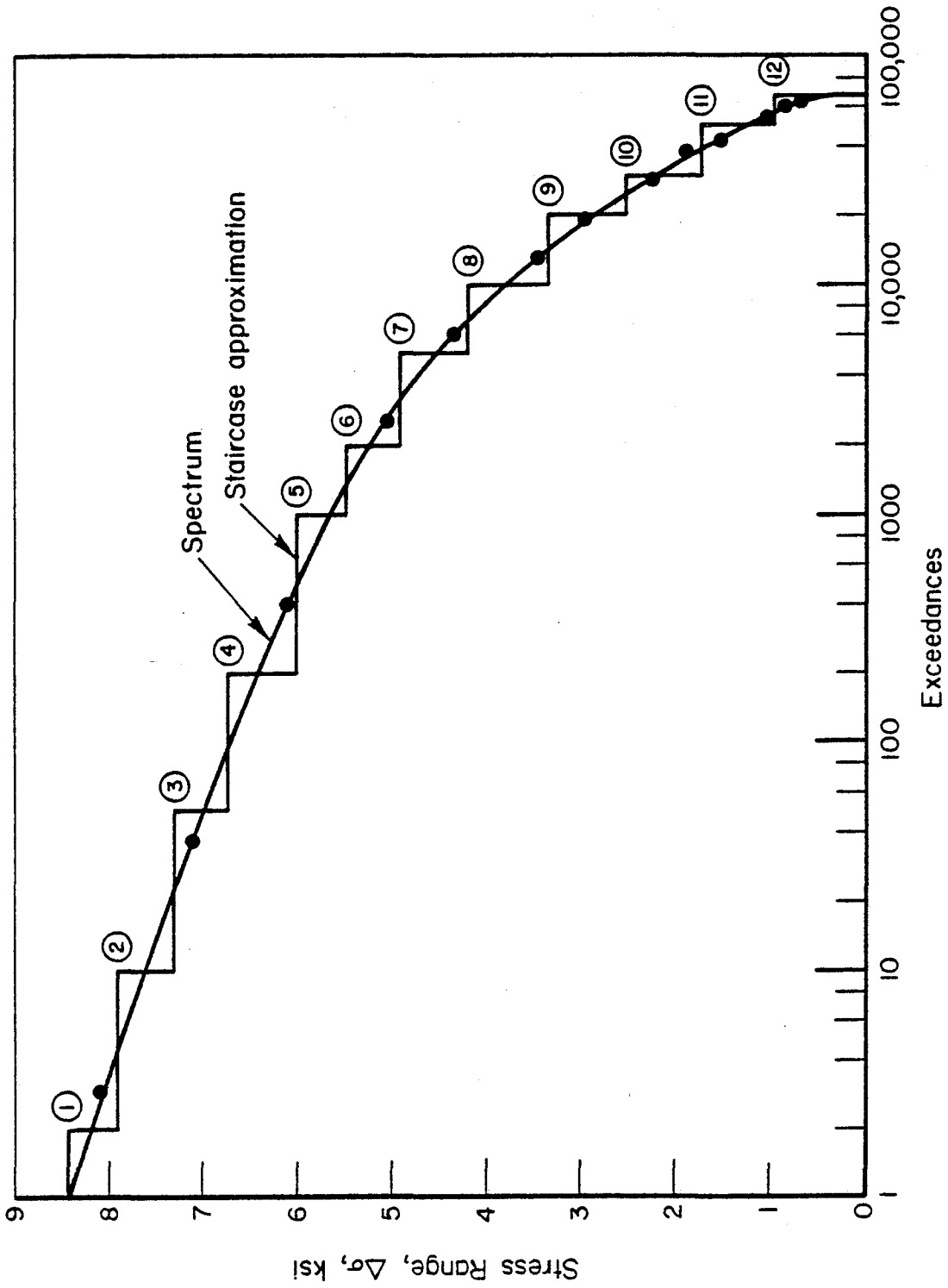
FIGURE 24. STRESS SPECTRUM FOR 1 MGT

probability of fracture is of concern, but they are unimportant for crack growth if there is little retardation.)

The simulated service stress history was developed on the basis of Table 6. Column 1 lists the 12 stress levels. Column 2 gives the stresses associated with these levels, which will be discussed later. The number of exceedances of each level, obtained from Figure 24, is given in Column 4. It follows from a subtraction of each pair of successive numbers in Column 3.

The occurrences represent the number of times a given level had to be applied in 67,000 cycles. It was assumed that on the average a train consists of about 100 cars or 400 axles. Thus, the 67,000 cycles represent approximately 170 trains. It was further assumed that these 170 trains consist of four different types: heavy trains (A), medium-weight trains with empty and loaded cars (B), long medium-weight trains (C), and light trains (D).

The highest load (stress Level 1) occurs only twice in 1 MGT. It is unlikely that both occurrences will be in one train. Thus, a train $A_1$ was designed (extremely heavy) to show one occurrence of Level 1 as indicated in Column 5 of Table 6. Other levels occur more often, but Levels 9 to 12 have relatively low frequencies of occurrence. The exceedances of the various levels for train $A_1$ are given in Column 6, showing that the number of axles totals exactly 400.

Since Level 1 occurs twice in 1 MGT, it follows that there could only be two trains of Type $A_1$. The total number of cycles at each level for two $A_1$ trains is given in Column 7 of table 6 (2 times Column 5). The cycles for the remaining 168 trains are given in Column 8. They follow from subtracting Column 7 from Column 4.

A train $A_2$ was designed, which is a heavy train with only 200 axles. It contains the next highest level (Column 9) and more loads of the lower levels, adding up to 200 cycles in Column 10. Since there remain six occurrences of Level 2, there were to be six $A_2$ trains. These six trains contained the number of cycles shown in Column 11 of Table 6 (6 times Column 9). Thus, the cycles for the remaining 162 trains were as given in Column 12 (Column 8 minus Column 11).

The other trains were established in a similar manner. The heavy $A_3$ train consisting of 400 axles occurred 12 times, which exhausted the remaining

TABLE 6. DEVELOPMENT OF LOAD HISTORY

| ① | ② | ③ | ④ | ⑤ | ⑥ | ⑦ | ⑧ | ⑨ | ⑩ | ⑪ | ⑫ | ⑬ | ⑭ | ⑮ | ⑯ | ⑰ | ⑱ | ⑲ | ⑳ | ㉑ | ㉒ | ㉓ | ㉔ | ㉕ | ㉖ | ㉗ | ㉘ | ㉙ |
|---|---|---|---|---|---|---|---|---|---|---|---|---|---|---|---|---|---|---|---|---|---|---|---|---|---|---|---|---|
| | Stress | | | Train $A_1$ | | | | Train $A_2$ | | | | Train $A_3$ | | | | Train B | | | | Train C | | | | Train D | | | | |
| Level | Range, ksi | Excee-dances | Occur-rences | Occur-rences | Excee-dances | X 2 | Rest | Occur-rences | Excee-dances | X 6 | Rest | Occur-rences | Excee-dances | X 12 | Rest | Occur-rences | Excee-dances | X 120 | Rest | Occur-rences | Excee-dances | X 20X | Rest | Occur-rences | Excee-dances | 10% Rest | | |
| 1 | 8.44 | 2 | 2 | 1 | 1 | 2 | -- | -- | -- | -- | -- | -- | -- | -- | -- | | | | | | | | | | | | | |
| 2 | 7.92 | 10 | 8 | 1 | 2 | 2 | 6 | 1 | 1 | 6 | -- | -- | -- | -- | -- | | | | | | | | | | | | | |
| 3 | 7.34 | 50 | 40 | 5 | 7 | 10 | 30 | 3 | 4 | 18 | 12 | 1 | 1 | 12 | -- | | | | | | | | | | | | | |
| 4 | 6.76 | 200 | 150 | 15 | 22 | 30 | 120 | 10 | 14 | 60 | 60 | 5 | 6 | 60 | -- | | | | | | | | | | | | | |
| 5 | 6.33 | 1,000 | 800 | 40 | 62 | 80 | 720 | 30 | 44 | 180 | 540 | 20 | 26 | 240 | 300 | 2 | 2 | 240 | 60 | 3 | 3 | 60 | -- | -- | -- | | | |
| 6 | 5.53 | 2,000 | 1,000 | 40 | 102 | 80 | 920 | 20 | 64 | 120 | 800 | 25 | 51 | 300 | 500 | 3 | 5 | 360 | 140 | 7 | 10 | 140 | -- | -- | -- | | | |
| 7 | 4.95 | 5,000 | 3,000 | 100 | 202 | 200 | 2,800 | 50 | 114 | 300 | 2,500 | 50 | 101 | 600 | 1,900 | 13 | 18 | 1,560 | 340 | 16 | 26 | 320 | 20 | 2 | 2 | 20 | | |
| 8 | 4.22 | 10,000 | 5,000 | 100 | 302 | 200 | 4,800 | 50 | 164 | 300 | 4,500 | 100 | 201 | 1,200 | 3,300 | 23 | 41 | 2,760 | 540 | 25 | 51 | 500 | 40 | 4 | 6 | 40 | | |
| 9 | 3.38 | 20,000 | 10,000 | 50 | 352 | 100 | 9,900 | 25 | 189 | 150 | 9,750 | 100 | 301 | 1,200 | 8,550 | 50 | 91 | 6,000 | 2,550 | 110 | 161 | 2,000 | 350 | 35 | 41 | 350 | | |
| 10 | 2.53 | 30,000 | 10,000 | 27 | 379 | 54 | 9,946 | 6 | 195 | 36 | 9,910 | 50 | 351 | 600 | 9,310 | 50 | 141 | 6,000 | 3,310 | 150 | 311 | 3,000 | 310 | 31 | 72 | 310 | | |
| 11 | 1.74 | 50,000 | 20,000 | 21 | 400 | 42 | 19,958 | 5 | 200 | 30 | 19,928 | 49 | 400 | 588 | 19,340 | 127 | 268 | 15,240 | 4,100 | 169 | 480 | 3,380 | 720 | 72 | 144 | 720 | | |
| 12 | 0.97 | 67,520 | 17,520 | -- | 400 | -- | 17,520 | -- | 200 | -- | 17,520 | -- | 400 | -- | 17,520 | 132 | 400 | 15,840 | 1,680 | 56 | 536 | 1,120 | 560 | 56 | 200 | 560 | | |

Sequence of 170 Trains (1 MGT)

```
II   B B A₃ B B B A₂ B B C B B D B B
I    B B A₃ B B B A₁ B B C B B D B B
II   B B A₃ B B B A₂ B B C B B D B B
III  B B A₃ B B B A₃ B B C B B D B B
II   B B A₃ B B B A₂ B B C B B D B B
II   B B A₃ B B B A₂ B B C B B D B B
I    B B A₃ B B B A₁ B B C B B D B B
II   B B A₃ B B B A₂ B B C B B D B B
III  B B A₃ B B B A₃ B B C B B D B B
II   B B A₃ B B A₂ B B C B B D B B
```

46

12 occurrences of Level 3. Also, Level 4 was exhausted by train $A_3$. This means that Level 5 was the highest level for the medium-weight trains B and C (400 axles for B and 536 axles for C). The 120 B trains and 20 C trains contained all the remaining occurrences of Levels 5 and 6. Thus, Level 7 was the highest level of the light-axle D train. The remaining occurrences of the other levels are given in Column 24. The remaining 10 trains were D trains, such that all load occurrences were accounted for.

The exceedance spectra for the different trains are shown in Figure 25. The total spectrum is made up by the number of trains indicated in Figure 25. There were 20 A trains, 120 B trains, 20 C trains, and 10 D trains in 1 MGT. Thus, the smallest repetitive block of trains that could be built had to contain 2 A, 12 B, 2 C, and 1 D. A total of 10 such blocks represented 1 MGT. B, C, and D were always of the same type in each block, but A appeared in three different forms, namely $A_1$, $A_2$, and $A_3$. The sequence in a block was selected as

$$BB\ A_3\ BB\ A_{1,2,3}\ BB\ C\ BB\ C\ BB\ D\ BB.$$

The first A in a block was always $A_3$, the second was either $A_1$, $A_2$, or $A_3$. This resulted in three different blocks denoted as Blocks I, II, and III. There remained two $A_3$ (10 were already accounted for), six $A_2$, and two $A_1$, which meant that the 10 blocks should consist of two blocks I, two blocks III, and six blocks II. The following sequence of 10 blocks totaling 170 trains and representing 1 MGT of traffic were selected and repeated during the experiments.

$$II,\ I,\ II,\ III,\ II,\ II,\ I,\ II,\ III,\ II.$$

The total block of 170 trains is shown at the bottom of Table 6.

The sequence of the stress levels in each train remains to be defined. In order to determine the effect of sequencing, two cases were considered in the experimental program. In some experiments, the cycles for the wheel loads of each train were assumed to occur in a high-low order. This means that the wheel-load sequence for each of the individual trains was as shown in Figure 26. As discussed in Section 5, these load ranges induce downward stress excursions from the residual stress level. Thus, the actual stress sequence for a given sequence of trains was as shown in Figure 27. In other experiments, the cycles of each train were randomized, whereas the

47
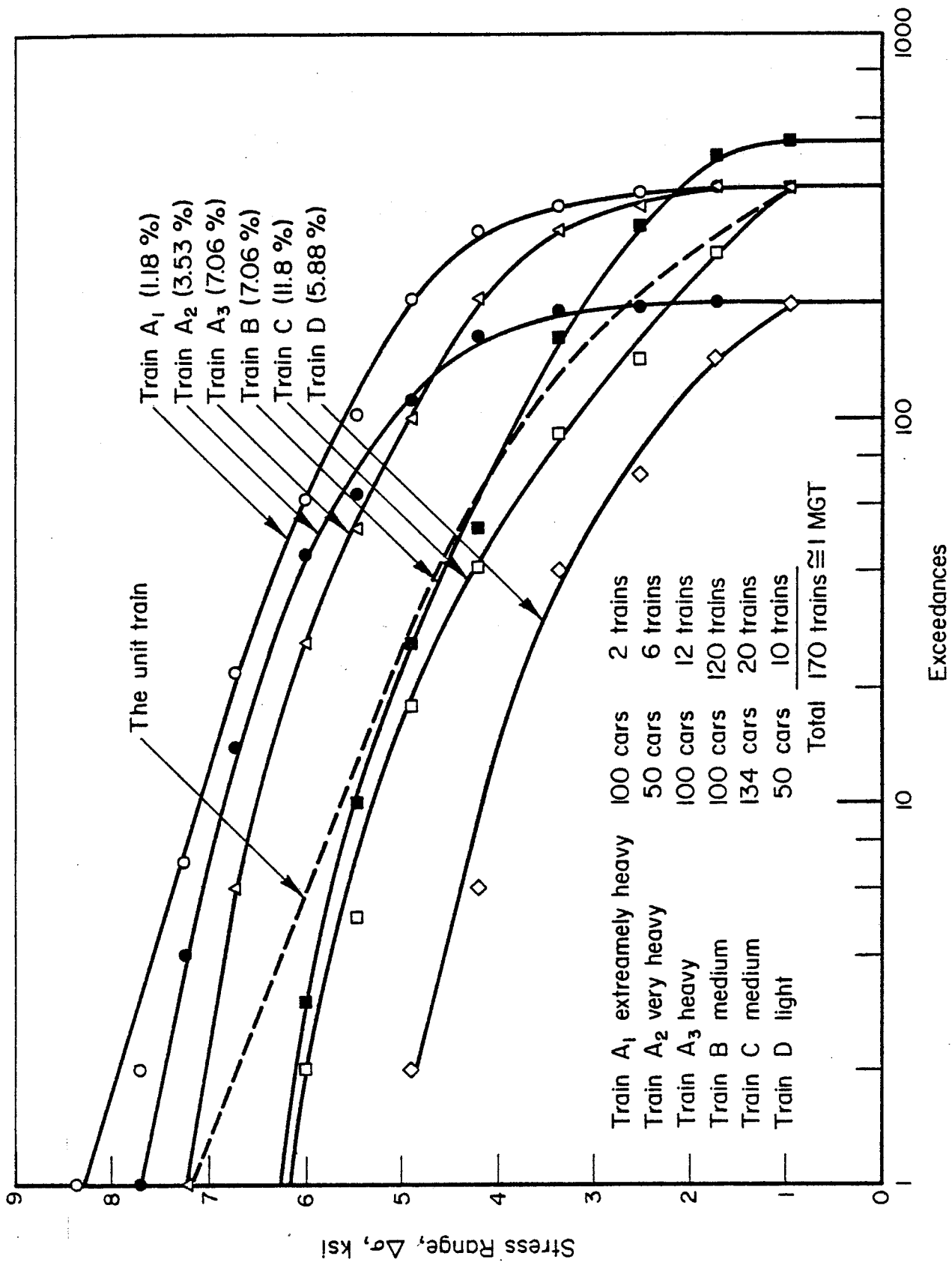
FIGURE 25. SPECTRA FOR SIX TYPES OF TRAINS

48

Each block represents a series of cycles. The length of the block is proportional to the number of cycles in the block.

Train A₁ (extremely heavy, 100 cars, 1.18 percent)

Train A₂ (very heavy, 50 cars, 3.53 percent)

Train A₃ (heavy, 100 cars, 7.06 percent)

Train B (medium, 100 cars, 7.06 percent)

Train C (medium, 134 cars, 11.8 percent)

Train D (light, 50 cars, 5.88 percent)

Stress Range
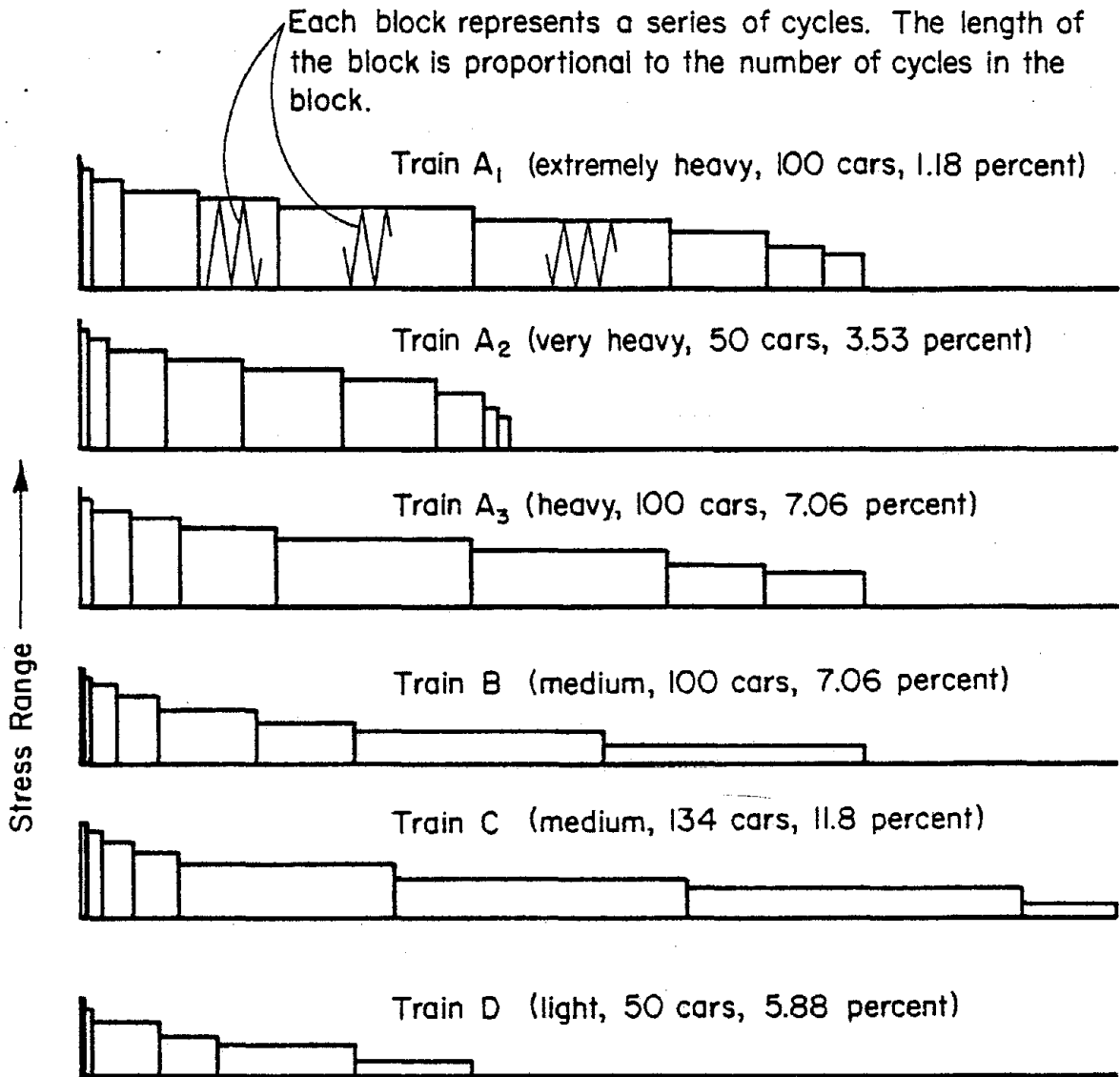
FIGURE 26.  TRAIN COMPOSITIONS FOR MIXED TRAFFIC
SPECTRUM, ALL LOADS INCLUDED

49

FIGURE 27. ACTUAL STRESS HISTORY FOR TRAIN SEQUENCE $A_1$-B-B
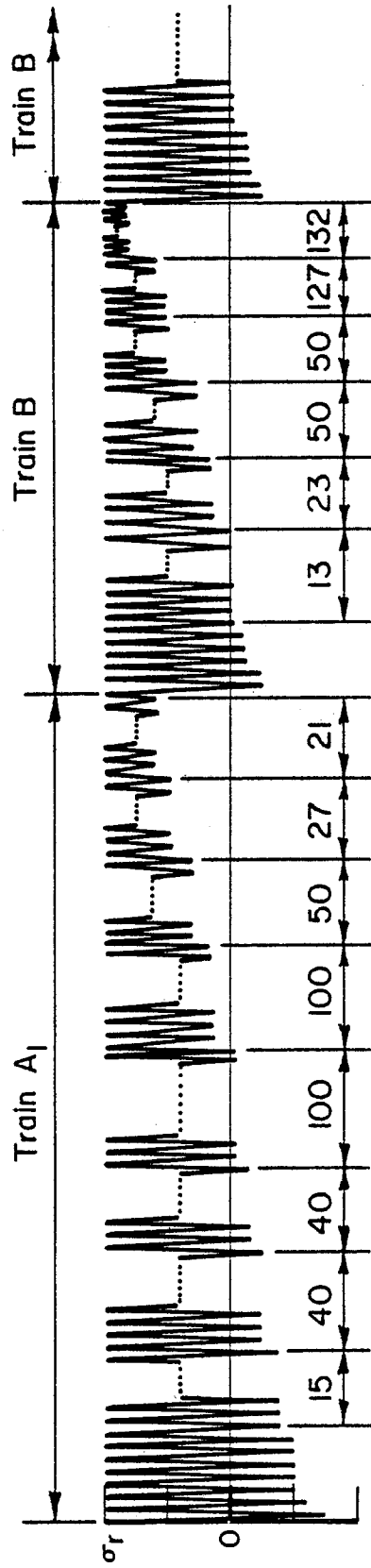
O = zero stress level

$\sigma_r$ = residual stress level

cycles of the lowest level (12) were omitted.

Similar procedures were followed for the two other spectra, separately for III and IV. They were converted into load exceedance diagrams and subsequently stress exceedance diagrams in the same manner as before using a conversion of 1 kip wheel load to 0.14 ksi stress range. The exceedance diagrams are shown in Figure 28, together with the staircase approximation by 12 levels.

The convenience of building the staircase approximation on the basis of exceedances rather than stress levels now becomes apparent. Levels 1 through 12 still have the same number of occurrences - only the stress values have changed. This means that the simulated service history that was developed in Table 6 is still applicable. The only thing that changes is the absolute value of the stress levels. Consequently, all spectra can be treated in the same way in tests as well as in computations. If the same conversion to stresses is used as before (1 kip wheel load corresponds to 0.14 ksi), the three spectra can be compared on the basis of stresses (see Table 7). Note in Table 7 that Level 12 was omitted from Spectra III and IV. Level 12 is only a small stress excursion that contributes little to crack growth. Omission of Level 12 reduces the number of cycles from 67,520 to 50,000 per MGT, which is a considerable savings in testing time.

## 6.3.  Simplified Stress Histories

Efficiency in testing and predictions requires the simplest possible stress history. On the other hand, the stress history should be realistic in the sense that test results and predictions are representative for actual service circumstances.

In order to evaluate possible simplifications, two stress histories were developed. The first was based on a reduced number of eight stress levels, as shown in Figure 29. Stress levels 3 to 10 were combined in pairs to form four new levels, 3 to 6. Table 8 shows the stress history, which is easily obtained from the previous one derived in Table 6.

Since Level 8 (Level 12 of the original stress history) is a very small stress range, it contributes little to crack growth. Therefore, a 7-level case was selected in which the cycles of the lowest level were omitted.

51
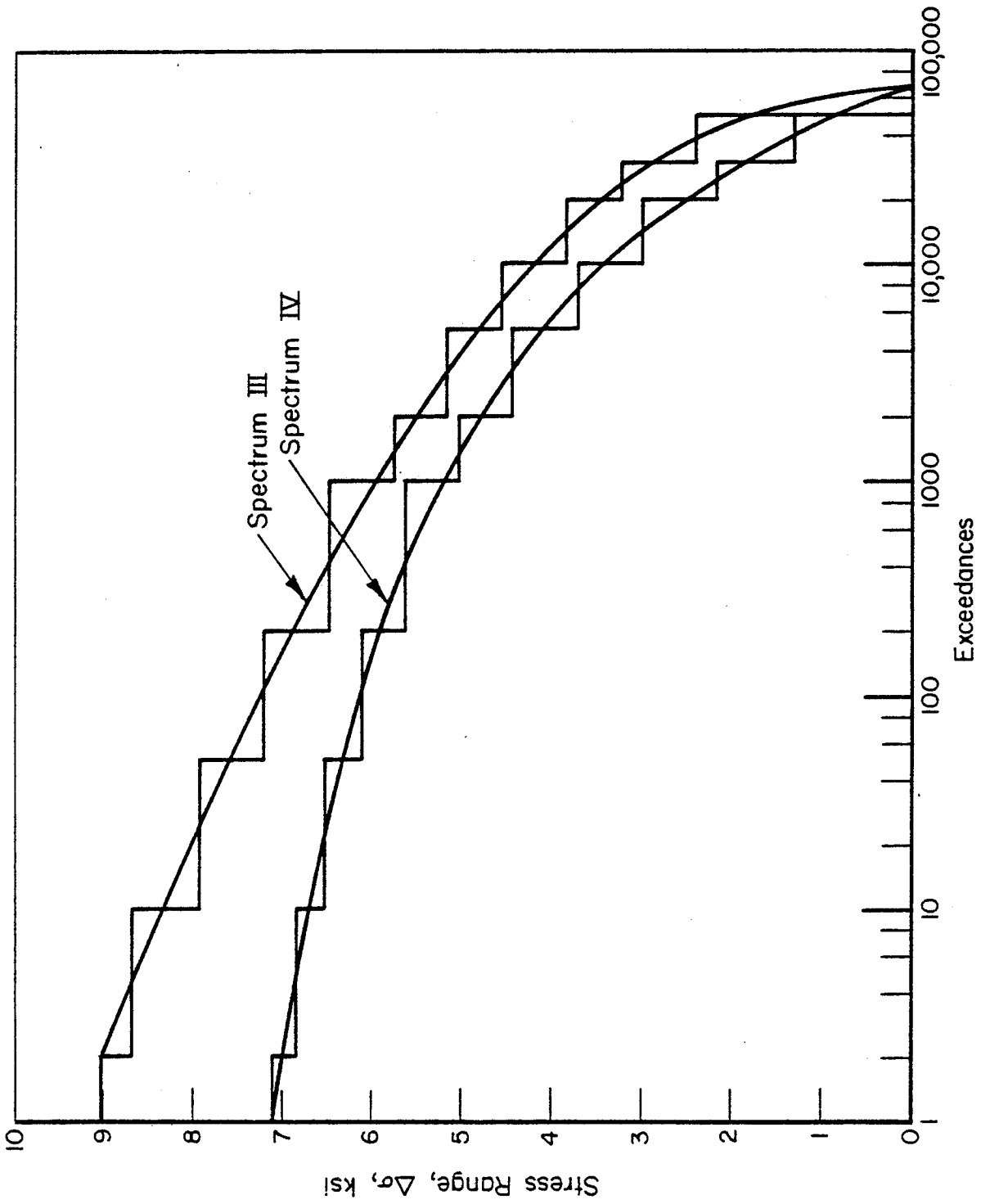
FIGURE 28.  STRESS SPECTRA III AND IV, BOTH FOR 1 MGT

52

TABLE 7. COMPARISON OF THREE TEST SPECTRA

| | | | Stress Range, ksi | | |
|---|---|---|---|---|---|
| Load Level | Exceedances | Occurrences | Spectrum I and II Combined | Spectrum III | Spectrum IV |
| 1 | 2 | 2 | 8.44 | 9.05 | 7.12 |
| 2 | 10 | 8 | 7.92 | 8.69 | 6.88 |
| 3 | 50 | 40 | 7.34 | 7.96 | 6.56 |
| 4 | 200 | 150 | 6.76 | 7.24 | 6.15 |
| 5 | 1,000 | 800 | 6.33 | 6.52 | 5.67 |
| 6 | 2,000 | 1,000 | 5.53 | 5.79 | 5.07 |
| 7 | 5,000 | 3,000 | 4.95 | 5.19 | 4.47 |
| 8 | 10,000 | 5,000 | 4.22 | 4.59 | 3.74 |
| 9 | 20,000 | 10,000 | 3.38 | 3.86 | 3.02 |
| 10 | 30,000 | 10,000 | 2.53 | 3.26 | 2.17 |
| 11 | 50,000 | 20,000 | 1.74 | 2.41 | 1.33 |
| 12 | 67,520 | 17,520 | 0.97 | omitted | |
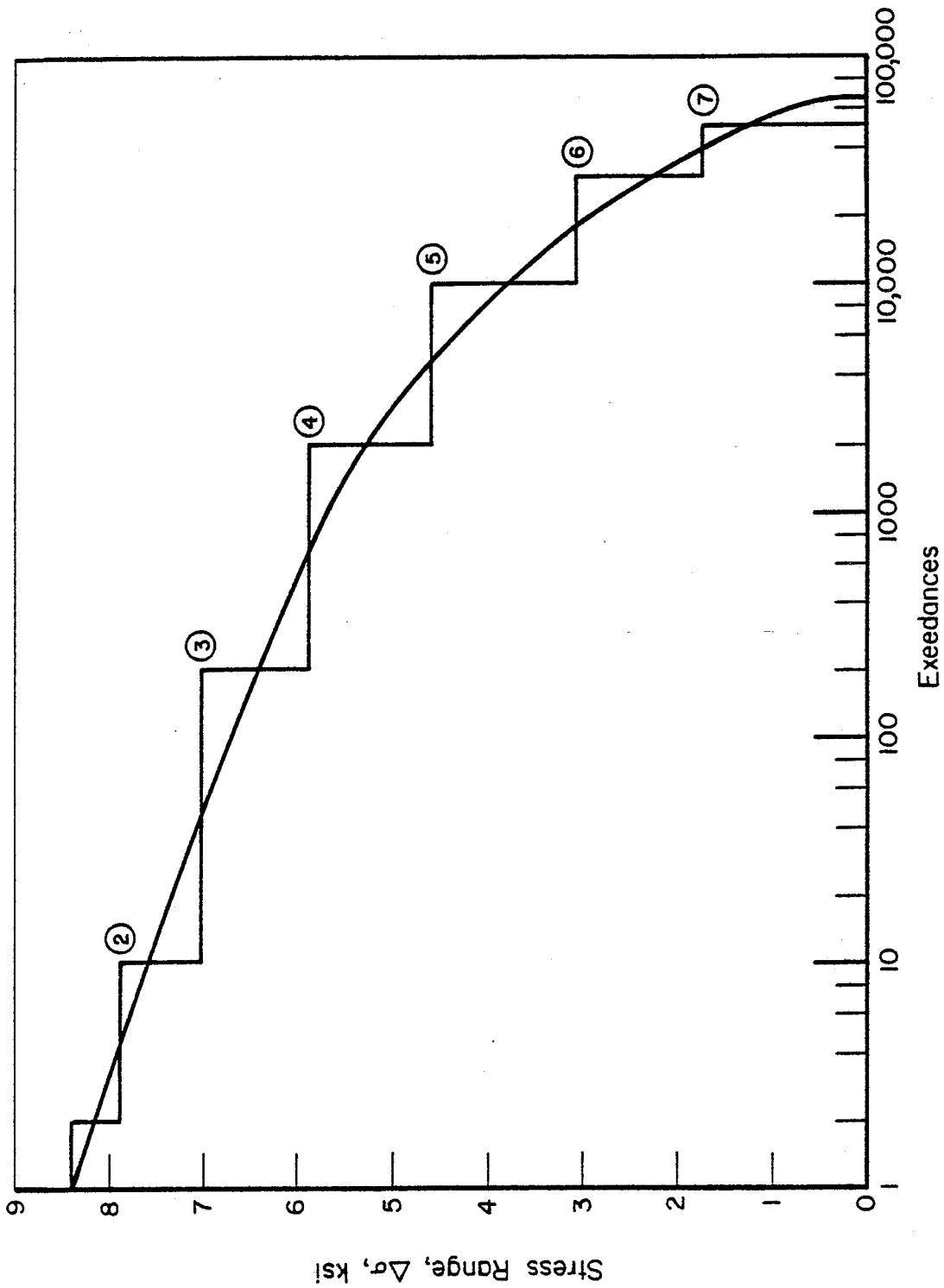
FIGURE 29. SEVEN LEVEL APPROXIMATION OF STRESS SPECTRUM FOR 1 MGT

TABLE 8. SIMPLIFIED HISTORIES WITH 8 AND 7 LEVELS

| Level | Stress Range, ksi | Exceedances | Occurrences | New Level | Exceedances | Occurrences | Stress Range, ksi | Train A$_1$ | Train A$_2$ | Train A$_3$ | Train B | Train C | Train D |
|---|---|---|---|---|---|---|---|---|---|---|---|---|---|
| 1 | 8.44 | 2 | 2 | 1 | 2 | 2 | 8.44 | 1 | -- | -- | -- | -- | -- |
| 2 | 7.92 | 10 | 8 | 2 | 10 | 8 | 7.92 | 1 | 1 | -- | -- | -- | -- |
| 3 | 7.34 | 50 | 40 | 3 | 200 | 190 | 7.05 | 20 | 13 | 6 | -- | -- | -- |
| 4 | 6.76 | 200 | 150 | 4 | 2,000 | 1,800 | 5.93 | 80 | 50 | 45 | 5 | 10 | -- |
| 5 | 6.33 | 1,000 | 800 | 5 | 10,000 | 8,000 | 4.59 | 200 | 100 | 150 | 36 | 41 | 6 |
| 6 | 5.53 | 2,000 | 1,000 | 6 | 30,000 | 20,000 | 3.04 | 77 | 31 | 150 | 100 | 260 | 66 |
| 7 | 4.95 | 5,000 | 3,000 | 7 | 50,000 | 20,000 | 1.84 | 21 | 5 | 49 | 127 | 169 | 72 |
| 8 | 4.22 | 10,000 | 5,000 | 8 | | | | -- | -- | -- | 132 | 56 | 56 |
| 9 | 3.38 | 20,000 | 10,000 | | | | | 400 | 200 | 400 | 400 | 536 | 200 |
| 10 | 2.53 | 30,000 | 10,000 | | | | | | | | | | |
| 11 | 1.74 | 50,000 | 20,000 | | | | | | | | | | |
| 12 | 0.97 | 67,520 | 17,520 | | | | | | | | | | |

55

Obviously, this reduces the number of cycles for 1 MGT from 67,000 to 50,000, which is a reduction of about 25 percent in testing time. The sequences for the individual trains are shown in Figure 30.

Another simplified stress history makes use of a hypothetical unit train. When using a unit train, all 170 trains constituting the 1 MGT are assumed equal and they contain the same load levels and the same number of cycles at each load level. If a unit train can be used, the computation of crack growth for prediction purposes is easier and can be accomplished in a shorter time. With all trains taken equal, the highest level that can be applied is the level that is exceeded 170 times or more in the 1 MGT, because it has to appear in every train. In order to maintain the levels of the original history, the clipping level was taken at level 4, which is exceeded 200 times (Table 9).

As shown in Table 9, the exceedances and the occurrences for the remaining levels are the same as in Table 6. The number of occurrences is simply divided by 170 to give the occurrences of each level for the unit train. This unit train is run 170 times to represent 1 MGT. The lowest level (12) is omitted (truncated), so that a unit train consists of 300 cycles.

In order to account for the clipping at Level 4, the stress range for that level was taken slightly higher than the corresponding levels in previous histories. The adjustment was only minor for two reasons.

1) Clipping results in the omission of only 20 load cycles. It simply means that all levels above 4 are reduced to Level 4. In Table 6 it is shown that Levels 1, 2, and 3 occur 2, 8, and 40 times, respectively; whereas, Level 4 occurs 150 times. In the case of unit trains, Level 4 occurs 170 times.

2) If the residual stress is lower than the stress range associated with Level 4, the levels higher than 4 will only cause higher compressive loads than Level 4. Their effective positive stress range will be about equal to the residual. Small adjustments were also made at the lower levels to compensate for the omission of Level 12.

56
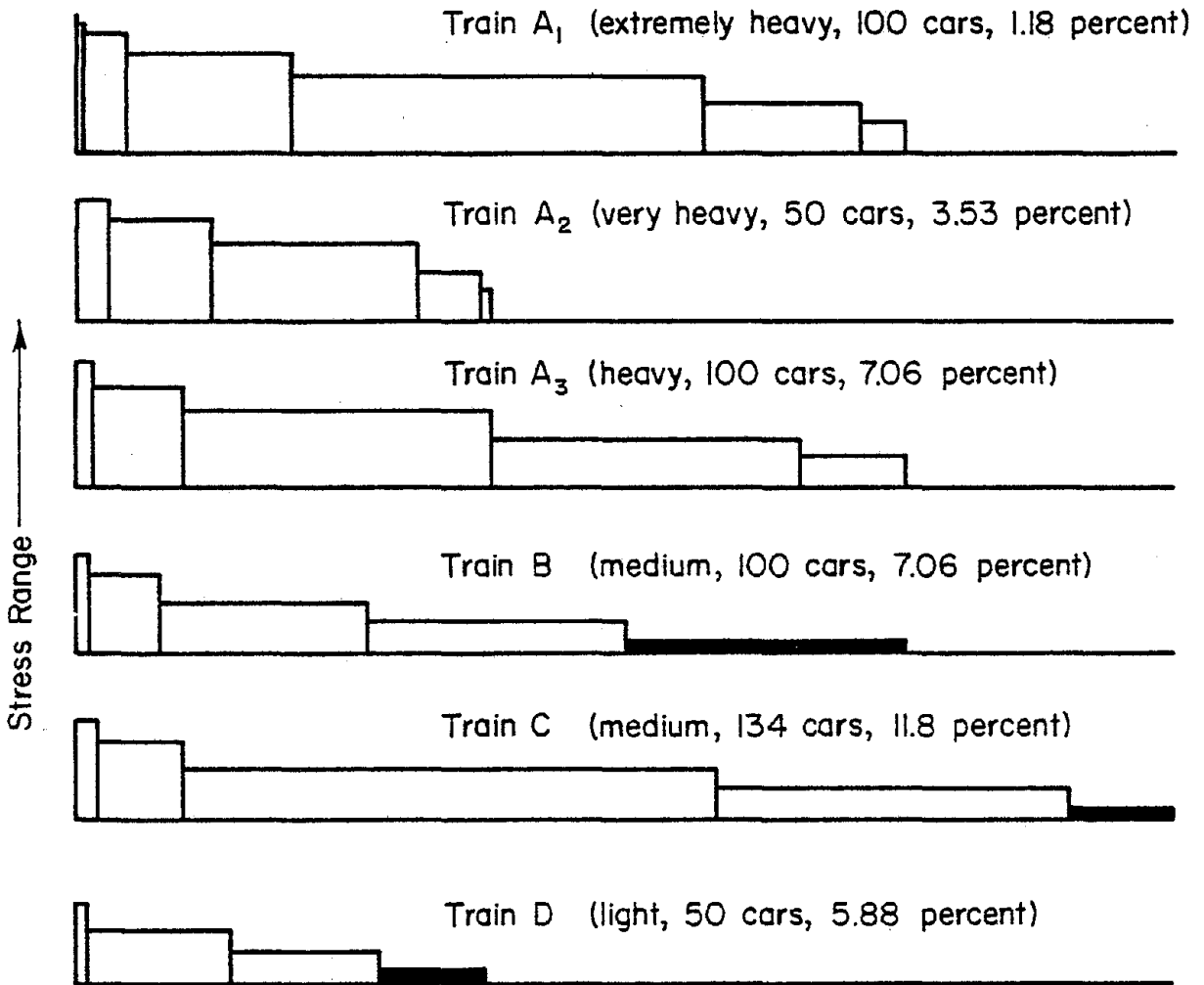
FIGURE 30. TRAIN COMPOSITION FOR MIXED TRAFFIC SPECTRUM, EIGHT LOAD LEVELS

Shaded load will be omitted upon further simplification (seven levels).

TABLE 9. THE UNIT TRAIN; 1 MGT = 170 TRAINS

| | | | | | | | | | Stress Range, ksi | |
| Level | Exceedances | Occurrences | Per Train | Cumulative | Adjusted Cumulative | Adjusted Occurrences | 170 X | Spectrum I and II Combined | Spectrum III | Spectrum IV |
|---|---|---|---|---|---|---|---|---|---|---|
| 4 | 200 | 200 | 1 | 1 | 1 | 1 | 170 | 7.24 | 7.84 | 6.03 |
| 5 | 1,000 | 800 | 5 | 6 | 6 | 5 | 850 | 6.03 | 6.52 | 5.67 |
| 6 | 2,000 | 1,000 | 6 | 12 | 12 | 6 | 1,020 | 5.55 | 5.79 | 5.03 |
| 7 | 5,000 | 3,000 | 18 | 30 | 30 | 18 | 3,060 | 4.95 | 5.19 | 4.46 |
| 8 | 10,000 | 5,000 | 29 | 59 | 60 | 30 | 5,100 | 4.22 | 4.59 | 3.74 |
| 9 | 20,000 | 10,000 | 59 | 118 | 120 | 60 | 10,200 | 3.50 | 3.86 | 3.02 |
| 10 | 30,000 | 10,000 | 59 | 177 | 180 | 60 | 10,200 | 2.53 | 3.26 | 2.17 |
| 11 | 50,000 | 20,000 | 118 | 295 | 300 | 120 | 20,400 | 1.69 | 2.41 | 1.33 |

58

## 6.4. Selection of Stress Levels

In view of the occurrence of compressive stresses, the service simulation tests were run on single-edge-notch specimens of 3-inch width, with a starter crack of approximately 1 inch. The main criterion for the selection of the stress levels was that the total duration of one test should be between 300,000 and 1,000,000 cycles in order to keep testing time at a minimum.

Since the stresses in the actual rail are not directly comparable with the stress in a tension specimen, it was not considered a shortcoming that the stress level was selected more or less arbitrarily with the test duration as the criterion. Since crack growth is uniquely described by the stress-intensity factor, generality of the approach is still warranted.

According to Figure 13, a wheel load of 19 kips produces a $\Delta K$ of approximately 8 ksi$\sqrt{\text{in.}}$ on a stiff roadbed. The single-edge-notch specimen has a starter crack of 1 inch. If this specimen were to have the same $\Delta K$ as the 1-inch crack in the rail, the stress range corresponding to a 19 kip wheel load can be calculated from the K-formulation of Equation (6.1),

$$K = \beta\, \sigma\sqrt{\pi a} = 8, \text{ksi}\sqrt{\text{in.}} \text{ or } \sigma = 2.7 \text{ ksi} \tag{6.1}$$

Thus, the stress conversion would be 2.7/19 = 0.14 ksi per 1000-pound wheel load. This conversion factor was used throughout for all spectra (e.g., compare Figures 23 and 24).

The residual stress in the rail caused a stress intensity of 12 ksi$\sqrt{\text{in.}}$ (Figure 13). Using the same argument as above, the simulated residual stress in the specimen should be 4.05 ksi, which would have to be applied as a maximum tensile stress in the specimen.

These stresses were too low to produce reasonable testing times. Therefore, it was decided to take the residual stress level equal to 6 ksi (this corresponds to a 9000-pound load on the specimen, which was the load during many previous tests).

It should be noted that if the test results for this specimen and these stresses can be predicted by a computational failure model, then the model should also be capable of predicting crack growth under different stresses in the rail, because the procedure is based on stress intensities.

## 6.5. Results of Service Simulation Tests

The test data are tabulated in Tables 10 and 11 and plotted in Figures 31, 32, and 33. Taking into account the material variability, it can be concluded that the various representations of one spectrum yielded practically identical results.

A summary of the test data is presented in Table 12 in terms of the crack growth life to failure. Also given in Table 12 are the crack growth lives to failure observed in the constant amplitude tests[1] for the rail samples used in the service simulation tests.

Consider first the experimental results for the combined spectra I and II. The crack growth lives vary from 11.5 to 19.8 MGT. Hence, the variability is less than a factor of 2, whereas analysis shows all tests nearly equivalent (see Section 7). On the other hand, the constant amplitude results for the same rail samples vary by a factor of 4 from 260 to 1030 kc. Obviously, the scatter in variable amplitude testing is considerably less than in constant amplitude testing, which is a rather common observation.[12]

Yet, the question might arise whether part of the variability of crack growth could be due to residual stresses originally present in the rail and partly remaining in the specimens. Therefore, two specimens were used for residual stress measurements.* Strain gages were mounted to the specimen surface, and cuts were made along side the gages. Subsequently, strain gages were mounted in holes cut by electric discharge machining in order to determine the subsurface residual stresses. There appeared to be residual stresses of some magnitude in a thin surface layer due to the machining operation. However, subsurface residual stresses were only of the order of 1 to 2 ksi, so that it seems unlikely that the scatter in crack growth behavior was caused entirely by residual stress.

Keeping in mind the natural material variability, the various test cases can indeed be considered equivalent from a technical point of view. A direct comparison for individual samples shows

    a)   7-level loading equivalent to unit trains (14 and 16
           MGT for sample 010 and spectra I and II)

---

* This work was performed by R. E. Mesloh.

60

TABLE 10. TEST DATA FOR COMBINED SPECTRA I AND II

| Sample 032 (032-1) 12 Levels | | Sample 032 (032-2) 7 Levels | | Sample 010 (010-2) 7 Levels | | Sample 038 (038-1) 8 Levels | | Sample 038 (038-2) Random | | Sample 014 (014-1) 8 Levels | | Sample 014 (014-2) Random | |
|---|---|---|---|---|---|---|---|---|---|---|---|---|---|
| a, in. | N, MGT | a, in. | N, MGT | a, in. | N, MGT | a, in. | N, MGT | a, in. | N, MGT | a, in. | N, MGT | a, in. | N, MGT |
| 1.07 | 0 | 1.07 | 0 | 1.07 | 0 | 1.07 | 0 | 1.07 | 0 | 1.07 | 0 | 1.07 | 0 |
| 1.073 | 0.1 | 1.207 | 3.5 | 1.087 | 0.8 | 1.074 | 0.2 | 1.123 | 1.9 | 1.116 | 2.6 | 1.115 | 4.1 |
| 1.084 | 0.5 | 1.257 | 4.7 | 1.137 | 3.2 | 1.124 | 3.4 | 1.173 | 3.8 | 1.166 | 4.6 | 1.165 | 7.5 |
| 1.105 | 2.5 | 1.307 | 5.9 | 1.187 | 5.3 | 1.174 | 5.6 | 1.223 | 5.3 | 1.216 | 6.5 | 1.216 | 10.0 |
| 1.123 | 4.3 | 1.357 | 6.9 | 1.237 | 6.9 | 1.224 | 7.2 | 1.323 | 7.8 | 1.266 | 8.0 | 1.266 | 12.0 |
| 1.173 | 10.4 | 1.407 | 7.8 | 1.287 | 8.3 | 1.274 | 8.4 | 1.373 | 8.8 | 1.316 | 9.1 | 1.316 | 13.6 |
| 1.223 | 12.4 | 1.157 | 8.6 | 1.337 | 9.4 | 1.324 | 9.3 | 1.423 | 9.6 | 1.366 | 10.0 | 1.365 | 14.8 |
| 1.273 | 13.9 | 1.507 | 9.2 | 1.387 | 10.3 | 1.374 | 10.1 | 1.573 | 11.7 | 1.416 | 10.7 | 1.415 | 15.8 |
| 1.323 | 15.1 | 1.557 | 9.8 | 1.437 | 11.0 | 1.424 | 10.8 | 1.623 | 12.1 | 1.466 | 11.3 | 1.466 | 16.6 |
| 1.373 | 16.2 | 1.607 | 10.2 | 1.487 | 11.6 | 1.474 | 11.4 | 1.673 | 12.4 | 1.516 | 11.7 | 1.516 | 17.2 |
| 1.423 | 17.0 | 1.657 | 10.6 | 1.537 | 12.1 | 1.524 | 11.8 | 1.773 | 12.8 | 1.566 | 12.1 | 1.566 | 17.6 |
| 1.473 | 17.6 | 1.707 | 10.9 | 1.587 | 12.6 | 1.574 | 12.2 | 1.873 | 13.1 | 1.616 | 12.3 | 1.615 | 18.0 |
| 1.523 | 18.2 | 1.757 | 11.2 | 1.637 | 12.9 | 1.624 | 12.5 | 2.03 | 13.3 | 1.666 | 12.6 | 1.665 | 18.4 |
| 1.573 | 18.6 | 1.807 | 11.5 | 1.687 | 13.2 | 1.674 | 12.7 | | | 1.716 | 12.8 | 1.716 | 18.6 |
| 1.623 | 19.0 | 1.857 | 11.5 | 1.737 | 13.4 | 1.724 | 12.9 | | | 1.766 | 12.8 | 1.766 | 18.8 |
| 1.673 | 19.2 | | | 1.787 | 13.6 | 1.774 | 13.0 | | | 1.816 | 12.9 | 1.816 | 18.9 |
| 1.723 | 19.7 | | | 1.837 | 13.8 | 1.824 | 13.1 | | | | | 1.865 | 19.0 |
| 1.773 | 19.8 | | | 1.887 | 14.0 | 1.874 | 13.2 | | | | | 1.915 | 19.1 |
| 1.823 | 19.8 | | | | | 1.924 | 13.2 | | | | | | |

TABLE 11.   TEST DATA FOR SPECTRA III AND IV

| Sample 032 (032-4) Spectrum III Random | | Sample 051 (051-1) Spectrum III Random | | Sample 020 (020-2) Spectrum III Unit Trains | | Sample 014 (014-3) Spectrum IV Random | | Sample 014 (014-4) Spectrum IV Unit Trains | |
|---|---|---|---|---|---|---|---|---|---|
| a, in. | N, MGT | a, in. | N, MGT | a, in. | N, MGT | a, in. | N, MGT | a, in. | N, MGT |
| 1.07 | 0 | 1.07 | 0 | 1.07 | 0 | 1.07 | 0 | 1.07 | 0 |
| 1.077 | 0.3 | 1.214 | 1.6 | 1.115 | 1.3 | 1.021 | 4.8 | 1.208 | 9.3 |
| 1.127 | 2.6 | 1.263 | 2.1 | 1.165 | 2.8 | 1.171 | 8.3 | 1.220 | 10.0 |
| 1.177 | 4.3 | 1.313 | 2.7 | 1.215 | 4.0 | 1.221 | 10.7 | 1.270 | 12.0 |
| 1.236 | 5.7 | 1.364 | 3.1 | 1.265 | 4.9 | 1.271 | 12.7 | 1,320 | 13.5 |
| 1.277 | 6.5 | 1.414 | 3.5 | 1.315 | 5.7 | 1.321 | 14.5 | 1.370 | 14.7 |
| 1.327 | 7.2 | 1.464 | 3.8 | 1.365 | 6.3 | 1.371 | 15.8 | 1.420 | 15.7 |
| 1.377 | 7.9 | 1.513 | 4.1 | 1.415 | 6.8 | 1.421 | 16.9 | 1.470 | 16.5 |
| 1.427 | 8.3 | 1.563 | 4.2 | 1.565 | 7.2 | 1.471 | 17.8 | 1.520 | 17.2 |
| 1.477 | 8.7 | 1.614 | 4.3 | 1.615 | 7.5 | 1.521 | 18.5 | 1.570 | 17.8 |
| 1.527 | 9.0 | 1.664 | 4.4 | 1.665 | 7.8 | 1.571 | 19.1 | 1.620 | 18.3 |
| 1.577 | 9.3 | | | 1.715 | 8.0 | 1.621 | 19.6 | 1.670 | 18.7 |
| 1.627 | 9.5 | | | 1.765 | 8.1 | 1.671 | 20.1 | 1.720 | 19.0 |
| 1.677 | 9.7 | | | 1.815 | 8.2 | 1.721 | 20.3 | 1.770 | 19.3 |
| 1.727 | 9.9 | | | 1.865 | 8.3 | 1.771 | 20.6 | 1.820 | 19.4 |
| 1.777 | 10.0 | | | 1.950 | 8.3 | 1.821 | 20.8 | 1.870 | 19.5 |
| 1.877 | 10.1 | | | | | 1.871 | 21.0 | 1.920 | 19.6 |
| | | | | | | 1.921 | 21.1 | 1.970 | 19.7 |
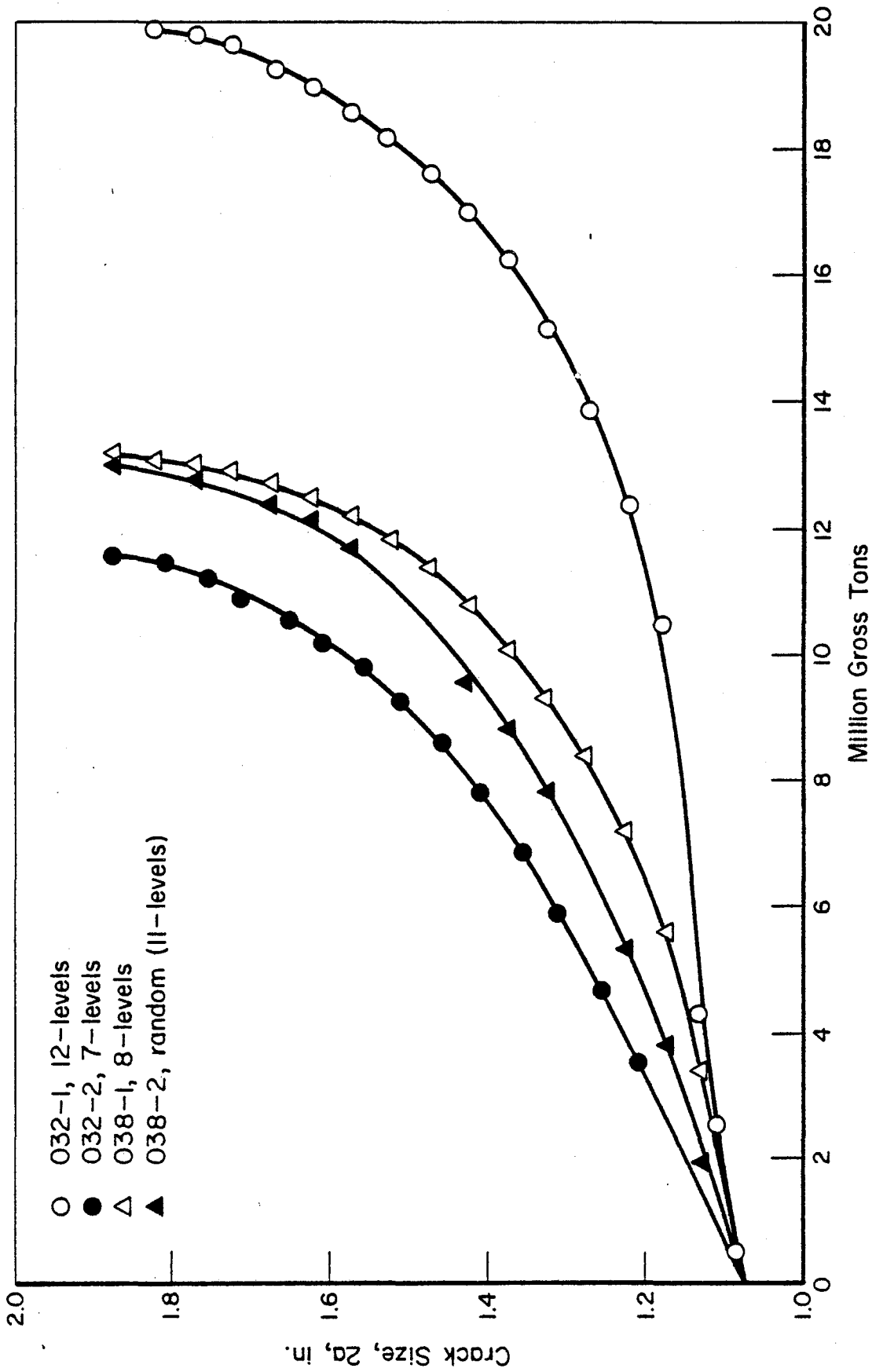
FIGURE 31. TEST DATA FOR COMBINED SPECTRA I AND II

The legend within the figure reads:

○  032-1, 12-levels
●  032-2, 7-levels
△  038-1, 8-levels
▲  038-2, random (11-levels)

Axis labels: Million Gross Tons (horizontal), Crack Size, 2a, in. (vertical)
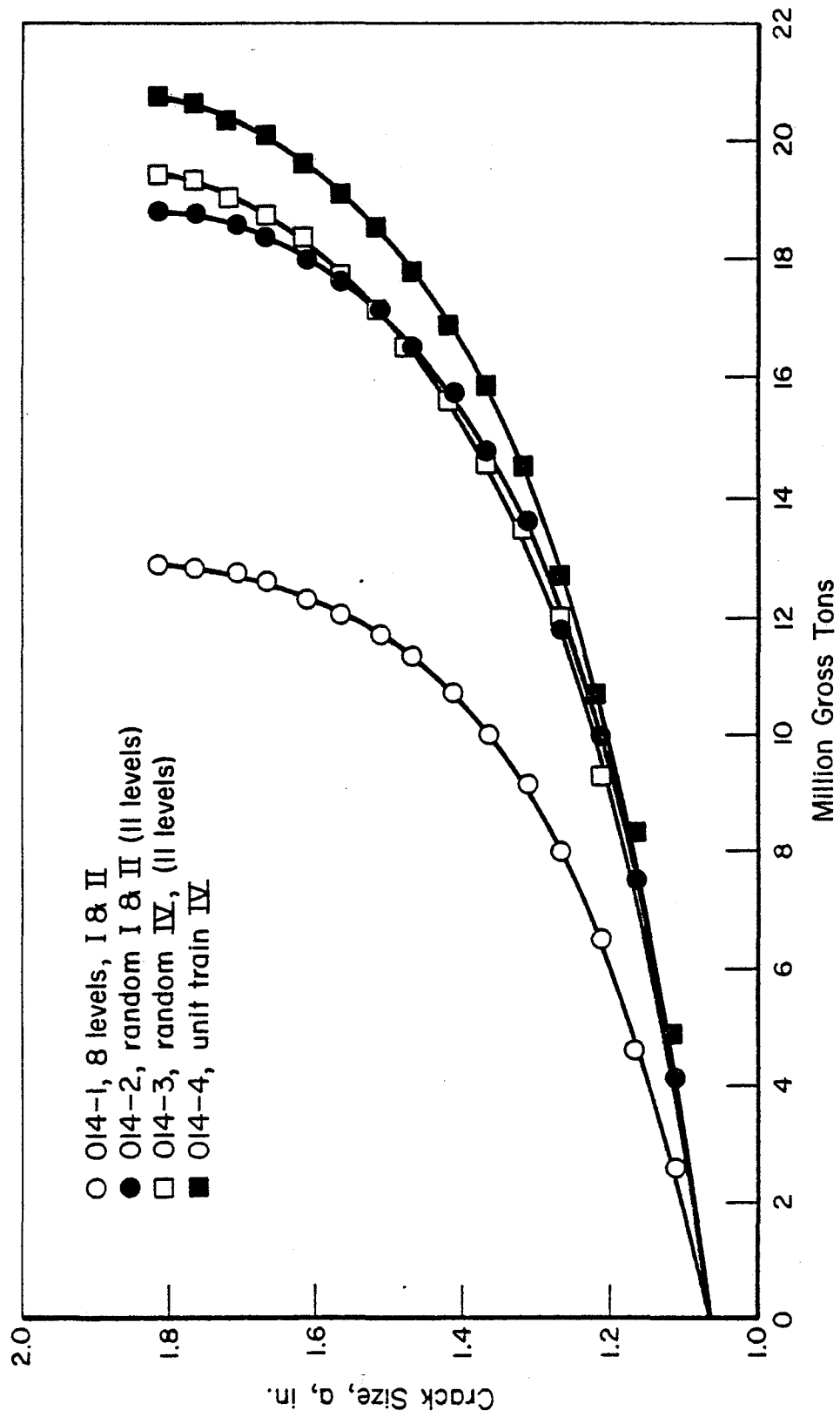
FIGURE 32.   SERVICE SIMULATION TESTS ON SAMPLE 014
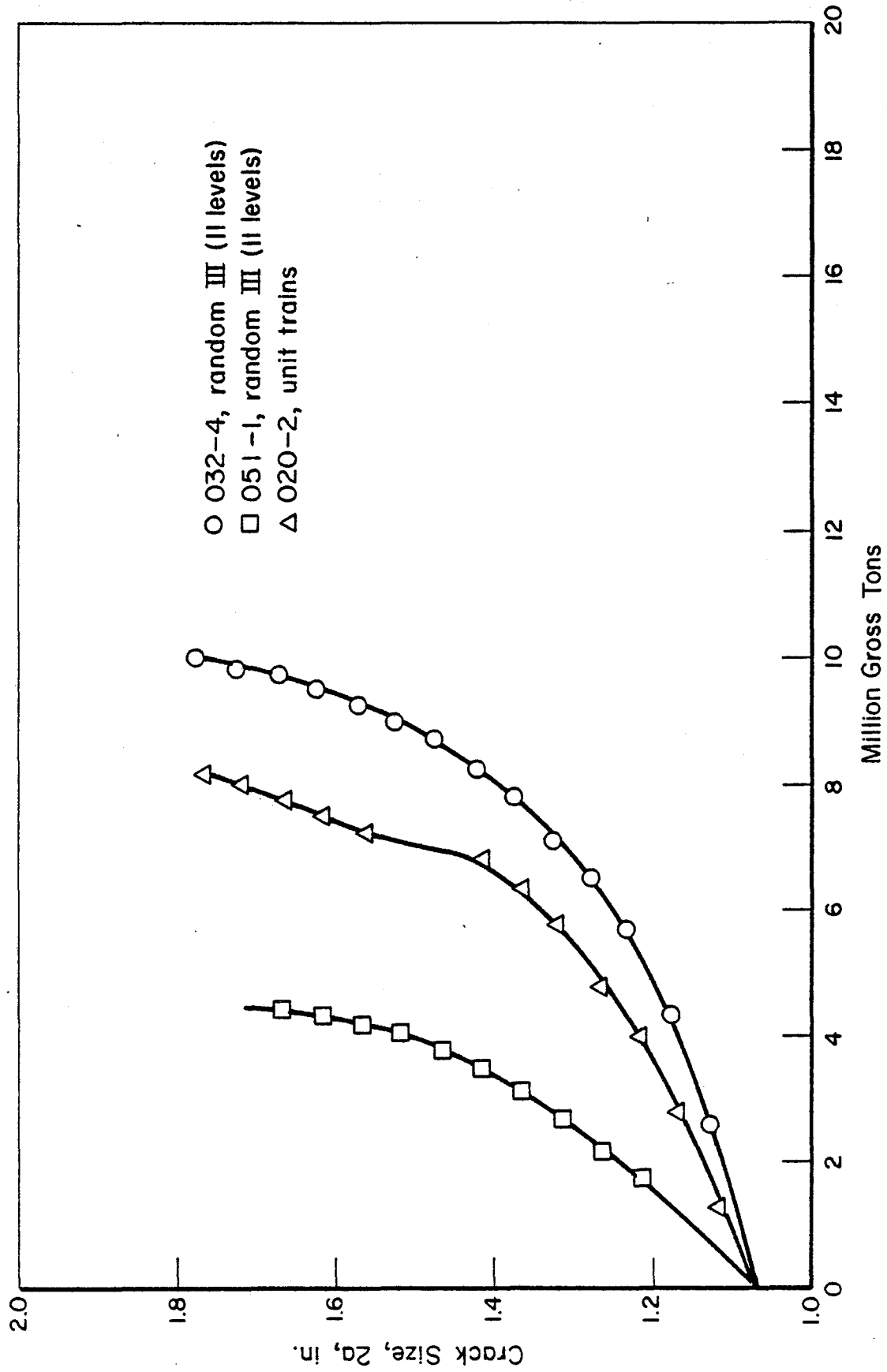
FIGURE 33. TEST DATA FOR SPECTRUM III

The figure shows Crack Size, 2a, in. (vertical axis, 1.0 to 2.0) versus Million Gross Tons (horizontal axis, 0 to 20).

Legend:
O 032-4, random III (II levels)
□ 051-1, random III (II levels)
△ 020-2, unit trains

b) Random loading equivalent to unit trains (21.1 and 19.7 MGT for sample 014 and spectrum IV)

c) The 8-level loading equivalent to the random loading (13.2 and 13.3 MGT for sample 038 and spectra I and II).

Thus, it is concluded that from an experimental point of view, the stress history is of secondary importance if seven or more levels are used. The sequence can either be random, train-by-train, or unit trains. Using this conclusion, it turns out that the average of all tests for the combined spectra I and II is 15 MGT; whereas, spectrum III averaged 7.6 MGT, and spectrum IV averaged 20.4 MGT. This shows that there is a systematic difference in the damaging effect of the three spectra. The following section will show how these results compare to the predicted behavior.

## 7. THE COMPUTATIONAL RAIL FAILURE MODEL

### 7.1. Crack Growth Retardation Models

A number of crack growth retardation models have been proposed in the literature[13-18]. In principle, all these models attempt to account for load interaction and retardation effects, usually in a semiempirical way. The best known models are the ones by Wheeler[13] and by Willenborg, et al[14]. They assume that crack growth will be retarded as long as the plastic zone due to a current load cycle is completely contained in the larger plastic zone due to a previous overload. The retardation itself is reflected by a retarded crack growth rate, which is lower than the crack growth rate to be expected on the basis of constant amplitude data at the same applied stress intensity.

As an example, consider the Wheeler model. The retarded crack growth rate is given as

$$\left(\frac{da}{dN}\right)_r = C_p \left(\frac{da}{dN}\right)_{linear} = C_p \ f(\Delta K) \quad , \tag{7.1}$$

where $(da/dN)_r$ is the retarded crack growth rate; $(da/dN)_{linear}$ is the constant amplitude crack growth rate; and $f(\Delta K)$ is the usual crack growth function,

e.g., Equation (3.5). The retardation factor, $C_p$, is given as

$$C_p = \left(\frac{r_{pi}}{a_o + r_{po} - a_i}\right)^m$$

(7.2)

In this equation, $r_{pi}$ is the current plastic zone and $a_i$ is the current crack size, $r_{po}$ is the plastic zone of a previous overload, and $a_o$ is the crack size at the occurrence of the overload. The exponent m has to be determined empirically.

The crack growth calculation is usually carried out as a cycle-by-cycle integration. Equation (7.2) is evaluated for each cycle and $(da/dN)_r$ is determined using Equation (7.1). The crack extension (da) is then added to the current crack size and so on. The computation of one crack growth curve may take between 1 and 30 minutes of computer time.

As shown in Sections 4 and 5, retardation does not play a significant role in the case of rail steels. Moreover, the retardation models available would not be able to handle retardation effects for cases with variable minimum load only, as considered here. However, the intention of this brief discussion is to evaluate the accuracy of predictions that can be obtained with these models.

The accuracy of the Willenborg model was considered by Engle and Rudd[19] using a limited number of variable amplitude crack growth results. The results turned out to be generally within a factor of 2. More elaborate accuracy checks were made by Broek and Smith[11] and by Schütz[20]. As an example, Figure 34 gives a comparison of one set of test data with curves predicted by different models and different sets of constant amplitude data.

Although the accuracy of most predictions in Figure 34 is very poor, much better results can be obtained if the retardation model is empirically adjusted. In this respect, the Willenborg model is the least versatile, since it contains no adjustable constants. If the Wheeler model is adjusted by determining the best value for m in Equation (7.2) for a set of variable amplitude data, the results for other predictions may come as close as within about 30 percent. This is shown[11] in Figure 35 which is a histogram of the ratio of predicted crack growth life and the crack growth life obtained in a test. All these cases are for relatively small spectrum variations.
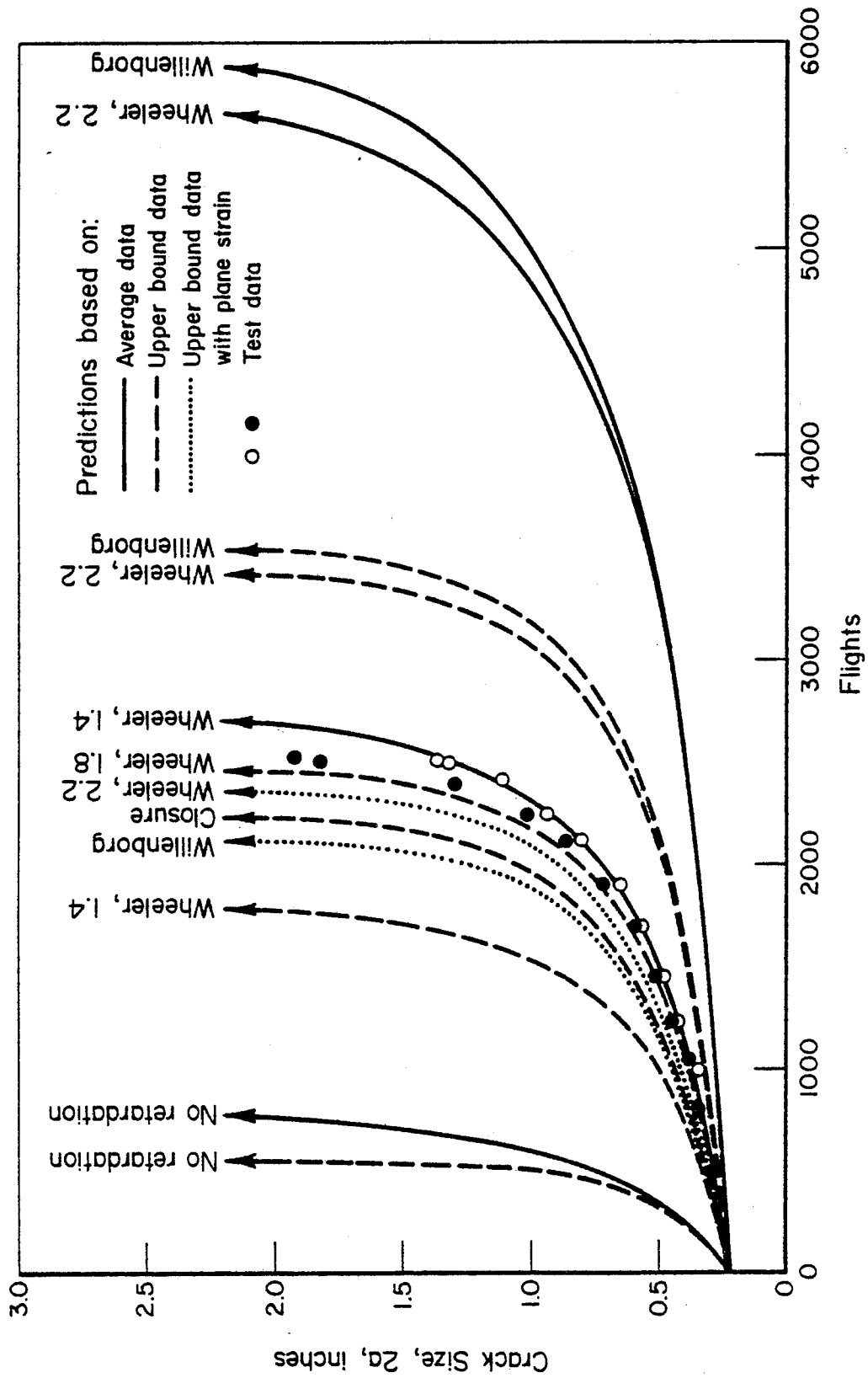
FIGURE 34. VARIOUS PROCEDURES FOR CRACK GROWTH CALCULATION COMPARED FOR 7075-T73 ALUMINUM, FLIGHT-BY-FLIGHT SERVICE SIMULATION USING FIGHTER SPECTRUM(11)
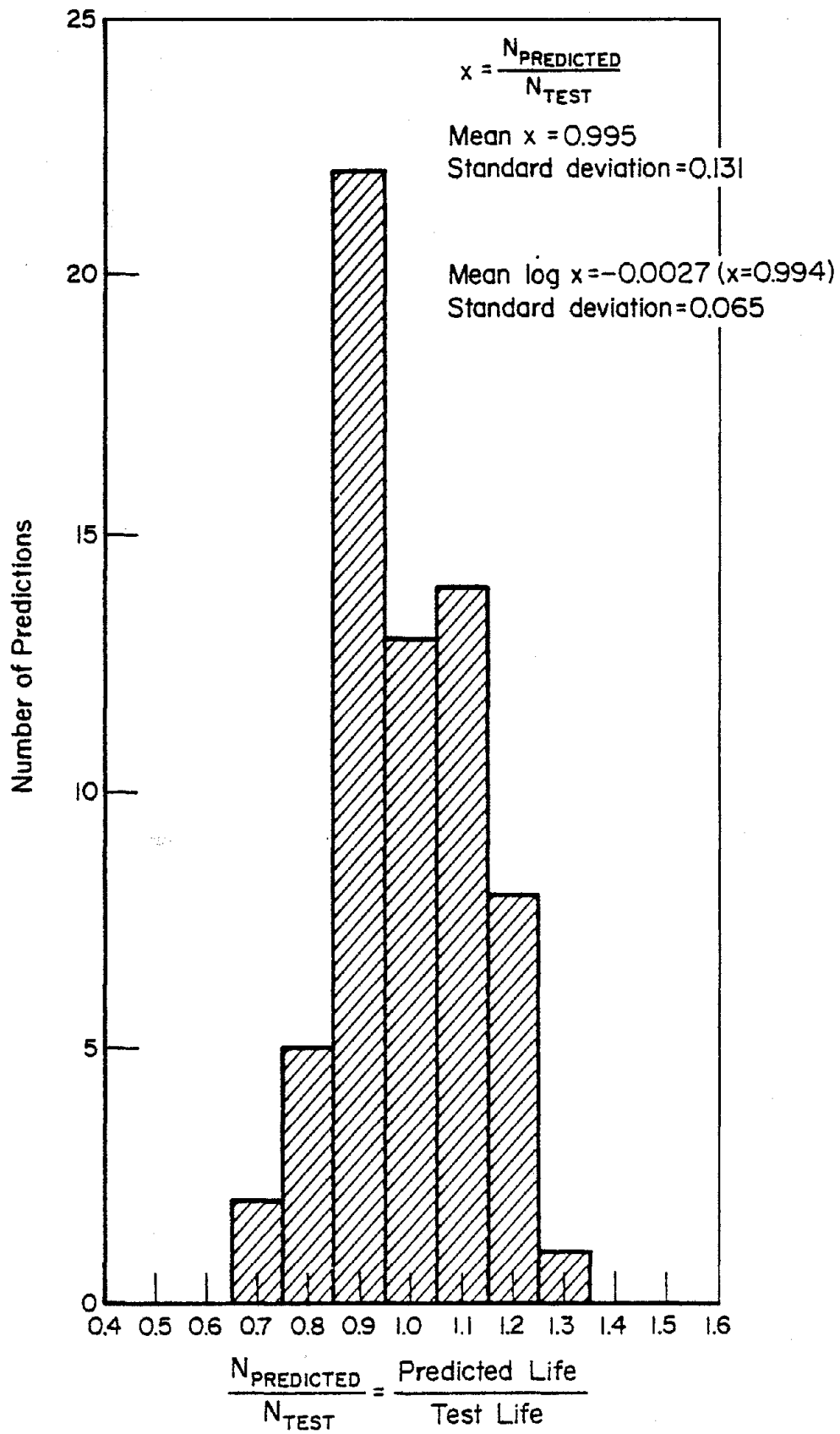
FIGURE 35. HISTOGRAM OF RATIOS BETWEEN BEST WHEELER PREDICTION AND
TEST RESULT FOR FLIGHT-BY-FLIGHT SERVICE SIMULATION USING
FIGHTER SPECTRUM TITANIUM AND ALUMINUM ALLOY

Similar comparisons involving larger spectrum variations were made by Schütz[20]. It turned out that predictions were generally within a factor of 2 of the test data with a few exceptions. Conservative as well as unconservative predictions were obtained in all accuracy checks[11,19,20].

Schütz[20] concluded that none of the models have shown convincing improvements over predictions made without retardation models (linear). He also concluded that there is no escape from realistic tests. Broek and Smith[11] were more optimistic, realizing that there will be inaccuracies in any prediction technique whether it be crack growth or weather. In the first place, the loads to be expected in the future are not known and may be appreciably different from the projections. In the second place, there are inaccuracies in stress analysis. Both may cause appreciable differences between predicted and actual crack growth.

The most important aspect of crack growth prediction is the material variability. Two cracks growing in the same material under exactly the same circumstances may show a factor of 2 difference in growth rates. Obviously, any model will predict the same result for both tests. Thus, if the prediction is exact for one test, it will be off by a factor of 2 for the other. This is not due to a deficiency of the model, but a mere consequence of anomalous material behavior. No matter how sophisticated the model, there can be no absolute accuracy.

If the material variability accounts for a factor of 2 and the predictions are based on average behavior, the predicted life will come within about 50 percent of the actual life in the general case, although some individual result may be predicted more closely. Thus, the predictions have to be made on a statistical basis, which shows the need for a reliability analysis.

It can be concluded that no crack-growth-prediction model can have absolute accuracy. Predictions within about 50 percent of the actual life should be considered satisfactory if material variability accounts for a factor of 2. This conclusion is of importance for the predictions for rail steels in the following.

## 7.2. Crack Growth Predictions

Predictions of the experimental results obtained in this program were made by means of linear integration. Since retardation was no consideration, a cycle-by-cycle integration was not necessary. Therefore, the integration was carried out in steps of 0.5 MGT according to the block diagram of Figure 36. The integration went stepwise through the load levels and occurrences for 0.5 MGT calculating the new crack size after each load level. Crack extension during $N_j$ cycles of level j was simply integrated as $N_j \cdot da/dN$.

The stress-intensity factor was calculated through the use of Equation (3.7) and the crack-growth rate from the rate Equation (3.5). The first predictions made use of the average growth rate equation for LT orientation and room temperature derived in phase II[2],

$$\frac{da}{dN} = 4.27 \times 10^{-9} \ (1-R)^2 \ (K_{max}^2 - K_{th}^2) \ \frac{K_{max}^{1.13}}{K_c - K_{max}} \quad \text{in./cycle} \quad (7.3)$$

with $K_{th} = 13.5$ ksi$\sqrt{\text{in.}}$, and $K_c = 55$ ksi$\sqrt{\text{in.}}$.

The predicted crack growth curves are compared with the test data in Figures 37 through 40. The predictions appear to be virtually insensitive to the spectrum represention: unit trains, 12-level, 11-level (random), 8-level, and 7-level gave almost identical results. Some test data are reproduced very well by the predictions, but others show a poorer fit. As discussed in the foregoing, this is mainly due to material variability which is most apparent from the sets of random data, e.g., for spectra I and II in Figure 38 and for spectrum III in Figure 39.

For subsequent predictions, the constants in Equation (3.5) were derived for the individual rail samples used for the service simulation tests. The values of the constants are given in Table 13. They were determined to give the best possible fit to the constant-amplitude crack growth curves. As shown in Figure 41, the constant-amplitude results are reproduced very well by the equations.

Using these constant-amplitude rate equations, crack growth predictions were made for each of the individual rail samples used in the service simulation tests. The predicted crack growth lives are shown in Table 14. Where comparative test results were available, they are shown between parentheses in the appropriate column of Table 14.

71

TABLE 12.  SUMMARY OF TRAIN-BY-TRAIN TEST DATA

| Rail Sample | Constant Amplitude, kc (Ref. 1) | Spectra I and II | | | | | Spectrum III | | Spectrum IV | |
|---|---|---|---|---|---|---|---|---|---|---|
| | | 7 Level, MGT | 8 Level, MGT | 12 Level, MGT | Random, MGT | Unit Trains, MGT | Random, MGT | Unit Trains, MGT | Random, MGT | Unit Trains, MGT |
| 010 | 260 | 14 | | | | ≈16(a) | | | | |
| 014 | 260 | | 12.9 | | 19.1 | | | | 21.1 | 19.7 |
| 020 | 1,300 | 11.5 | | 19.8 | | | | 8.3 | | |
| 032 | 410 | | 13.2 | | 13.3 | | | | | |
| 038 | 1,030 | | | | | | 10.1 | | | |
| 051 | 1,050 | | | | | | 4.4 | | | |

(a)  Only approximate end result available; intermediate data could not be retrieved due to malfunctioning of computer during automatic crack growth recordings.

TABLE 13.  CONSTANTS FOR EQUATION (3.5) FOR RAIL SAMPLES USED FOR SERVICE SIMULATION TESTS

| Rail Sample | $K_c$, ksi | $K_{th}$, ksi | C | m | Constant Amplitude Life, kc |
|---|---|---|---|---|---|
| 010 | 55 | 12 | $2.22 \times 10^{-7}$ | 1 | 260 |
| 014 | 50 | 13.5 | $2.6 \times 10^{-7}$ | 0.96 | 260 |
| 020 | 60 | 14.5 | $4.61 \times 10^{-11}$ | 3.30 | 1,300 |
| 032 | 50 | 13.5 | $1.25 \times 10^{-8}$ | 1.79 | 410 |
| 038 | 70 | 10 | $1.35 \times 10^{-7}$ | 0.8 | 1,030 |
| 051 | 55 | 13.5 | $1.80 \times 10^{-11}$ | 3.64 | 1,050 |
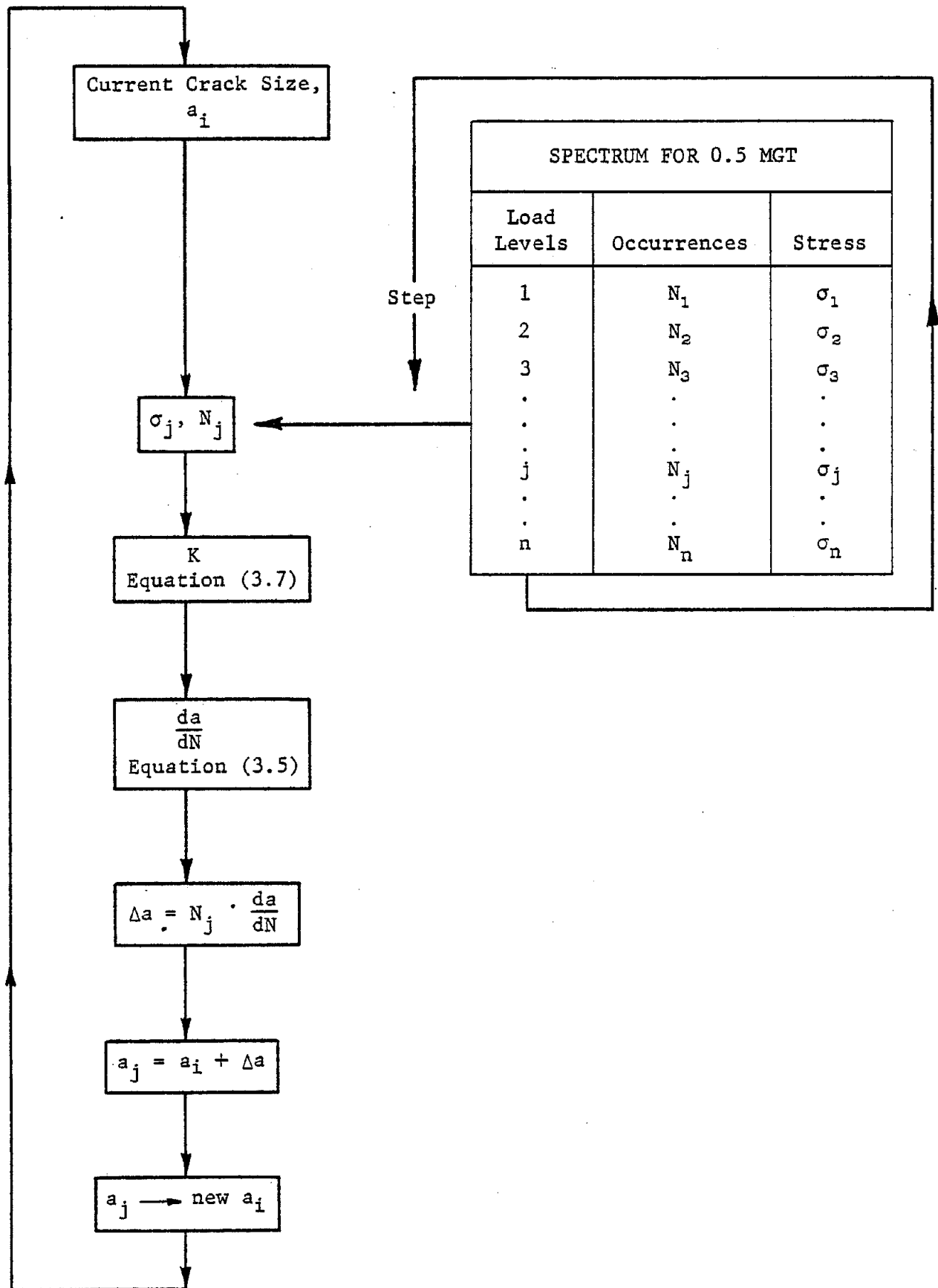
FIGURE 36. BLOCK DIAGRAM FOR CRACK GROWTH INTEGRATION
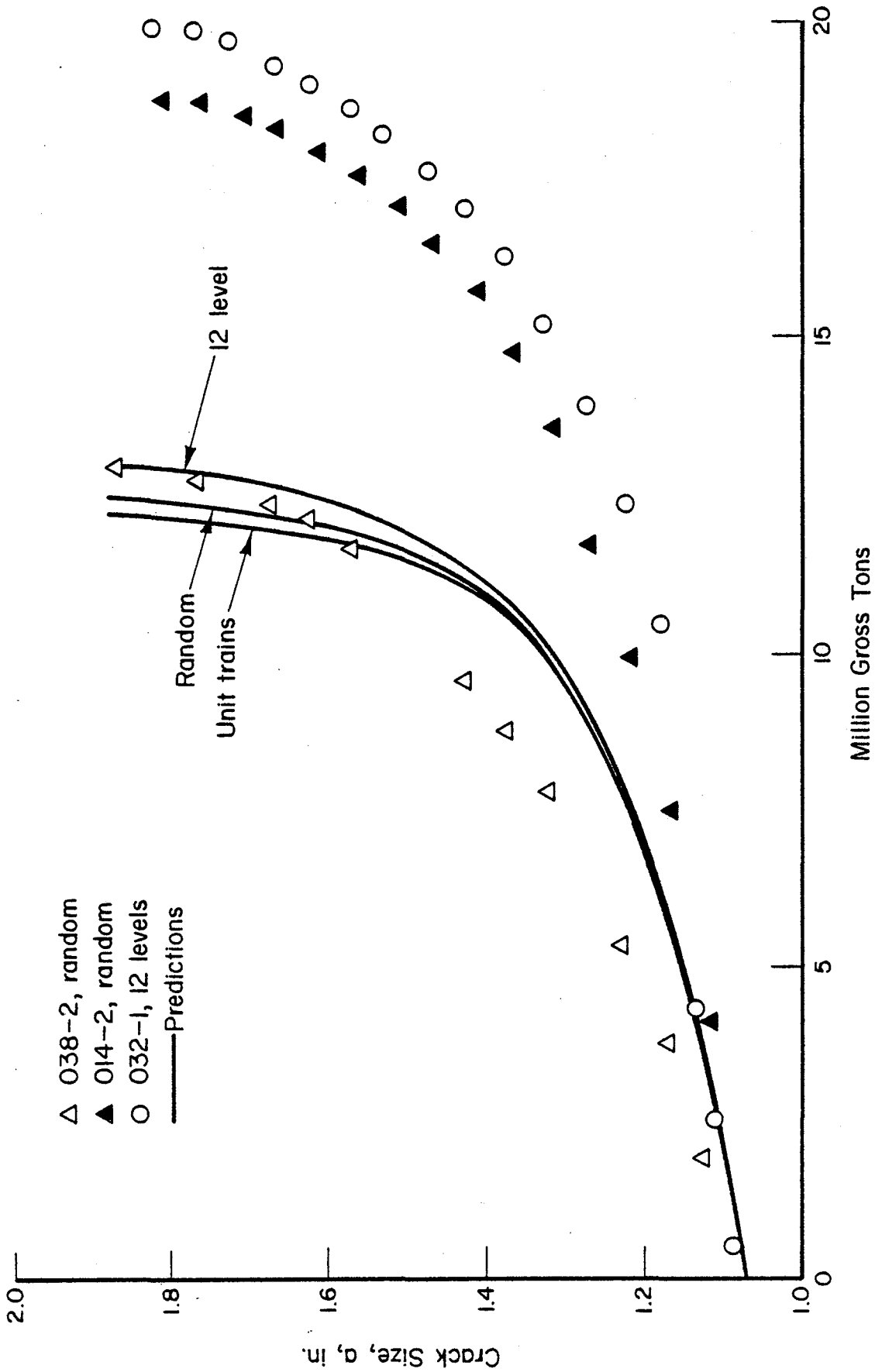
FIGURE 37.  TEST DATA AND PREDICTIONS (CURVES) FOR COMBINED
SPECTRA I AND II; 12 LEVELS AND RANDOM
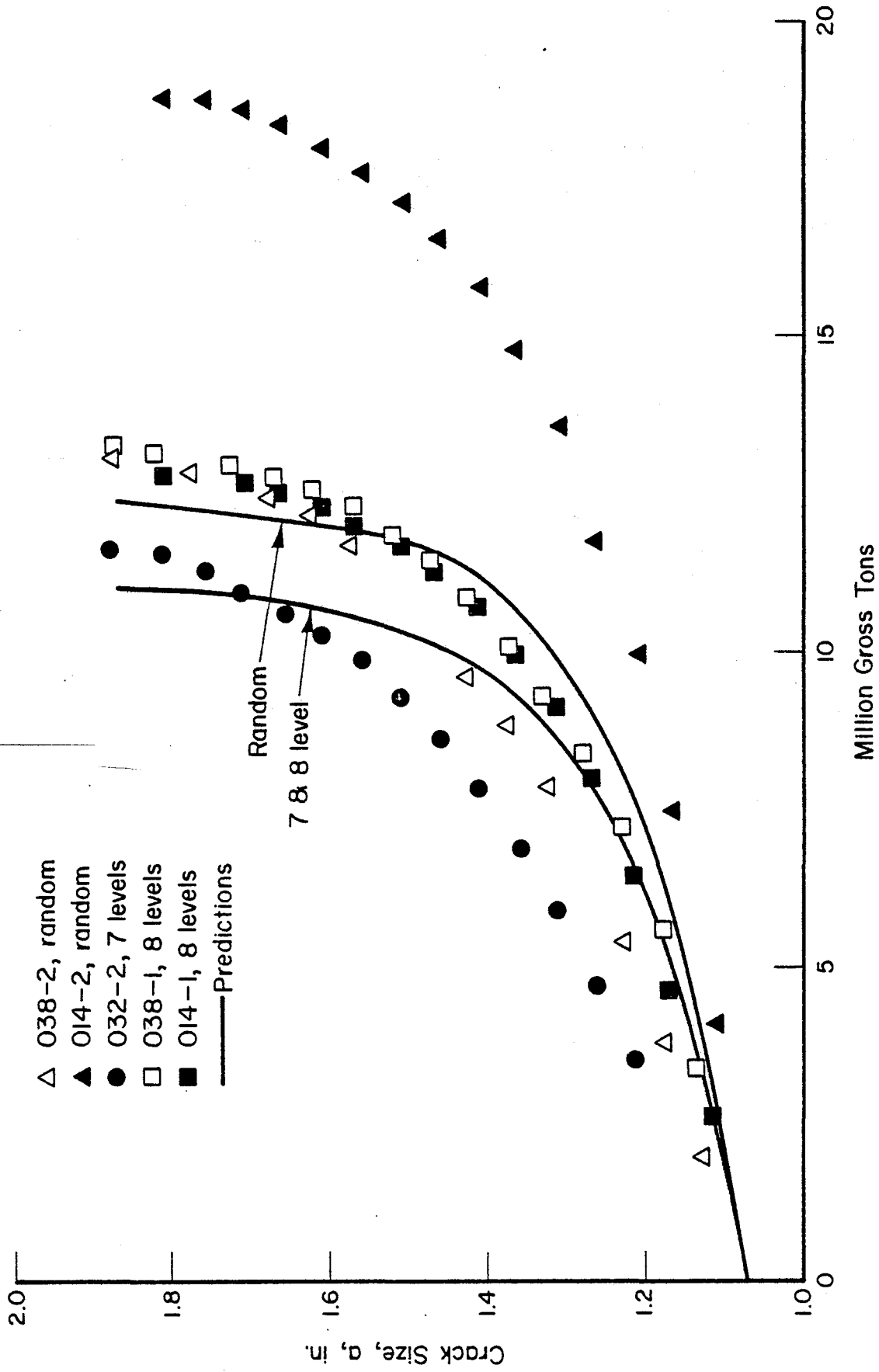
FIGURE 38. TEST DATA AND PREDICTIONS (CURVES) FOR COMBINED SPECTRA I AND II; 7 AND 8 LEVELS AND RANDOM

75
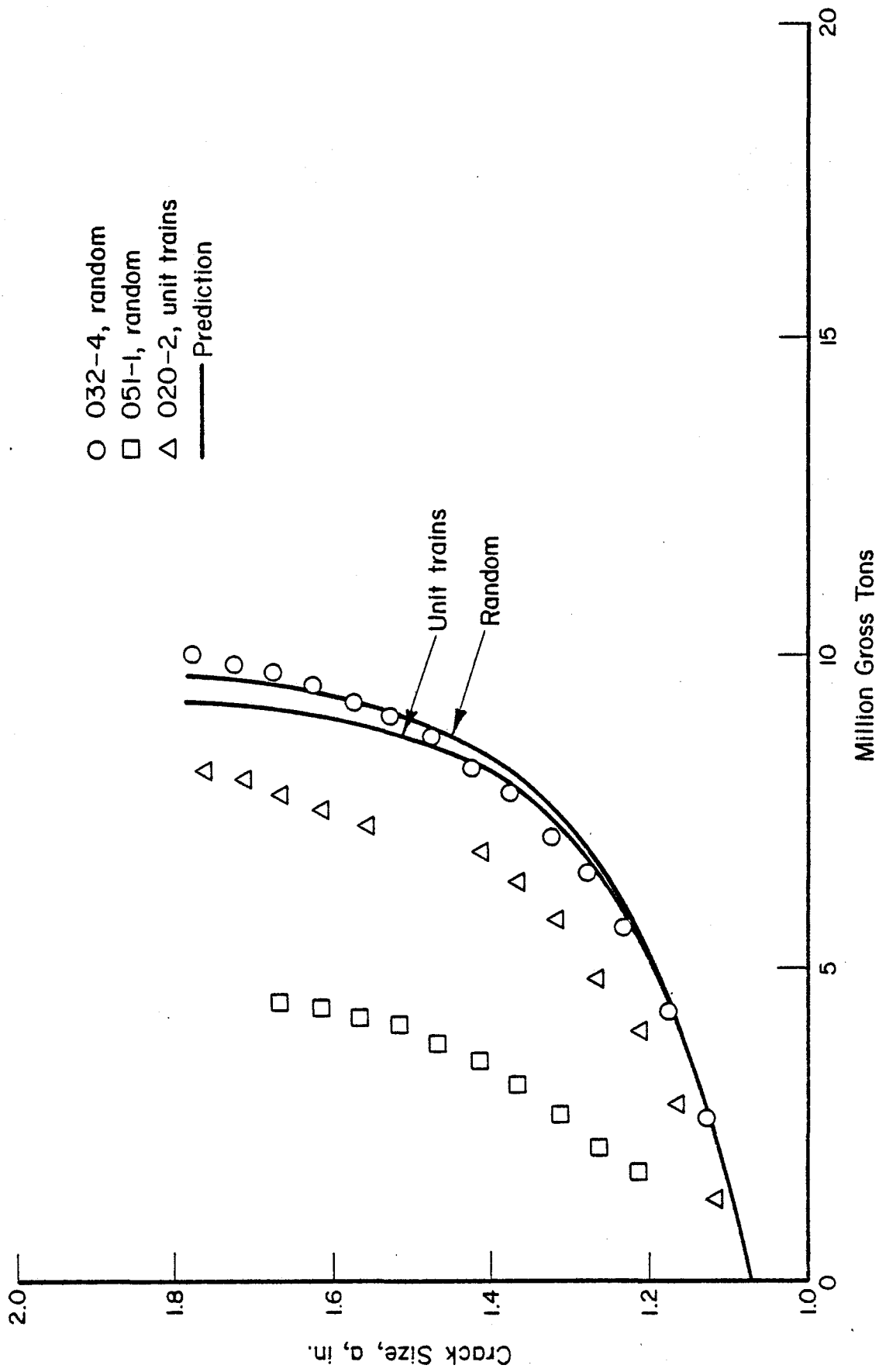
FIGURE 39. TEST DATA AND PREDICTIONS (CURVES) FOR SPECTRUM III

76
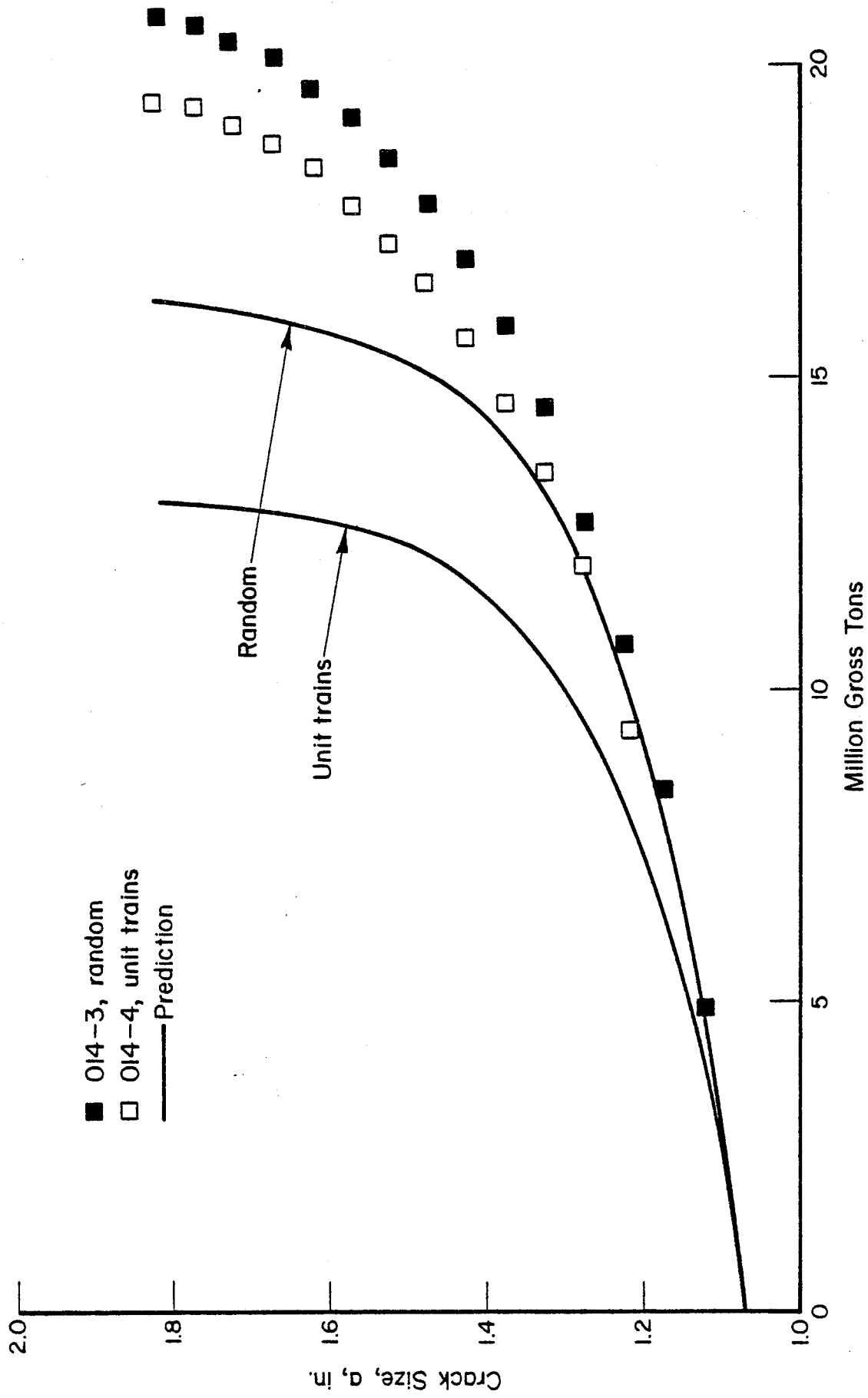
FIGURE 40. TEST DATA AND PREDICTIONS (CURVES) FOR SPECTRUM IV

Data points: Test
Curve: Integrated rate equations
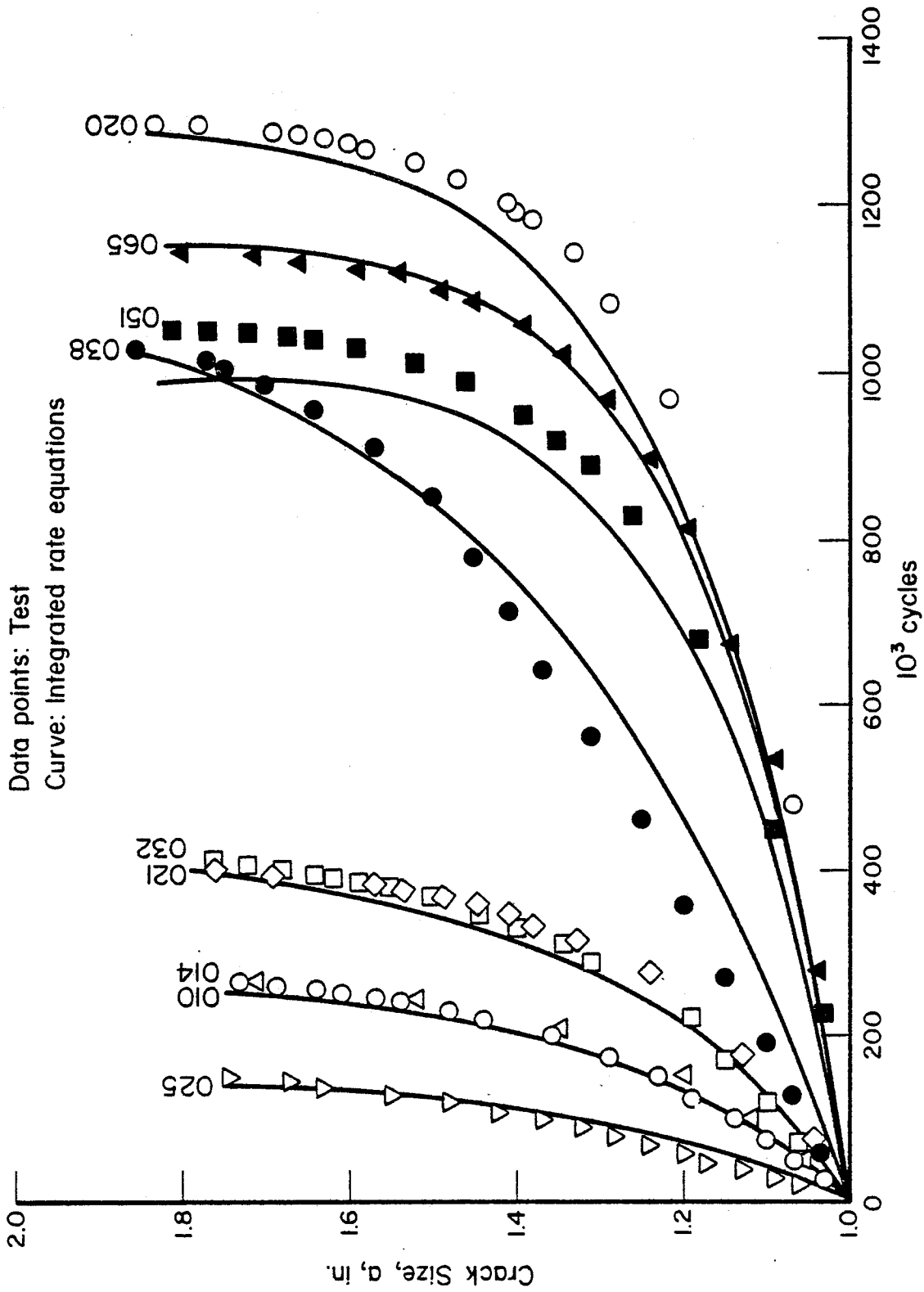
FIGURE 41. PREDICTIONS OF CONSTANT AMPLITUDE DATA WITH
EQUATION (3.5) AND CONSTANTS OF TABLE 13

78

TABLE 14. CRACK GROWTH PREDICTIONS

Life from 1.07 in. to Failure in MGT.

| Rail Sample | Constant Amplitude Life, kc | Spectra I and II Combined | | | | | Spectrum III | | Spectrum IV | |
|---|---|---|---|---|---|---|---|---|---|---|
| | | 12 Level | 8 Level | 7 Level | Random 11 Level | Unit Trains | Random 11 Level | Unit Trains | Random 11 Level | Unit Trains |
| 014 (Tests) | 260 | 7.5 | 6.5 (12.9) | 6.5 | 7.5 (19.1) | 7.3 | 5.7 | 5.6 | 9.6 (21.1) | 7.7 (19.7) |
| 010 (Tests) | 260 | 8.7 | 7.5 | 7.5 (14.2) | 8.7 | 8.5 (≈16) | 6.6 | 6.5 | 11.2 | 9.0 |
| 032 (Tests) | 410 | 10.6 (19.8) | 9.2 | 9.2 (11.5) | 10.6 | 10.3 | 8.0 (10.1) | 7.9 | 13.6 | 11.0 |
| 038 (Tests) | 1,030 | 39.4 | 33.9 (13.2) | 33.9 | 39.3 (13.3) | 38.2 | 29.5 | 28.9 | 50.8 | 40.6 |
| 051 (Test) | 1,050 | 23.6 | 20.4 | 20.4 | 23.6 | 22.9 | 17.7 (4.4) | 17.4 | 30.4 | 24.4 |
| 020 (Test) | 1,300 | 34.3 | 29.5 | 29.5 | 34.3 | 33.2 | 25.7 | 25.2 (8.3) | 44.2 | |
| Avg. (Tests) | | 12.6 (19.8) | 10.9 (13.0) | 10.9 (12.9) | 12.6 (16.2) | 12.3 (≈16) | 9.5 (7.2) | 9.3 (8.3) | 16.2 (21.1) | 13.0 (19.7) |
| Ratio | | 0.64 | 0.84 | 0.84 | 0.78 | 0.77 | 1.32 | 1.12 | 0.77 | 0.66 |

The predictions for the individual samples reflect the large variability that existed in the constant amplitude data, 260 to 1300 kc or a factor of 5. This same factor is found for the predicted lives under spectrum loading; e.g., for sample 014, a life of 7.3 MGT for spectra I and II unit trains and a life of 33.2 MGT for sample 020. As noticed earlier, the test data showed variations of less than a factor of 2 only.

The predictions clearly show a small but systematic effect of spectrum representation; the 7 and 8 level representation shows a slightly shorter predicted life than the 12-level, 11-level random, and the unit train representation. The random history is likely to be the most representative of service loading. Thus, it can be concluded that a 12-level train-by-train sequence and a unit train sequence give adequate predictions, since they lead to the same result as random loading.

The last lines of Table 14 give the predicted lives based on the average data of Equation (7.3) and the average test data. Those data show that the relative difference of the various spectrum representations is correctly predicted; there is an almost constant ratio between the predicted and achieved life for a given spectrum representation. The results enhance the conclusion that a unit train representation can be used for the prediction of service data.

The difference in spectrum severity is properly reflected by the prediction procedure. The predicted lives for random loading using average data are 12.6, 9.5, and 16.2 MGT, respectively, for the three spectra, showing a relative magnitude of 1:0.75:1.29. The average actual lives are 16.2, 7.2, and 21.1 with a relative magnitude of 1:0.44:1.30. The absolute values of the predicted average lives and the actual average lives are well within 35 percent — their ratios vary from 0.64 to 1.32 as shown in the last line of Table 14.

Considering the achievable accuracy in crack growth predictions, those based on average crack growth data are quite satisfactory. They are well within a factor of 2 for the individual test data (with one exception) and they are within 35 percent of the average test data. Predictions based on the baseline data of the individual rail samples are much worse, because the variability of the results of service simulation tests turned out to be much smaller than of constant amplitude tests.

The results to this point can be summarized as follows:

a) 12-level, 11-level random, and unit train spectrum representations give the same results in tests as well as predictions.

b) 7-level and 8-level spectrum representations give somewhat shorter lives, which would make predictions more conservative.

c) The best predictions are obtained with a rate equation based on average data.

d) The relative severity of different spectra is adequately reflected in predicted crack growth.

One alternative still has to be considered. This is the representation of the entire stress spectrum by a single parameter, i.e., the root mean squares (RMS) value of the stresses. The RMS value of the stress can be substituted in the stress-intensity equation to give a $\Delta K_{RMS}$. It could then be postulated that crack growth in service is a unique function of the $\Delta K_{RMS}$ of the spectrum. Crack growth predictions would then be based on direct integration of constant amplitude data, while using $\Delta K_{RMS}$ for any given spectrum instead of $\Delta K$. This procedure has been attempted in other applications with variable success[21-23].

The $\Delta K_{RMS}$ values were calculated for the service simulation tests and the crack growth rates per MGT were determined from the test data. The results are plotted in Figure 42. Note that the R-ratios given are defined as $R = (K_{max} - \Delta K_{RMS})/K_{max}$. Also shown in Figure 42 are trend lines for constant amplitude data[1]. The constant amplitude growth rates were converted from inch/cycle into inch/MGT through multiplication by 67,520, the number of cycles in one MGT.

It is obvious from the rate data that the service simulation tests would not be accurately predicted by direct integration of constant amplitude curves on the basis of $\Delta K_{RMS}$. Attempting to do this would be complicated by the R-ratio effect. Since the R-ratio for a given stress history is a fixed value, an arbitrary choice of the R-ratio for the constant amplitude data would have to be made. The generality of that choice would be questionable.

A more realistic possibility would be to determine the average curve for all the service simulation test data and to make predictions by
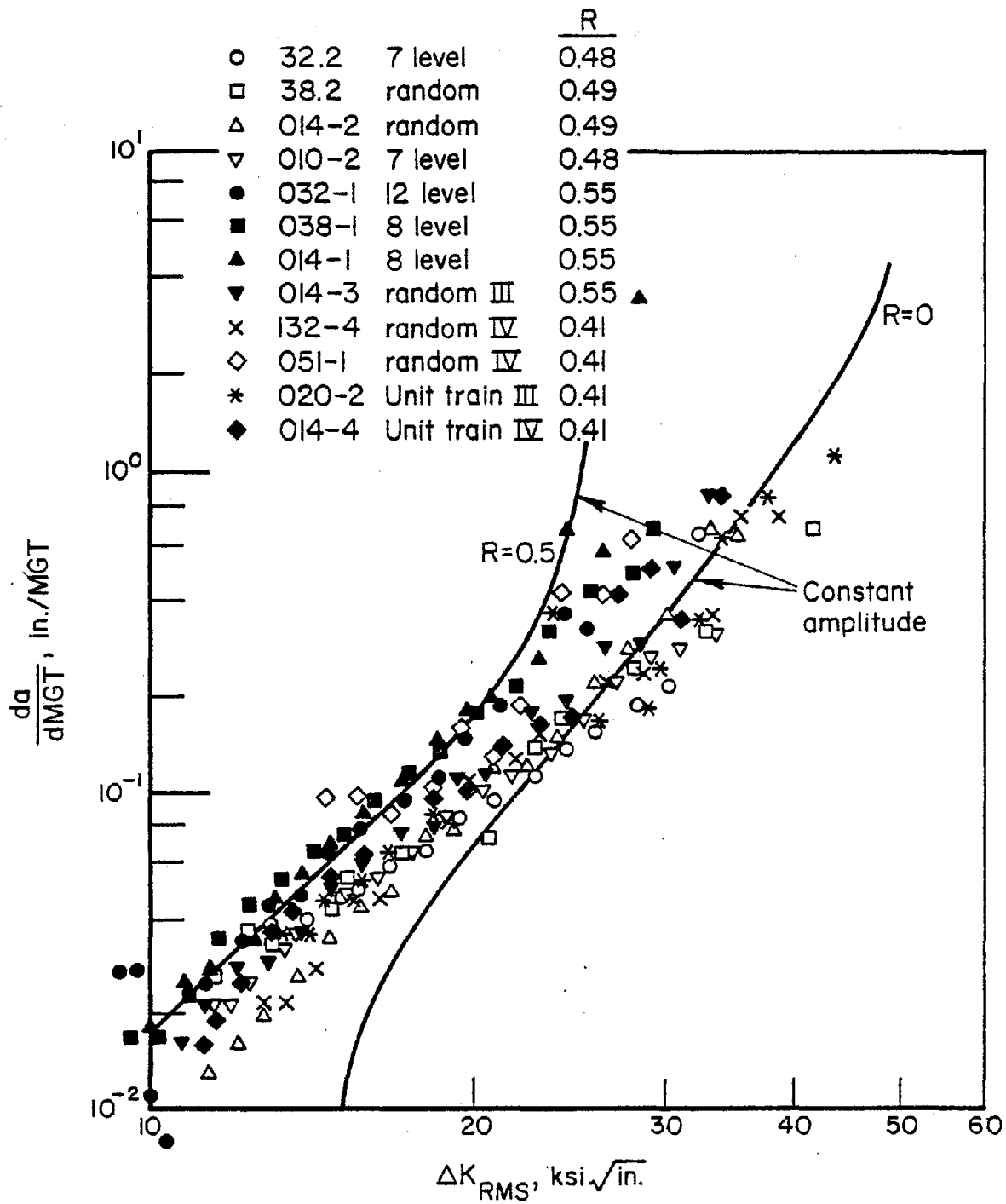
FIGURE 42. CRACK GROWTH PER MGT AS A FUNCTION OF $\Delta K_{RMS}$ FOR THE SERVICE SIMULATION TESTS

integrating this curve rather than the constant amplitude curve. Figure 42 shows a scatter of rate data of the order of a factor of 2. Thus, predictions based on an average curve would generally be within a factor of 2 also, although there seems to be a systematic effect of R-ratio.

The disadvantages of this prediction procedure are (1) that it has to be based on service simulation test data, which would have to be generated first on a rather large scale to consolidate the approach and (2) generalization to elliptical cracks and mixed mode situations would be very questionable (see Section 8). It is therefore concluded that the prediction procedure, based on load level integration as discussed earlier, is more general and more versatile. In addition, it is equally easy to apply.

## 7.3.  The Failure Model

A failure model is required for the prediction of the growth of service cracks in rails. Such predictions have to be made to serve as a basis for operational management decisions on measures to reduce rail failures. These measures may consist of limiting speed or traffic, upgrading track, renewing track, or increasing inspection frequency. The statistical nature of all of the input information to a crack growth prediction asks for a reliability analysis in which the statistical variation of crack growth is surveyed.

The purpose and use of crack growth predictions set forth the following requirements for a failure model:
- a)  Crack growth computation should be extremely fast, because many repetitional computations will be made in a reliability analysis.
- b)  Crack growth predictions should have the accuracy that is realistically achievable; i.e., they should be within a factor of 2 or better of the actual behavior under the circumstances assumed in the predictions.
- c)  Spectrum representation should be realistic enough to warrant adequate prediction of the effect of spectrum variations (e.g., those caused by the above measures to reduce rail failures). On the other hand, it should

be simple enough for expeditious crack growth computations.

d)  Generalization to the more complex circumstances of a
rail should be possible.

The failure model presented in the foregoing sections has these qualifications
as discussed below.

As for the requirement of rapid computation, the generation of
one propagation curve, such as the ones in Figures 37 through 40, took
approximately 3 computer seconds.  Increasing the step size from 0.5 to
1 MGT or larger would further reduce computer time, which certainly should be
done if small initial crack sizes have to be considered.  Smaller initial
cracks will show less crack extension per MGT so that larger steps will be
permissible.  It was shown in other work[1] that step sizes causing on the
order of 5 percent crack extension do not impair the results to a noticeable
degree.  Recalculation of the curves in Figure 37 through 40 on a programmable
pocket calculator using 1 MGT step sizes showed differences in predicted
crack growth lives of less than 3 percent.

The speed of calculation was also the reason why the crack incre-
ment per load level was approximated by $N_j$ x $(da/dN)_j$ (Figure 36).  A
more rigorous integration would be to apply, e.g., a Simpson integration rule
over the increment.  However, since the crack increments per load level are
extremely small, the growth rate over the increment is practically constant.
Thus, the final result would only change by a few percent which is a secondary
effect in comparison to other approximations.

As discussed in Section 7.1, the best achievable accuracy in crack
growth predictions is of the order of 30 percent on life; whereas, in most
cases, a factor of 2 is more realistic.  It cannot be expected that more
sophisticated prediction models will improve this situation, since it is
due to the variability of the input data and the material variability in
particular.  Thus, the accuracy of the present predictions is within the
range of what is practically achievable.

It was shown that random, 12-level approximation, and unit train
approximation of the spectrum gave essentially the same results in tests as
well as in computations.  As a result, a 12-level approximation, as well as a
unit train approximation, can be used with confidence to predict crack growth

under random or quasi-random service loading. The sequence tests showed that the train-by-train representation is a realistic simulation of the actual stress variations in service. The spectrum approximations used permit an easy and expeditious calculation of crack growth, particularly in the unit trains.

The spectrum representation developed is considered an essential part of the failure model. The use of fixed exceedances to determine the discrete stress levels ensures generality of the procedure. Any of the developed train-by-train sequences can be regenerated with a simple algorithm for a different spectrum — only the stress levels have to be adjusted.

The generalization of the failure model to cracks in rails poses some difficulties which will be discussed in Section 8. Since the same difficulties would be associated with any other model, they are not considered a reason for rejection of the present model.


## 8.   APPLICATION TO RAIL CRACKS


### 8.1.   The Nature of Rail Cracks

The most common types of rail cracks are illustrated in Figure 43. One type of crack occurs in the web at the bolt holes for the rail joints. They usually grow under 45 degrees as indicated in Figure 43.

Three main types of cracks occur in the rail head. They are

1) The transverse fissure, growing in the vertical transverse plane, ultimately leading to a break through the entire cross-section of the rail.

2) The vertical split head growing in a vertical longitudinal plane, ultimately leading to the breaking off of the side of the head over some length so that the wheel flanges lose support and a derailment occurs. Although the crack is shown in the central plane in Figure 43, it can occur in any parallel plane.

Bolt hole cracks

Vertical split head

Horizontal split head

Transverse fissure
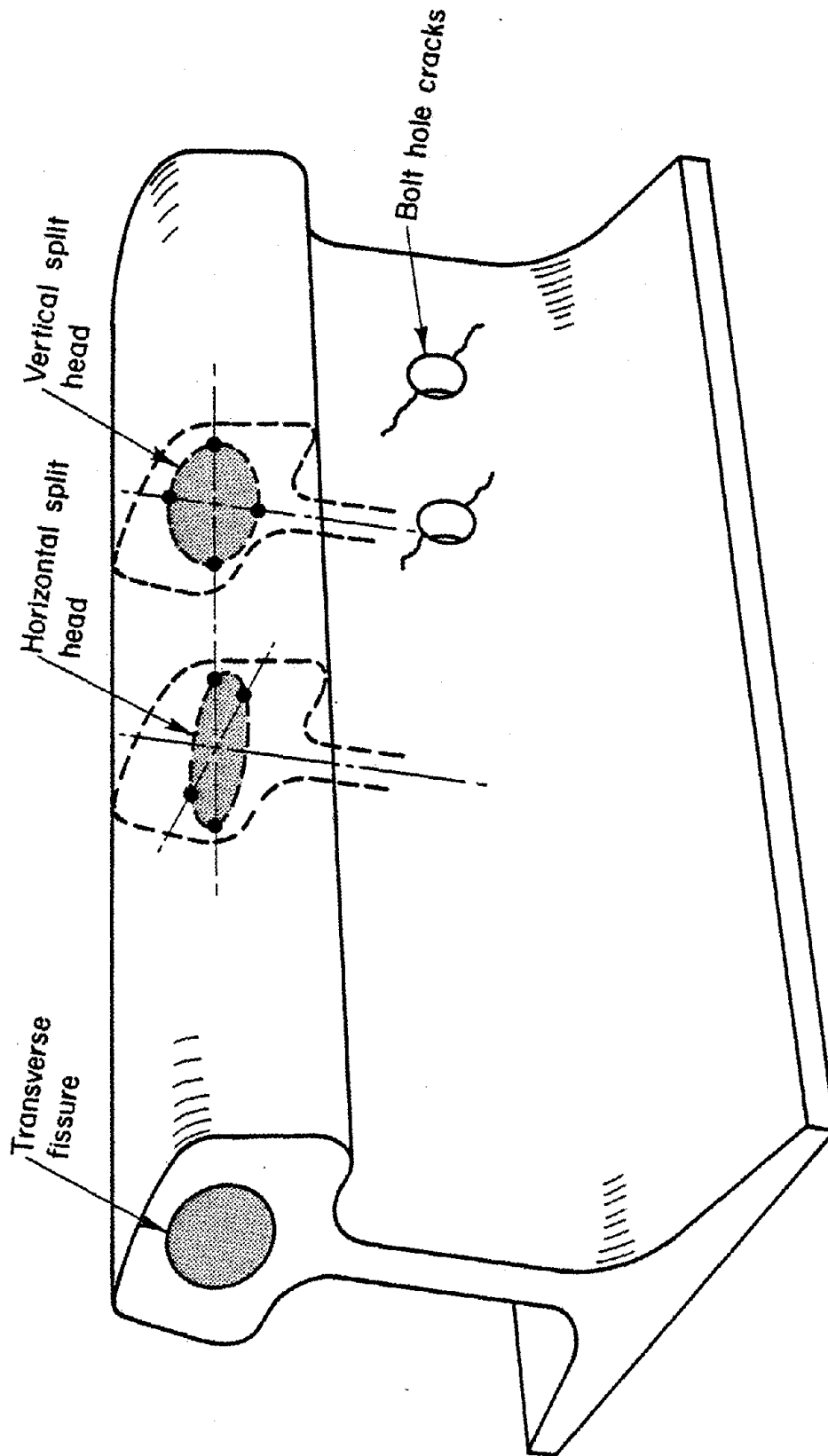
FIGURE 43. MOST COMMON TYPES OF RAIL CRACKS

86

3) The horizontal split head growing in a horizontal plane, ultimately leading to the breaking out of the running surface over some length. Figure 43 shows the crack in the central plane, but it can occur at any depth under the top surface.

Initially, all cracks are of quasi-circular or quasi-elliptical shape, but they change shape while growing due to stress gradients and external boundaries. The discussions in the following sections will be limited to the three head cracks.

## 8.2. Cyclic Loading of Head Cracks

An engineering stress analysis of intact and cracked rail was made by Johns et al.[9] in another DOT/TSC-sponsored program. Some observations made from that work of relevance to the present report are discussed in this section.

The stress distribution in the rail is uneven. As a result, the stress intensity of a crack varies along the crack front. This is illustrated for a transverse fissure in Figure 44 for the case of a 19,000-pound wheel load right above the crack. The implication is that crack growth rates will be different at different locations along the crack front so that the crack will change shape. Moreover, the crack growth properties depend upon the direction of crack growth which further contributes to crack shape changes. Finally, as a result of the stress gradients in the rail head, the shape of the K-distribution varies with crack size and crack location (Figure 44). Similar variations of K along the crack front occur for horizontal and vertical split heads.

When a wheel moves over the location of the crack, the stress intensity builds up from zero to the values shown in Figure 44 and then decreases again when the wheel moves away. This is illustrated in Figure 45 for two points of the crack front (top and bottom). Similar plots for the vertical and horizontal split head are presented in Figures 46 and 47. (All three figures are for a 19,000-pound wheel load.) Since the calculations are for elastic stress fields, the stress intensity is proportional to wheel load. Thus, the stress intensities for a 38,000-pound wheel load would be twice as high, and the cyclic variation of the stress intensity for any wheel load can be determined on the basis of Figures 45 - 47.
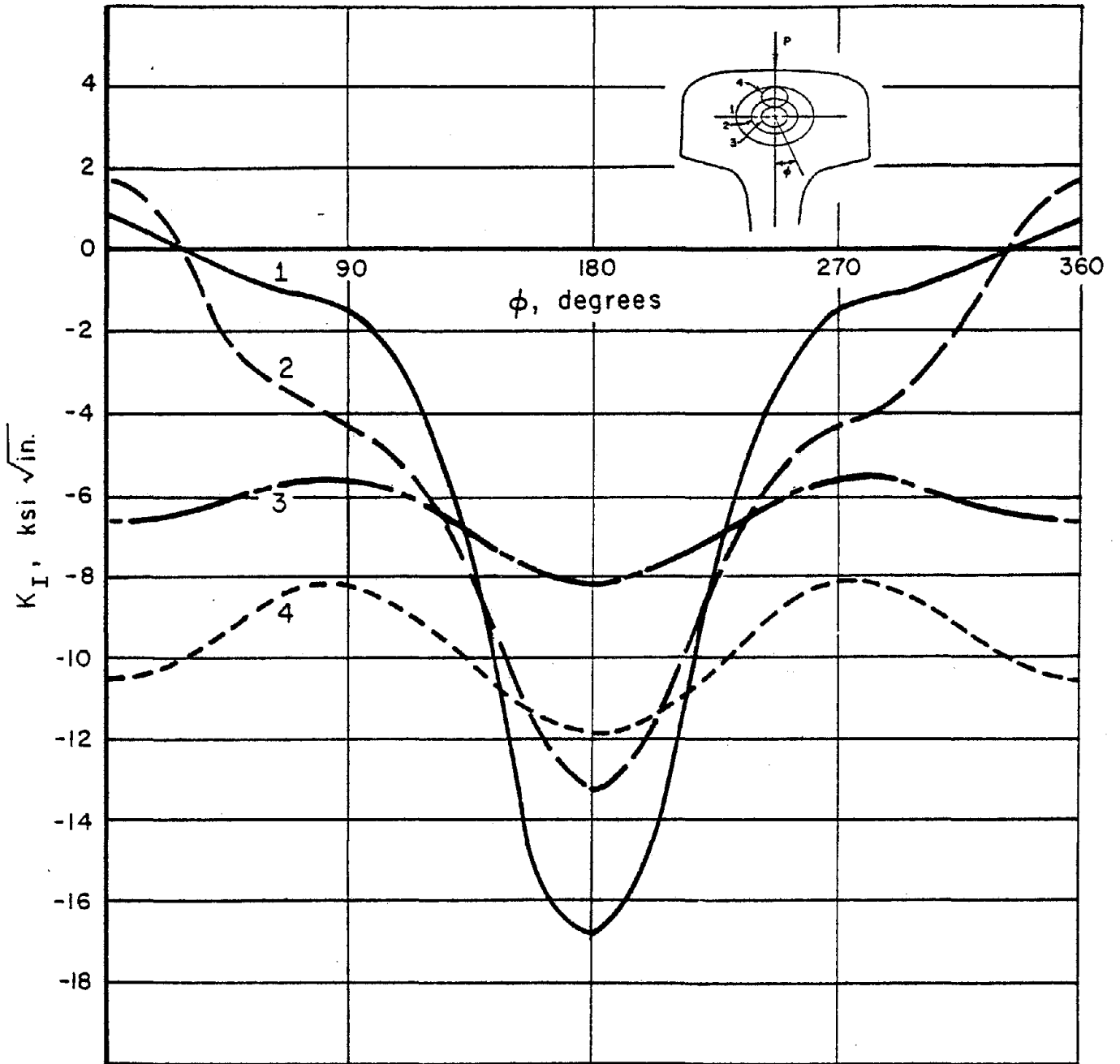
FIGURE 44. STRESS INTENSITY FACTOR $K_I$ FOR THREE TRANSVERSE
FISSURE SIZES AND TWO LOCATIONS; 19,000
POUND VERTICAL LOAD OVER CRACK[9]
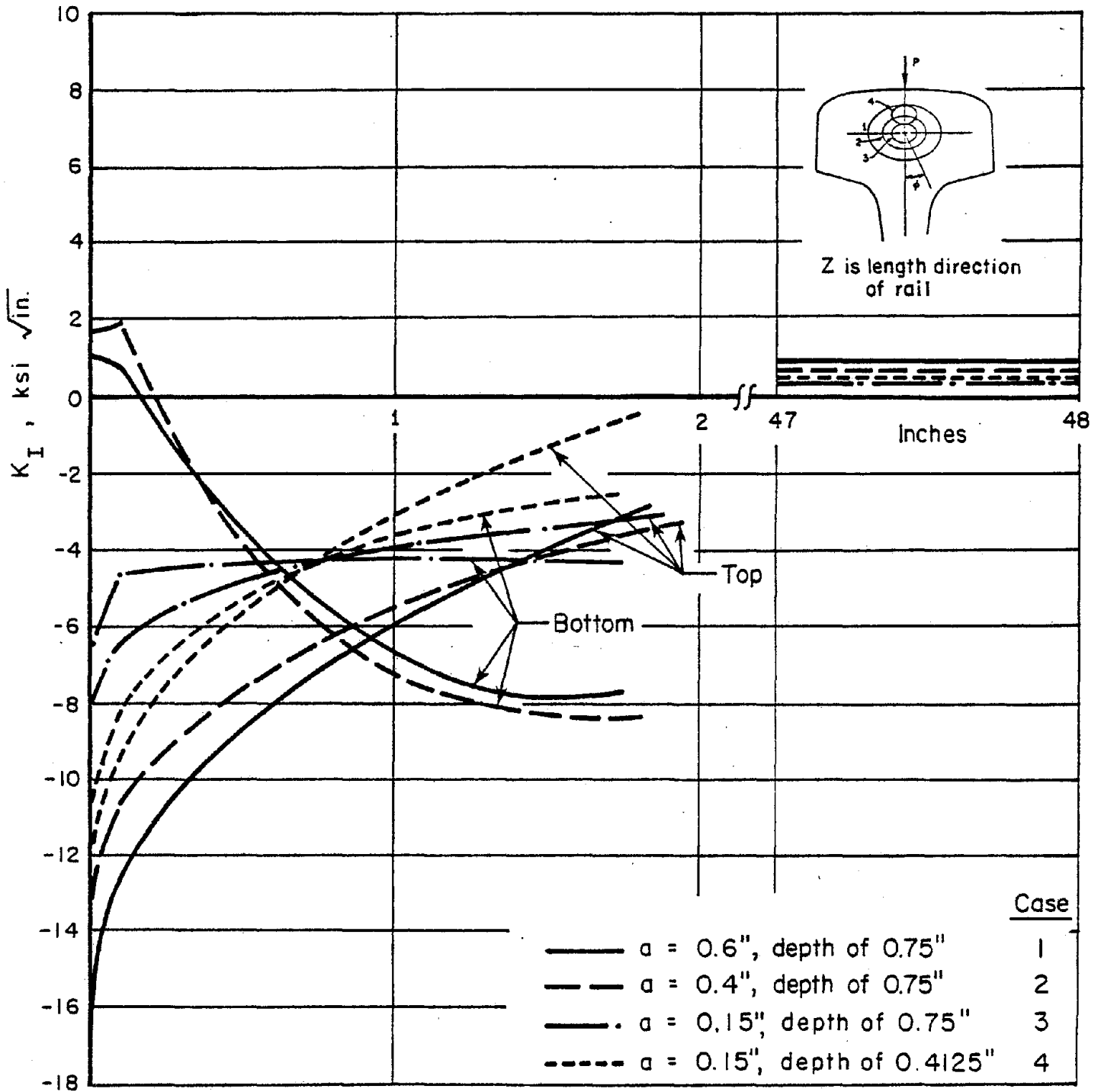
FIGURE 45. STRESS INTENSITY FACTOR $K_I$ VERSUS FLAW POSITION ON TOP
AND BOTTOM OF A TRANSVERSE FISSURE; 19,000 POUND
VERTICAL LOAD[9]
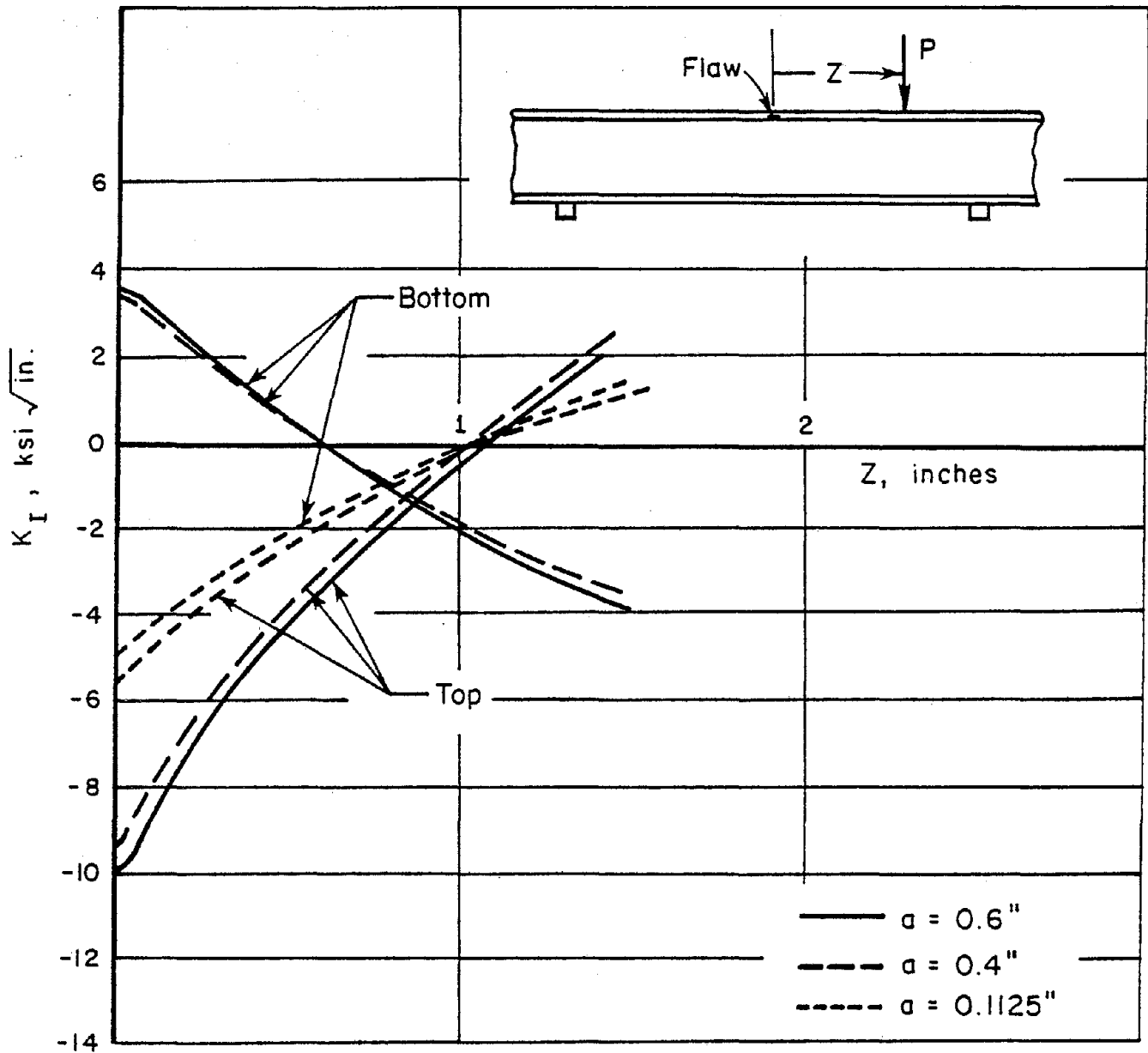
FIGURE 46. STRESS INTENSITY FACTOR $K_I$ VERSUS FLAW POSITION ON TOP AND BOTTOM OF VERTICAL SPLIT HEAD; 19,000 POUND LOAD[9]
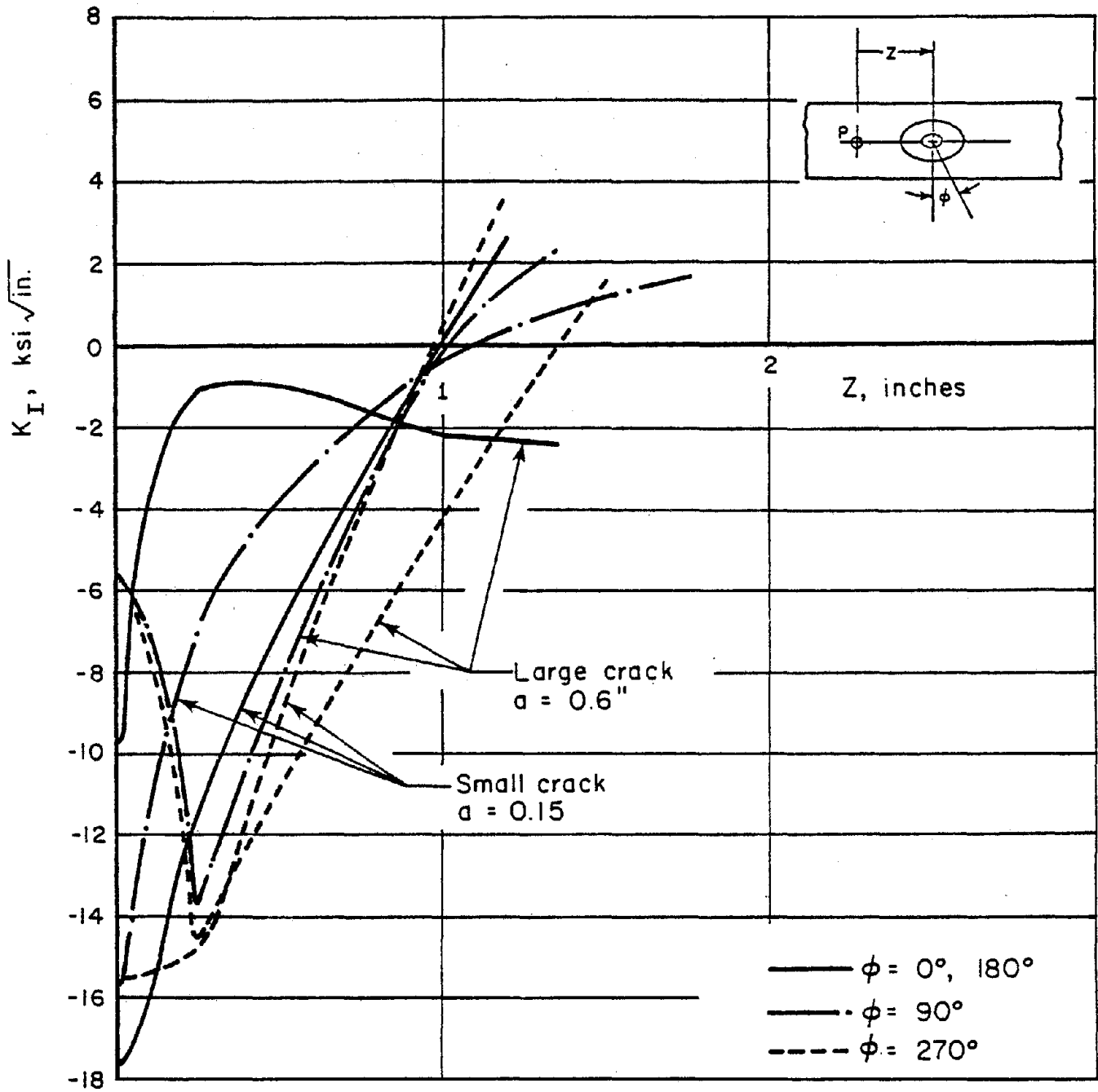
FIGURE 47. STRESS INTENSITY FACTOR $K_I$ VERSUS FLAW POSITION AT FOUR
LOCATIONS ON CRACK FOR HORIZONTAL SPLIT HEAD; 19,000
POUND LOAD CRACK 0.30 INCH BELOW RAIL SURFACE

91

Shown in these figures are the opening mode stress intensity factors, i.e., $K_I$ for mode I. The rail also experiences shear stresses, which result in mode II and III stress intensities $K_{II}$ and $K_{III}$. For the crack locations considered, $K_{II}$ and $K_{III}$ are quite small for the transverse fissure and the vertical split head. For the case of a horizontal split head, $K_{II}$ attains a considerable magnitude as is demonstrated by Figure 48.

The mode I stress intensities appear to be predominantly negative (Figures 45 through 47). This is a result of the wheel loads causing predominantly compressive stress in the rail head. Negative stress intensities are not a physical reality, since the faces of the crack will close under the action of compressive stress, so that effectively there is no crack. However, rails contain residual tensile stresses, which have to be superimposed on the cyclic stresses due to wheel passage. As a result, the cyclic variations of the stress intensity as shown in Figures 44 through 47, do not take place from zero but from a positive region depending upon the stress intensity due to residual stress. Figures 49 through 51 show the stress intensities resulting from a given residual stress field.[9] Since the residual stress varies from point to point, the resulting stress intensities vary along the crack front.

## 8.3. Operation of the Failure Model in General

Formal execution of the rail failure model for the case of an actual rail crack is quite complex. The computation requires the following ingredients:

1)  Stress distribution in the rail head for a given wheel load.

2)  For the given type of flaw, the stress intensity for a range of flaw sizes, shapes and positions.

3)  Stress intensities due to residual stresses for a range of flaw sizes, shapes, and positions.

4)  A wheel-load spectrum.

5)  Crack growth properties for the various directions in which a flaw of a given type will propagate.
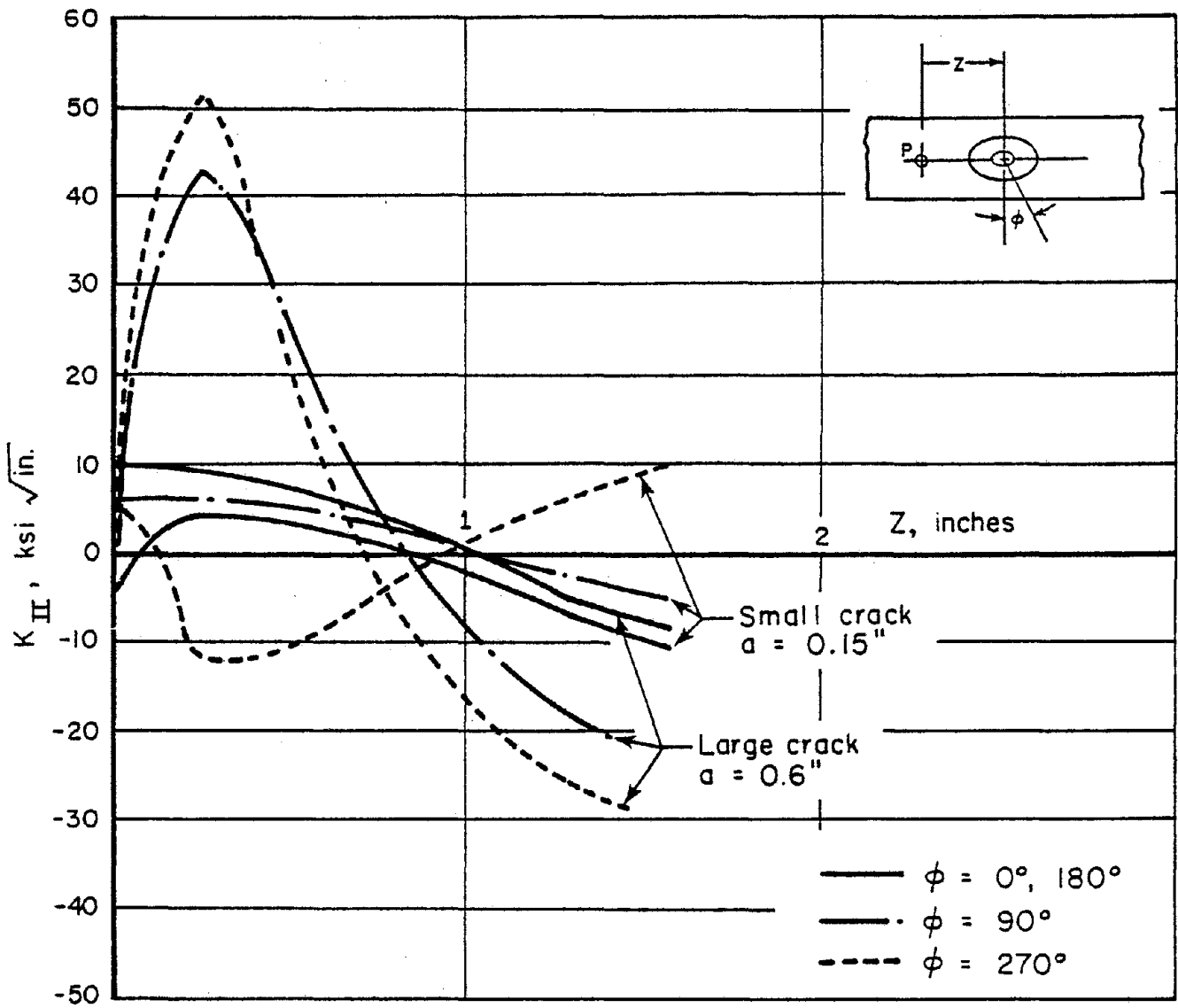
FIGURE 48.  STRESS INTENSITY FACTOR $K_{II}$ VERSUS FLAW POSITION FOR
            HORIZONTAL SPLIT HEAD; 19,000 POUND VERTICAL LOAD
            CRACK 0.30 INCH BELOW RAIL SURFACE[9]
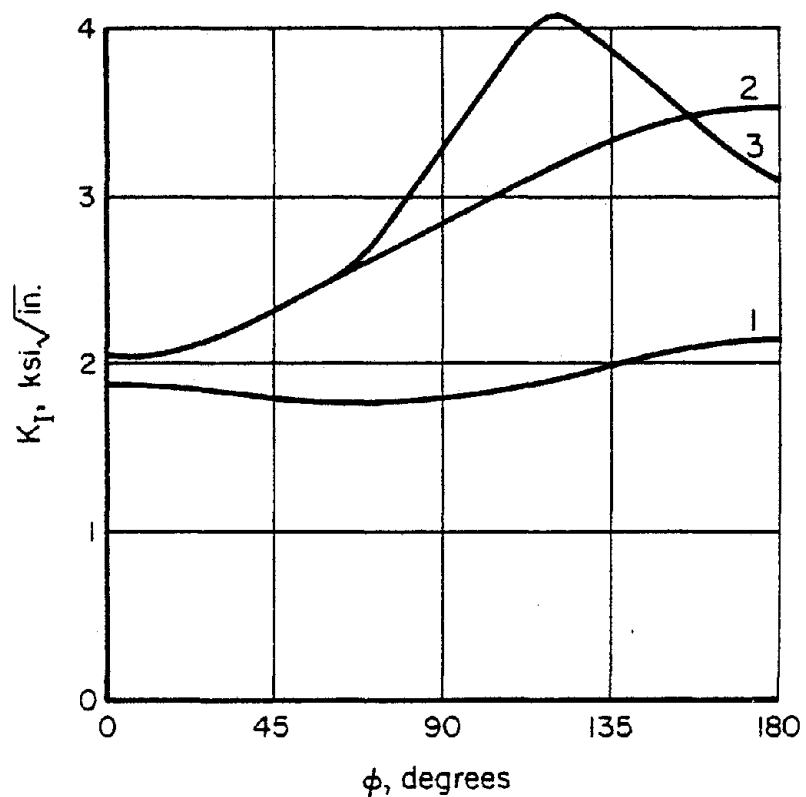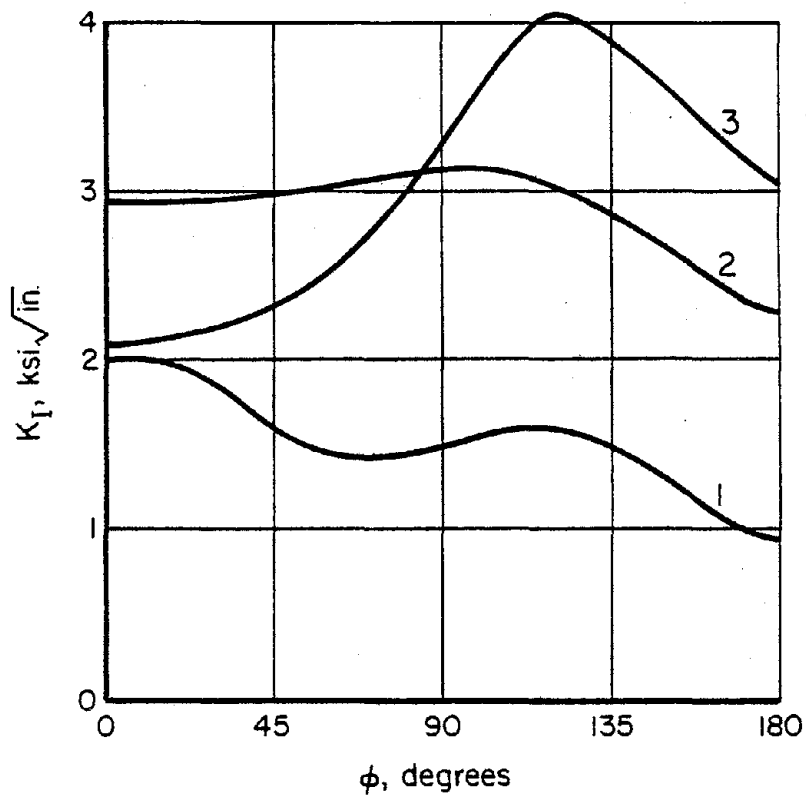
$K_I$ FOR O.R.E. RESIDUAL STRESS DISTRIBUTION

FIGURE 49.  DISTRIBUTION OF STRESS INTENSITY $K_I$ FOR THREE
TRANSVERSE FISSURE DEFECT SIZES IN TWO GROWTH
ORIENTATIONS CAUSED BY RESIDUAL STRESS[9]

94
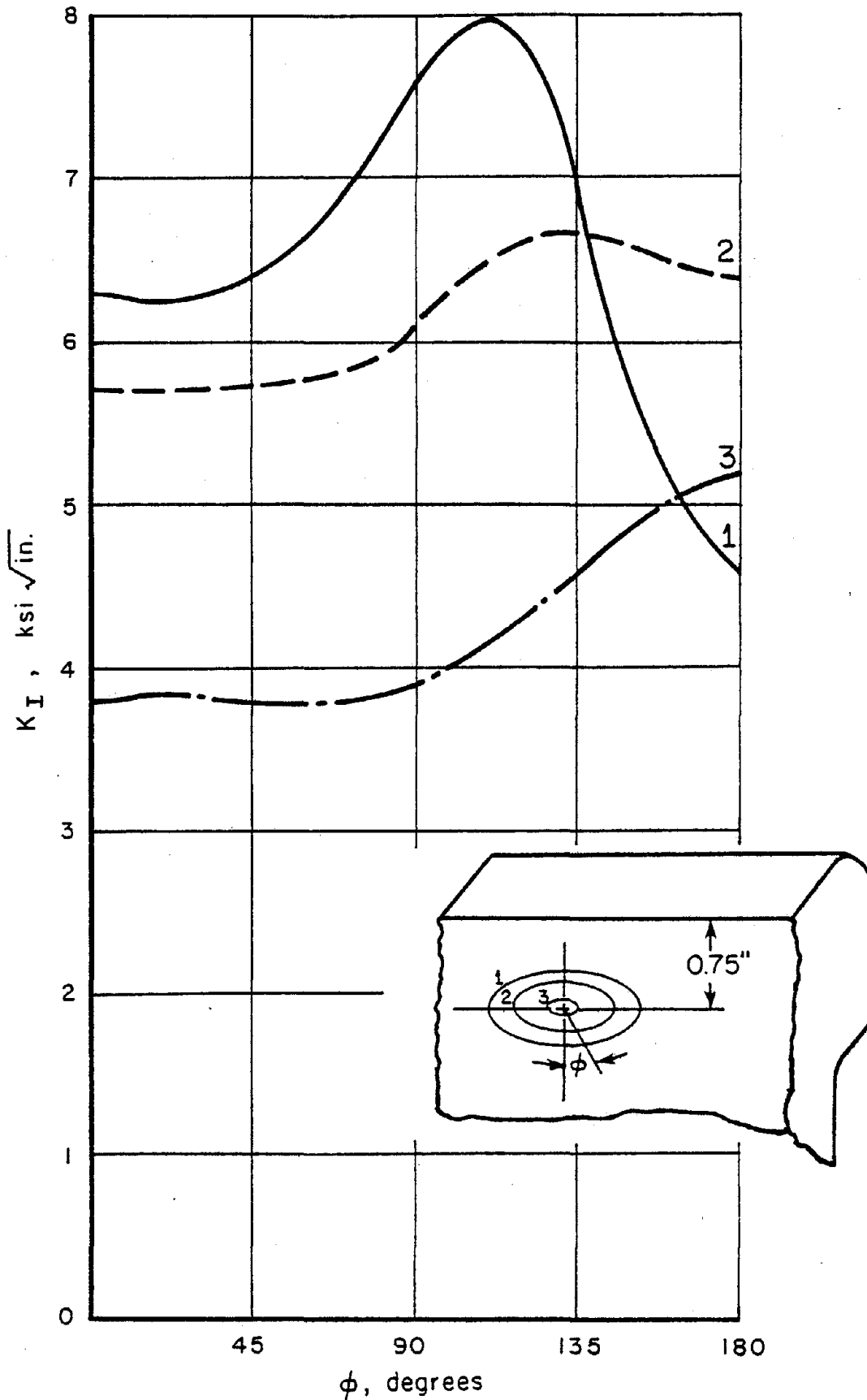
FIGURE 50. STRESS INTENSITY FACTOR $K_I$ FOR THREE VERTICAL SPLIT
HEAD DEFECT SIZES DUE TO RESIDUAL STRESS[9]
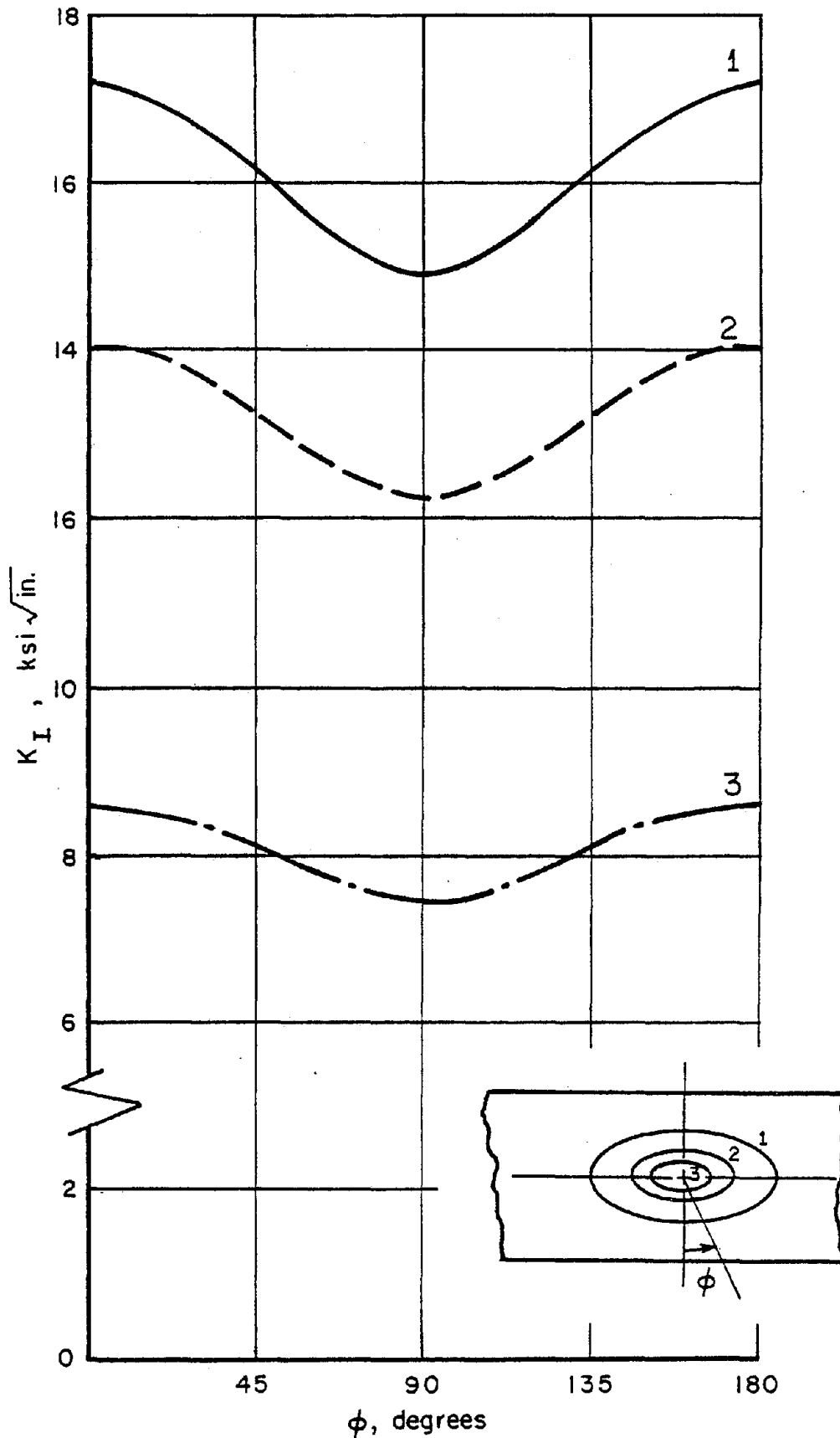
FIGURE 51. STRESS INTENSITY FACTOR $K_I$ FOR THREE HORIZONTAL SPLIT
HEAD DEFECT SIZES DUE TO RESIDUAL STRESS; CRACK
PLANE 0.30 INCH BELOW RAIL SURFACE[9]

Execution of the rail failure model consists of the following steps:

a)  Determine the wheel loads associated with the 12 exceedance levels of the spectrum (Figure 24, assuming that the 12-level spectrum approximation is used).

b)  Express the wheel loads of all 12-levels as a multiple of 19,000 pounds (it is assumed that stress intensities available are for 19,000 pounds wheel loads).

c)  Determine the cyclic variation of the stress intensity for a number of locations around the initial flaw, e.g., at $\theta = 0$, 90, 180 and 270 degrees (Figure 44). This should be done for $K_I$, $K_{II}$, and $K_{III}$.

d)  By using the multiples of 19,000 pounds, determine the cyclic stress intensities for all 12 levels and at the 4 locations under Step (c).

e)  Determine the effective cyclic stress intensities using one of the mixed mode cracks growth criteria[2]:

$$K_{Ieff} = f(K_I, K_{II}, K_{III}) \quad .$$

f)  Determine the stress intensity due to residual stress at the 4 locations.

g)  Superpose e and f for all 12 levels.

h)  Calculate crack growth rate at each of the 4 locations using the crack growth properties for each of the 4 directions. Start with load level 1. (Crack growth will be different in all 4 directions, so that the crack shape will change). Assuming that changes of crack size and shape are only minor, repeat calculation for all 12 levels to obtain growth in 1 MGT.

i)  After 1 MGT, changes in crack size and shape whould be accounted for. Thus, Steps (c) through (h) should be repeated, etc.

## 8.4. Present Shortcomings and Limitations

The information available at this time prohibits formal execution of the procedure outlined in Section 8.3. Areas where information is lacking are the following:

1) For a given type of crack, stress intensities have been calculated only for one flaw location, one flaw shape and three flaw sizes. This means that the change of shape of the flaw cannot be accounted for. But even if the flaw is assumed to be of constant shape, an important problem remains. As can be seen from Figures 44 through 47, two diametrical opposite points of the crack front experience largely different stress intensities. Thus, these two locations will experience different growth and as a result, the center of the flaw will move so that stress intensity values would be needed for a different flaw location.

   With stress intensities available for only three flaw sizes, very crude interpolations have to be made for intermediate flaw sizes. In view of the changes in flaw shape and location discussed above, interpolation for different flaw sizes becomes even more questionable.

2) At this time, little useful information is available as to the residual stress distribution in U.S. rail.[9] The information contained in Figures 49 through 51 is illustrative material only. Since crack growth rates depend strongly on residual stress (see Section 9.5), it is of primary importance that residual stress fields are accurately determined. Subsequently, stress intensities should be made available for many crack sizes, shapes, and locations for reasons discussed under (1).

3) A rationale to treat mixed mode cracking is not yet available. Several possibilities were discussed in a previous report[2], and it was concluded that the maximum principal stress concept and the strain-energy density concept are possible candidates. In both cases, the combined effects of Modes I, II, and III loading can be expressed in terms of an effective

Mode I stress intensity, $K_{Ieff}$. The crack growth rate then follows from the usual growth rate expression, such as Equation (3.5) in which all Mode I stress intensity are replaced by $K_{Ieff}$.

So far, no experimental verification of these concepts has been obtained. This is due to the fact that mixed mode crack growth cannot be maintained in an experiment[2]. Extensive mixed mode testing performed under the present program will be reported separately[24].

If the mixed mode concepts mentioned above are applicable, the mixed mode loading is likely to have little effect on the growth of rail cracks, since it turned out[9] that for transverse fissures and vertical split heads, the Mode II and III stress intensities are only of the order of 30 percent of the Mode I values. This means that $K_{Ieff}$ would be only about 5 percent higher than the acting $K_I$. Bolt hole cracks are growing perpendicular to the maximum tensile stress, so that they are growing in pure Mode I. As a result, mixed mode loading might be a problem only in the case of horizontal split heads (Figure 48).

It appears that the lack of stress-intensity factors for rail cracks and the unknown residual stress fields are the most severe limitations to the applicability of the failure model. Until this important information becomes available, the failure model will be of limited use only.

## 8.5. Crack Growth Predictions for Rail Cracks

Under the limitations discussed in Section 8.4, crack growth calculations were made for three types of rail cracks: transverse fissure, horizontal split head, and vertical split head. The calculations followed the steps itemized in Section 8.3, but some simplifications had to be made because of said limitations. These simplifications consisted of the following.

Initial flaw sizes were taken equal to the smallest flaw sizes for which stress-intensity factors were available (Figures 45 through 47). Since the stress intensity was known for three crack sizes only (two, in the case of the horizontal split head) stress-intensity factors for intermediate sizes were approximated by linear interpolation. The stress-intensity variation due to residual stress was taken proportional to the data in Figures 49 through 51, except that the absolute values were changed to determine the effects of residual stress on crack growth.

Crack growth was calculated in steps of 2 percent crack extension (i.e., the stress intensity was assumed constant over a 2 percent crack increment). The propagation of two diametrically opposite crack front locations was calculated independently. However, by using the stress intensities of Figures 44 through 51 it was implicitly assumed that the cracks did not change shape or position. Only Mode I growth was considered. Average crack growth properties were used and the effect of crack growth direction was accounted for.

As a consequence of these necessary simplifications, the resulting crack growth curves and crack growth lives should not be used in an absolute sense. However, they do indicate the relative severity of the three types of flaws, the effect of the magnitude of the residual stress, and the relative effect of the wheel load spectrum.

Predicted curves for a transverse fissure, a vertical split head, and a horizontal split head are presented in Figure 52. The vertical split head is predicted to be the most critical of the three, growing from 0.3-inch to 1.5-inches in 35 MGT (less than 2 years with an annual traffic of 20 MGT). Naturally, the relative severity of the three types of flaws may change if lateral loading would be included. However, it is likely that the
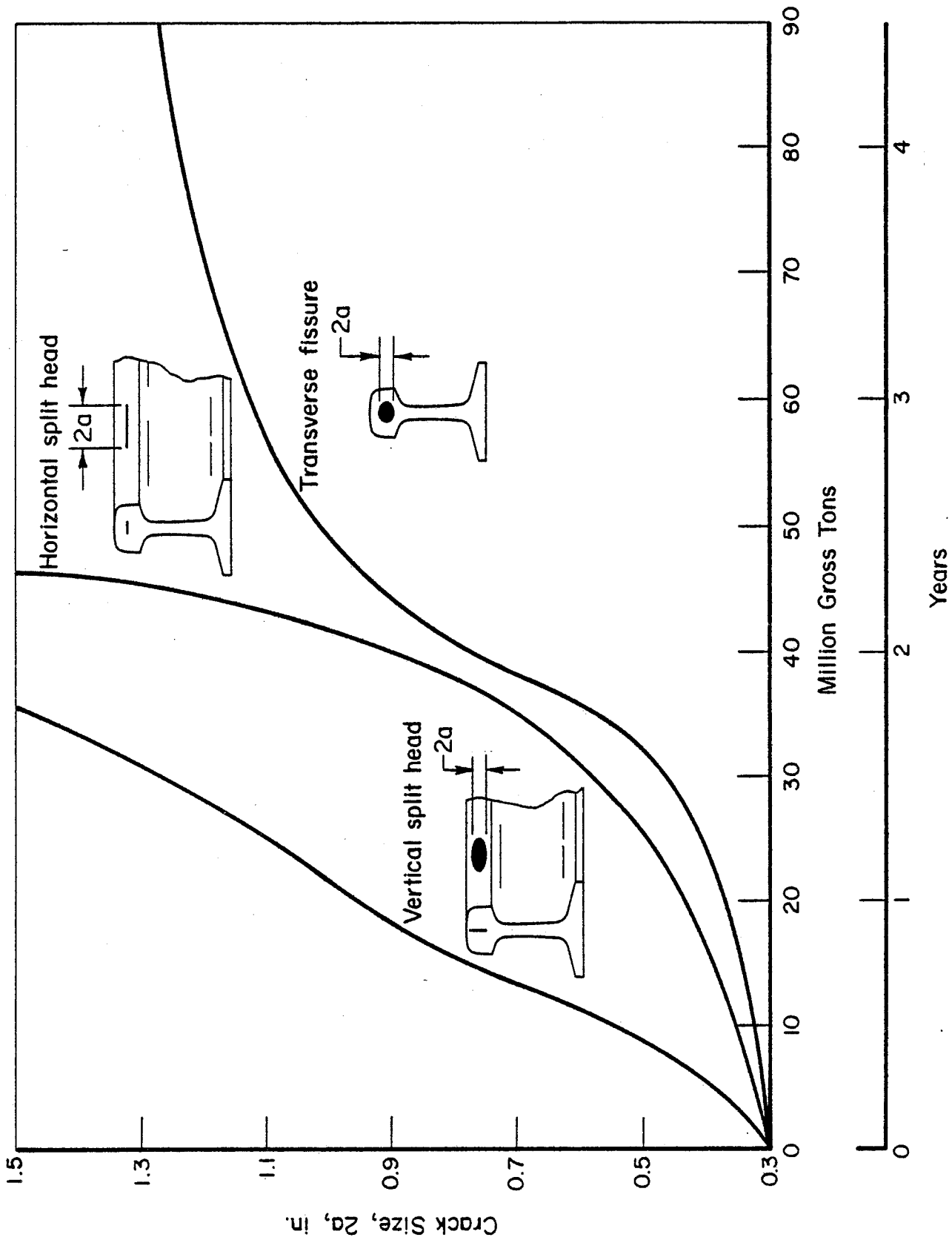
FIGURE 52. GROWTH OF THREE TYPES OF CRACKS UNDER COMBINED SPECTRA I AND II

vertical split head remains the most severe, because in general this type of crack will not occur in the center of the head as assumed here. If the crack is off center, the bending of the rail head under off-center loads is likely to have a larger affect on the stress intensity. These cases could not be considered here, because stress-intensity factors are not yet available, neither for the case of lateral loading nor for the case of off-center cracks.

Figure 53 shows the growth curves for horizontal and vertical split heads under the three different spectra discussed in Section 6. The relative severity of the spectra clearly comes out; crack growth to failure of a horizontal split head takes 1½ years under spectrum III, and 3 years under spectrum IV. (Reference should be made here to the remarks made above about the absolute values obtained in these predictions.)

The growth of a transverse fissure in rails on a hard roadbed*and a soft roadbed is shown in Figure 54. Growth to failure of a transverse fissure takes place over a period of 7 years on a hard roadbed under spectrum IV. It takes only 1½ years on a soft roadbed under spectrum III.

The effect of residual stress level is shown in Figures 55, 56 and 57 for three types of cracks and combined spectra I and II. The residual stress was assumed to be 0.7 and 1.3 times the values used for the previous predictions.

Generally speaking, the vertical split head can still be considered the most dangerous type of crack, because it shows faster growth than the other types if all circumstances are equal. However, Figures 56 and 57 show that if a transverse fissure or horizontal split head happen to be initiated in a rail with high residual stress, their growth can be just as fast or faster than the growth of a vertical split head in a rail with lower residual stress. By the same token, a vertical split head can be of lesser consequence if occurring in a rail with low residual stress. The large effect of the residual stress level on crack growth shows the importance of a thorough investigation of the magnitude of residual stresses in service as a function of time, track condition, and type of traffic (load spectrum).

_____

*Where a hard roadbed would have a track modulus greater than 4000 psi, and a soft roadbed would have a modulus of less than 2000 psi.
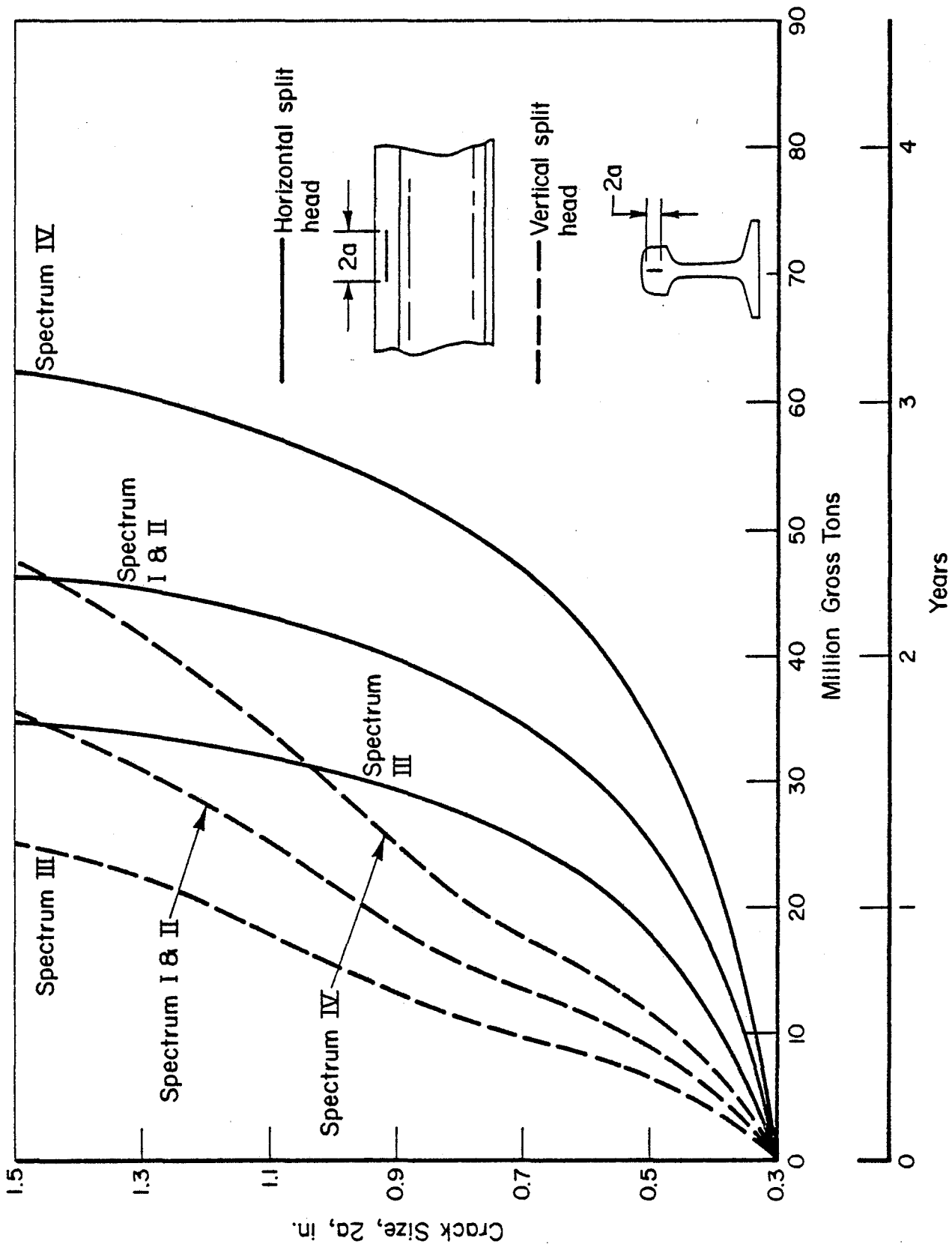
FIGURE 53. CRACK GROWTH OF HORIZONTAL AND VERTICAL SPLIT HEAD
UNDER THREE DIFFERENT SPECTRA
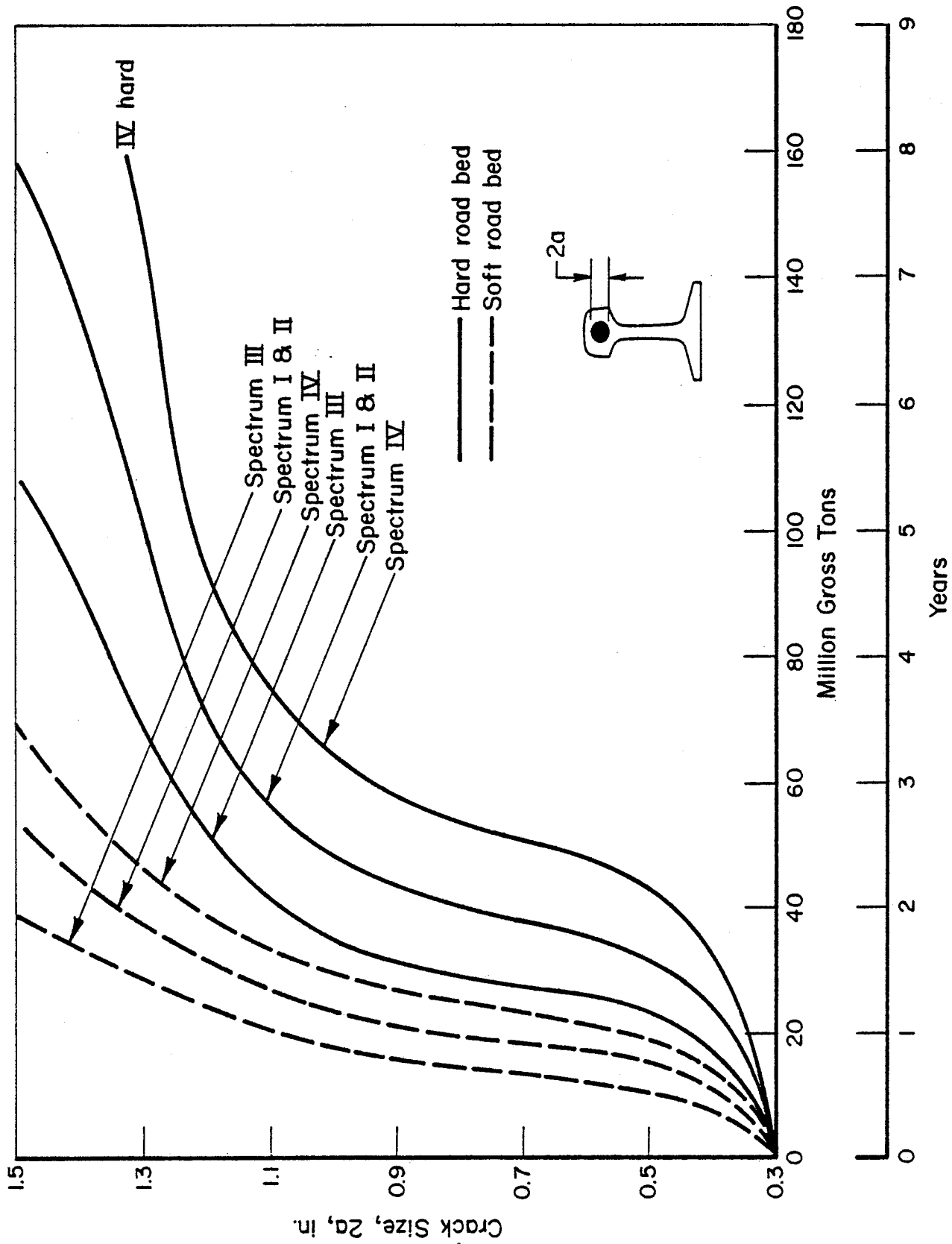
FIGURE 54. GROWTH OF A TRANSVERSE FISSURE AS A FUNCTION OF LOAD SPECTRUM AND ROADBED CONDITION
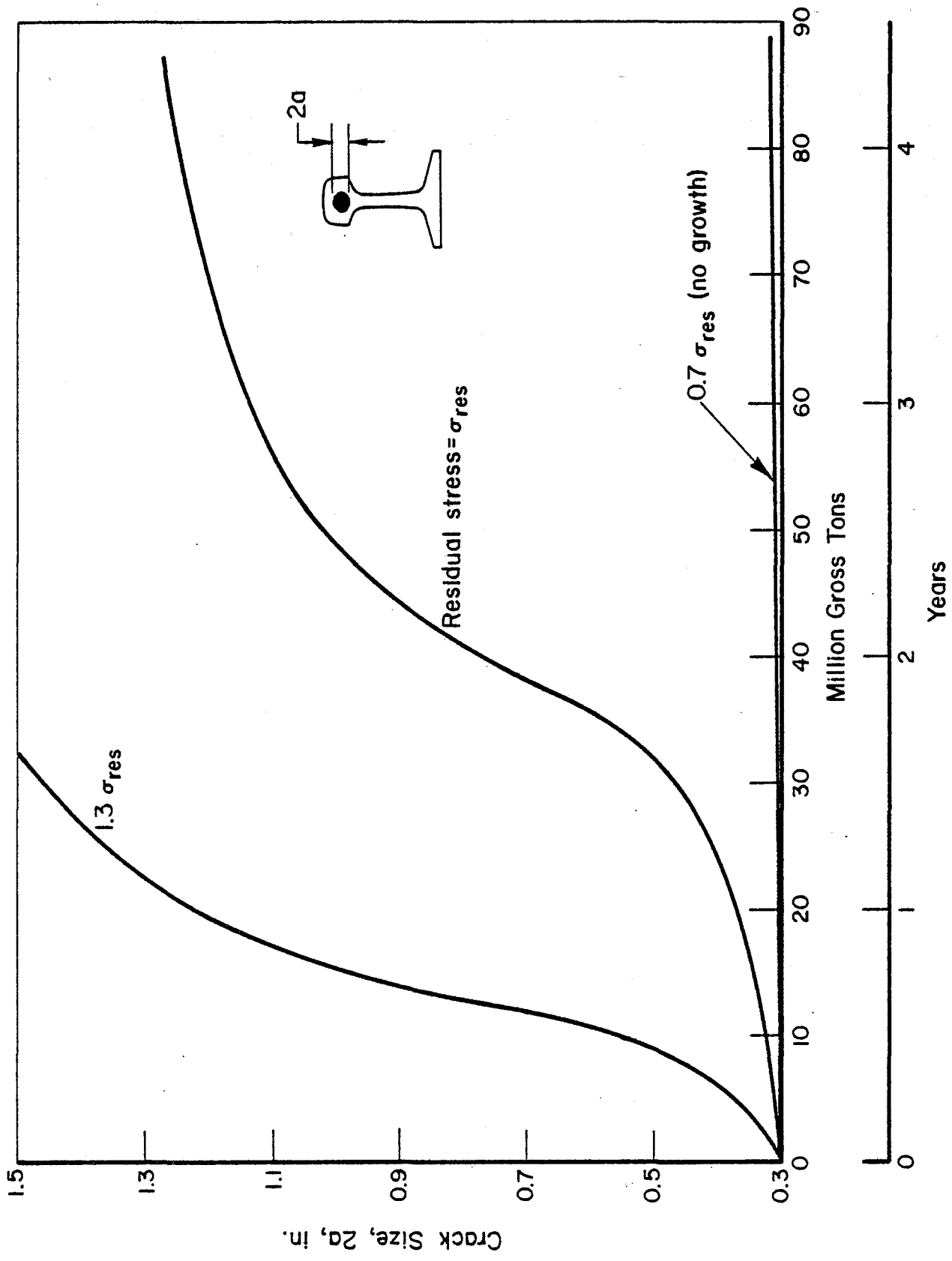
FIGURE 55. EFFECT OF RESIDUAL STRESS LEVEL ON GROWTH OF TRANSVERSE FISSURE

105
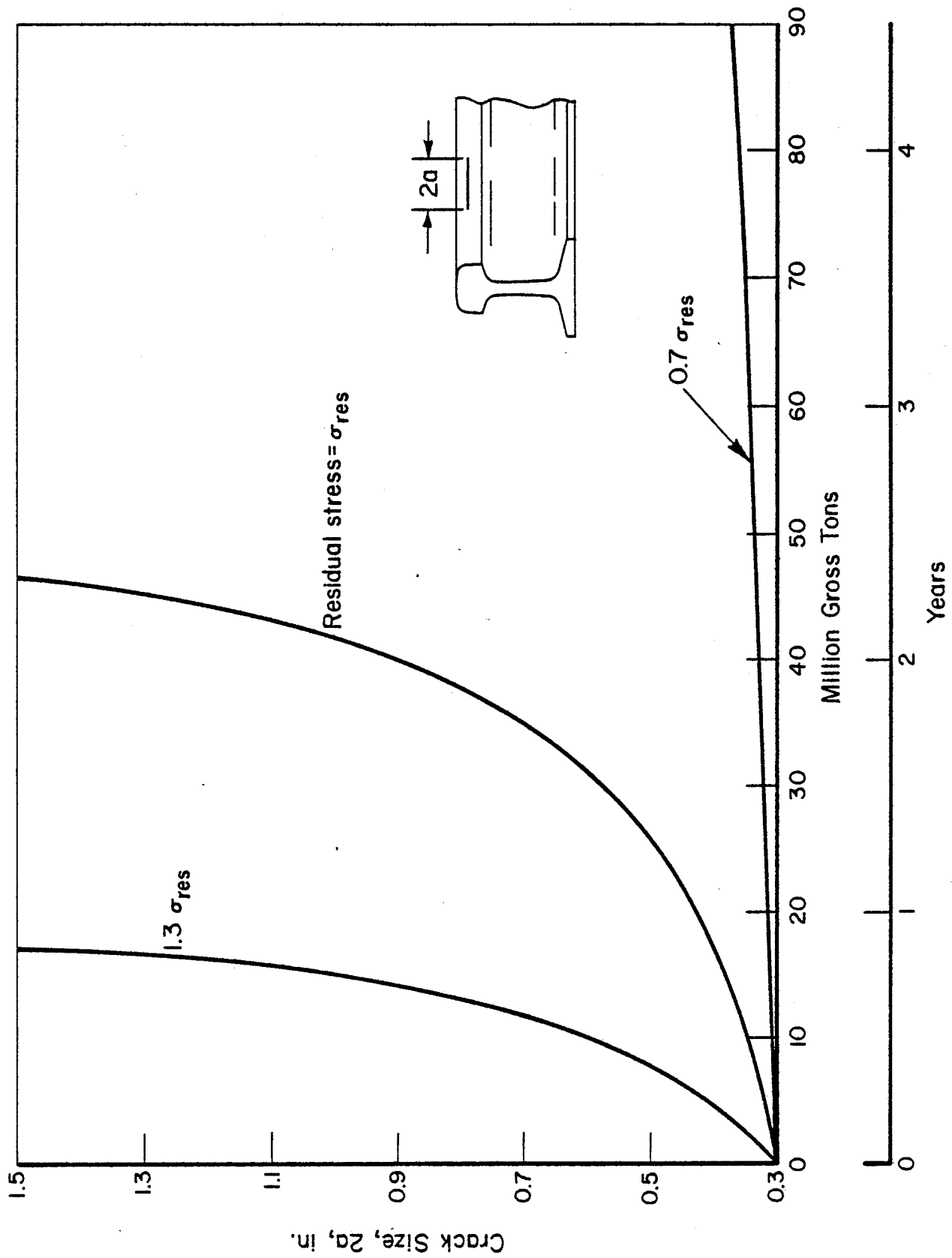
FIGURE 56. EFFECT OF RESIDUAL STRESS ON GROWTH OF HORIZONTAL SPLIT HEAD

106
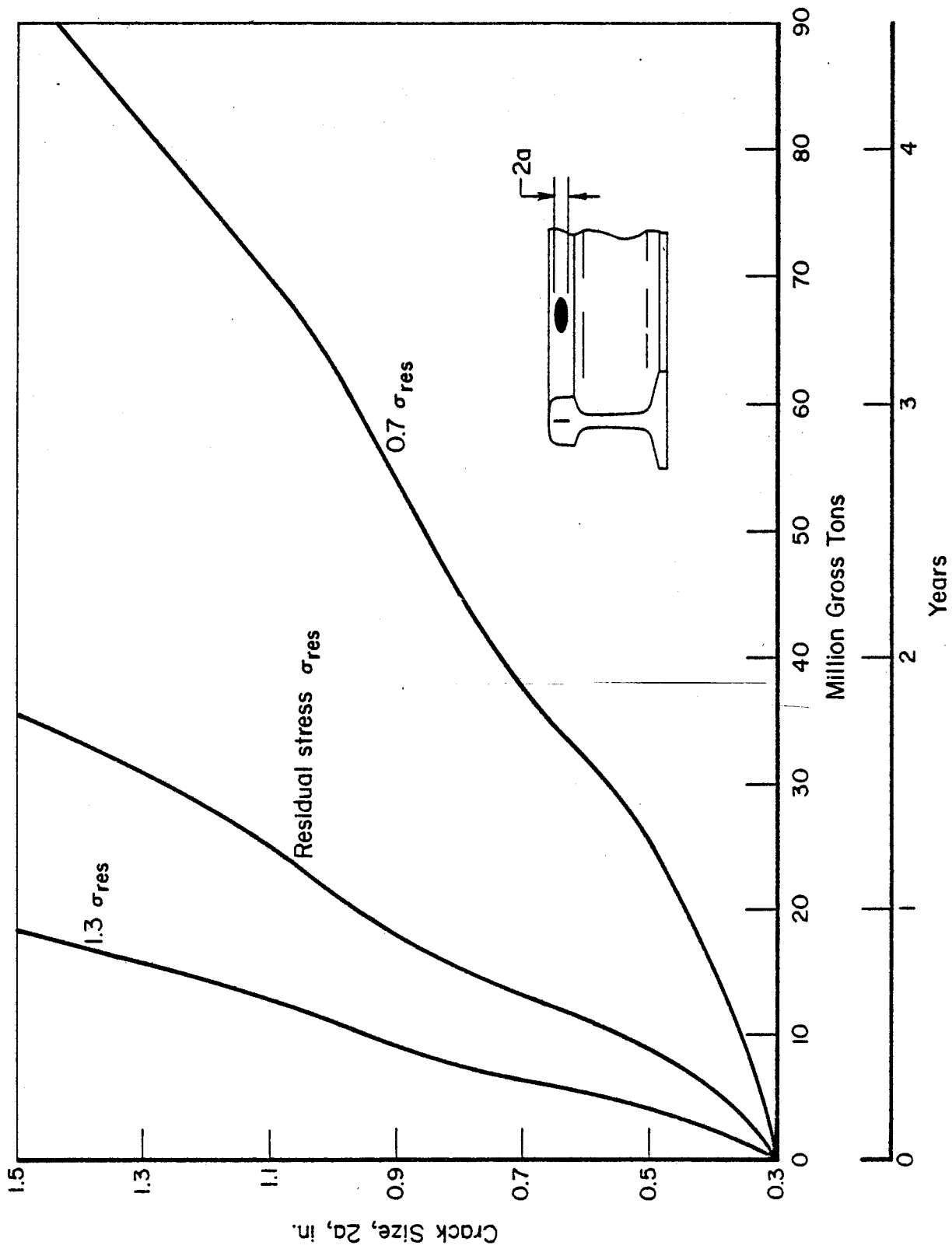
FIGURE 57. EFFECT OF RESIDUAL STRESS ON GROWTH OF VERTICAL SPLIT HEAD

## 8.6. Outlook

The foregoing results have shown the potential of the rail failure model (crack growth prediction model). It was pointed out that the results can only be used in a comparative sense, because of the doubtful assumptions that had to be made with regard to stress-intensity factors and crack shape. Moreover, the load spectra used were for vertical loads only, since stress intensities for lateral loads are still lacking. Finally, the occurrence of mixed mode cracking had to be neglected and the magnitude of the residual stress was taken arbitrarily.

When more detailed information on stress intensities and residual stress becomes available, more refined crack growth predictions can be made. However, regardless of the completeness of this information, the crack growth predictions will not have great accuracy, as was shown by the predictions for the service-simulation tests. It was pointed out that inaccuracies of predictions are largely due to the variability in material behavior. This indicates the need for a statistical treatment of the problem in the context of reliability analysis.

## 9. USE OF THE FAILURE MODEL

### 9.1. Management Decisions

The occurrence of rail failures is a serious problem for economical operation and safety of railroads. The gravity of the train accident statistics over a 10-year period between 1963 and 1972 can be noted from the fact that 5756 train accidents were caused by broken rails[25].

In order to reduce the chance of failures, actions can be taken to reduce the speed of trains, decrease the wheel loads, upgrade the track, inspect more frequently for cracks and remove them, or any combination of these measures. All of these actions are costly and may be of equal or greater consequence for economical operation than the acceptance of failures. At present, it is not possible to evaluate, with high precision, the economic consequences of any of these alternative measures. Hence, it is difficult

to determine which measure (or measures) would be the most cost-effective for a given railroad or length of track at a given point in time.

The situation would be largely improved with a computational scheme to aid management decisions to ensure safe but economical operations with regard to the rail failure problem. This scheme should provide answers to questions such as

- How much of a reduction in defect or failure rate would be obtained for upgraded track?
- What would be the reduction in failure rate if speeds or loads were reduced (or the converse)?
- What would be the reduction in failure rate if inspections were carried out more frequently?
- In order to get significant reductions in failure rate, would it be necessary to utilize the same measures for all the track in a line, or should attention be focussed differently in certain areas, depending upon specific local operating conditions?

If quantitative answers to these questions were obtained, the cost reductions due to lower failure rates could be evaluated and compared with the costs of preventive measures. This would enable selection of the most cost-effective maintenance intervals and inspection intervals. At the same time, regulatory authorities could utilize the computations to obtain quantitative information on the estimated level of safety of railroad track in a given condition and under certain traffic conditions.

The time to observe damage in a structure is a function of the damage detection capability as well as the cumulative response capability of the structure to its imposed environment. Therefore, elements characterizing flaws, initiation, growth, loading history, environment, inspection, etc., are necessary considerations for a model representative of the life-cycle integrity of a rail. The variability in the response of the structure in such a complex total environment must be given particular attention. This variability is a function of the stochastic behavior of the individual elements determining rail life-cycle performance and is a mixture of both independent and dependent processes. Accordingly, a candidate method for

109

estimating the integrity of a rail during its operational life-cycle is likely to be one that relies on the application of reliability technology.

In order to develop a reliability analysis, the processes that lead to rail failure must be thoroughly understood. Predictive models of fatigue crack initiation, crack propagation, and fracture must be employed. Simultaneously, models that can provide information on the magnitude and sequence of stresses that are experienced by a rail as a result of certain traffic must be available. These models then can be combined to predict when failure will occur. The outcome will be a probability of failure or failure rate. The analysis should permit variation of the track and maintenance parameters. Then it can be utilized to determine how the probability of failure changes for different track conditions, different traffic, maintenance, and inspection.

Not all of the models to be used in the reliability analysis nor all of the input data are currently available. Some of the input data and models presently are being generated and developed under FRA/TSC programs (1,2,9,10). Part of the data base was generated under the present program.

## 9.2. Reliability Analysis for Railroads

Reliability analysis attempts to determine the rate of failure or the probability of failure of a given product for certain conditions of usage and maintenance. This is illustrated in Figure 58, in terms of parameters, input, processors, and output. Basically, this scheme is the same for reliability analysis of any product, but each case is different in detail.

The parameters are those associated with track condition, track geometry and maintenance, those associated with the traffic type and speed, the type of material, and the inspection technique. The particular conditions of all parameters are reflected in the input data for the reliability analysis. These input data are measured data, or data predicted by physical models, or both.

The track and traffic parameters induce stresses in the rail, which cause fatigue. Thus, the track and traffic parameters have a bearing on the stress spectrum as an input. However, this spectrum must be developed first

PARAMETERS        PRODUCT        COMPONENTS        MAINTENANCE

INPUT        USAGE        COMPONENT PROPERTIES        INSPECTION MAINTENANCE PROCEDURES

FAILURE MODEL

RELIABILITY ANALYSES PROCEDURES        MATHEMATICAL EXECUTION

OUTPUT        FAILURE RATE
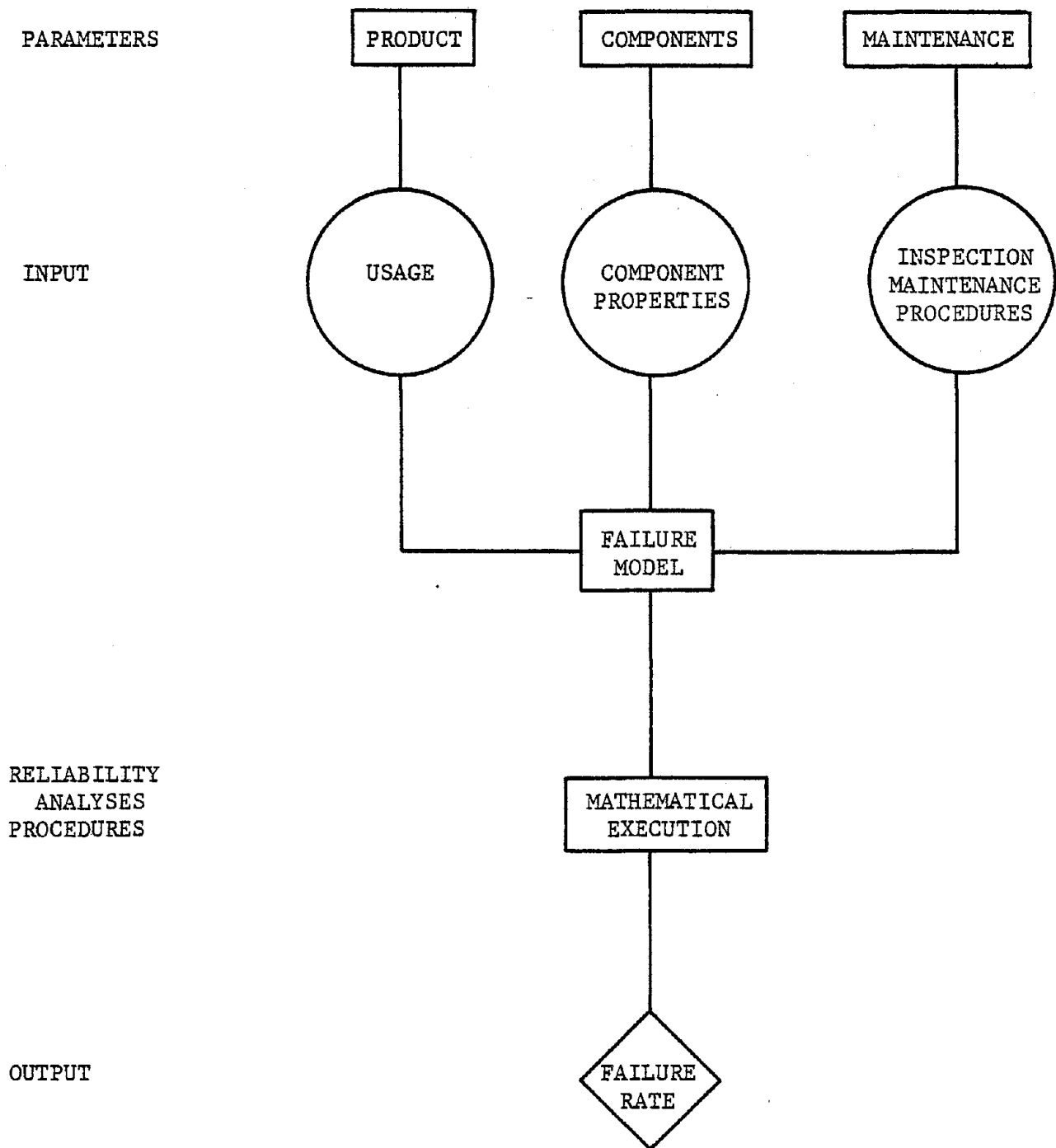
FIGURE 58.   RELIABILITY ANALYSIS

111

from measured load spectrum data and/or a model that can predict the load spectrum combined with a stress analysis that converts loads into stresses. Hence, the measured input data are a load spectrum.

Another stress input that reflects track and traffic conditions consists of residual stress data. In principle, these stresses would be obtained from an elastic-plastic stress analysis. However, stress analysis of rails has not been developed to a point that it can adequately predict residual stresses. Therefore, measured data will be needed. Stresses resulting from thermal cycles, stress variations due to seasonal variations in roadbed stiffness, etc., should, in essence, be predicted through a spectrum generation model and a stress analysis.

Material input data will be experimental data because, at present, no models exist to infer fatigue, crack growth, and fracture properties from more basic material parameters. The same is believed to be true for the input data on inspection.

The reliability analysis starts out by establishing a statistical representation for each set of input data. The large variability of crack growth behavior observed in the present program shows that statistical representation may be necessary. When the statistical models are established, the input data can be treated to derive the descriptive parameters (or constants) for these statistical models. With the given stress history, the reliability analysis then starts predicting when and where cracks will initiate, how fast they will grow, and when they will cause fracture, depending upon the frequency and type of inspection. After complete mathematical execution, the analysis can give as an output

- Probability of crack initiation as a function of time
- Probability of occurring of a crack of certain size as a function of time
- The failure rate (probable numbers of failures at any given time) for a given inspection of interval.

## 9.3. Level of Sophistication of Reliability Analysis

There is a tendency to want to model more complex behavioral processes mathematically as one's insights grow. This tendency should be viewed with some caution until such time that demonstrations are made to determine whether more sophisticated modeling does result in greater accuracy than simpler schemes. This is especially considered a useful caution in considering the rail reliability analysis.

Consider the most primitive reliability analysis. It would use all available rail failure data to establish one statistical distribution. The statistics would reflect total ignorance as to what causes rail failures but they would implicitly contain the effects of all those parameters. This model would predict, with great accuracy, the number of failures to expect next year if operating conditions remain constant. But it would provide no clues as to how to reduce the number of failures nor to evaluate more economical inspection or maintenance procedures.

A somewhat less primitive model would recognize that different types of track, different types of traffic, different conditions of track, speed, maintenance, and inspection affect failure rates. Again, taking all failure statistics of many years of service, failure rates could be subdivided in as many different categories as necessary. Failure rates then could be determined for different conditions. There still could be complete ignorance of what stresses exist and of the physics of fracture.

Is this second model indeed as primitive as it looks? With good accuracy, it will predict the failure rate for a given traffic and track type. It will show how and how much this failure rate will be reduced by maintenance or reduced speed, etc. This is exactly what the railroad engineer wants. Indeed, it is the most sophisticated model that can be conceived. It requires no physical understanding, but it is of perfect technical adequacy.

Unfortunately, the data base for this perfect reliability analysis has not been salvaged nor even properly recorded from the experience of more than a century of railroad operation. The problem that must be faced is to regenerate this experience at the lowest possible cost. In order to do this, mathematical and physical models have had to be established and developed in order to draw on statistics of a lower level that can be generated faster

than the actual service experience. A possible simple approach would be to (1) measure stress histories at a large number of sites and (2) subject a large number of rails to these stress histories in the laboratory. Thus, one would encompass all material variables. There would be no need for a spectrum generation model nor for stress analysis or damage integration models. Accurate predictions could be made and the results would be technically useful. However, the generation of the data covering sufficient variables would be prohibitively expensive.

The next level of complexity would be to do the same tests on coupons of rail steel instead of rails. Instead of stress spectra, one would measure load spectra. A stress analysis model then would be required.

With further sophistication and refinement, one could go to even more basic statistics, such as those of the basic material properties. Then one is faced with developing models predicting basic fatigue initiation and crack growth data on the basis of metallographic structure.

With each such step, there will be requirements for new data bases in order to develop lower level statistical distributions, new models, and new and more assumptions. It can be envisioned that each further step down becomes a more costly development process, with the real possibility that there will be much reduced accuracy, due to the many models and assumptions involved.

It is obvious that there is an optimum between expenditures and achievement. The optimum will move slowly to greater complexity as knowledge accumulates and larger computers are used. It is also obvious that the optimum will be close to, but below, the level of understanding of the physical processes at any given time. An attempt to go beyond that requires many more assumptions and may cause much lower accuracy. On the basis of these considerations, it can be concluded that the crack growth prediction model developed in this report provides an adequate input to reliability analysis. The accuracy of crack growth prediction is limited, but was shown to be largely due to material variability.

## 10. REFERENCES

1. Feddersen, C. E., Buchheit, R. D., and Broek, D., "Fatigue Crack Propagation in Rail Steels", Battelle Report on DOT-TSC-1076, to TSC,(1976).

2. Broek, D., and Rice, R. C., "Fatigue Crack Growth Properties of Rail Steels", Battelle Report on DOT-TSC-1076, to TSC, (1977).

3. Broek, D., "Elementary Engineering Fracture Mechanics", Noordhoff, (1974).

4. Schijve,J., and Broek, D., "Crack Propagation Tests Based on a Gust Spectrum With Variable Amplitude Loading", Aircraft Engineering, 34, (1962), pp 314-316.

5. Stephens, R. I., Chen, D. K., and Hom, B. W., "Fatigue Crack Growth With Negative Stress Ratio Following Single Overloads in 2024-T3 and 7075-T6 Aluminum Alloys", ASTM STP 595, (1976), pp 27-40.

6. Broek, D., "Fail Safe Design Procedures", AGARDograph AG 176, (1974), pp 121-166.

7. Bernard, P. J., Lindley, T. C., and Richards, C. E., "Mechanisms of Overload Retardation During Fatigue Crack Propagation", ASTM STP 595, (1976), pp 78-97.

8. Adetifa, O. A., Gowda, C. V. B., and Hopper, T. H., "A Model for Fatigue Crack Growth Delay Under Two-Level Block Loads", ASTM STP 595, (1976), pp 142-156.

9. Johns, T. G., Davies, D. B., McGuire, P. M., Sampath, S. G., and Rybicki, E. G., "Engineering Analysis of Stresses in Railroad Rail: Phase I", Battelle Report to TSC, (1977).

10. Ahlbeck, D. R., Harrison, H. D., Prause, R. H., and Johnson, M. R., "Evaluation of Analytical and Experimental Methodologies for the Characterization of Wheel/Rail Loads, FRA OR&D Report 76-276, (1976).

11. Broek, D., and Smith, S. H., "Spectrum Loading Fatigue Crack-Growth Predictions and Safety Factor Analysis", NADC Report 76383-30, (1976).

12. Schijve,J., "The Accumulation of Fatigue Damage in Aircraft Structural Materials", AGARDograph AG 157, (1972).

13. Wheeler, O. E., "Spectrum Loading and Crack Growth", J. Basic Engineering, 94, (1972), p 181.

14. Willenborg, J. D., et.al., "A Crack Growth Retardation Model Using an Effective Stress Concept", AFFDL-TM-71-1, FBR, (1971).

15. Habibie, B. J., "Fatigue Crack Growth Prediction"(In German), Messer-schmidt-Bölkow-Blohm Report No. UH-03-71, (1971).

16. Hanel, J. J., "Crack Growth Prediction Under Variable Amplitude Loading on the Basis of a Dugdale Mode" (In German), German Society for Materials Testing, (1973).

17. Bell, P. D., and Wolfman, A., "Mathematical Modeling of Crack Growth Interaction Effects", ASTM STP 595, (1976), pp 151-171.

18. Jacoby, G. H., Nowack, H., and Van Lipzig, H. T. M., "Experimental Results and a Hypothesis for Fatigue Crack Propagation Under Variable Amplitude Loading", ASTM STP 595, (1976), pp 172-182.

19. Engle, R. M., and Rudd, J. L., "Analysis of Crack Propagation Under Variable Amplitude Loading Using the Willenborg Retardation Model", Presented at the AIAA Structures and Dynamics Conference, Las Vegas, Paper 74-369, (1974).

20. Schütz, W., "Calculation Methods for Fatigue Life and Crack Propagation", Section 4 of AGARDograph on Fatigue Design of Fighters, To be published.

21. Schijve, J., "The Accumulation of Fatigue Damage in Aircraft Materials and Structures", AGARDograph AG 157, (1972).

22. Barsom, J. M., "Fatigue-Crack Growth Under Variable Amplitude Loading in ASTM-A514-B Steel", ASTM STP 536, (1965).

23. Strating, J., "Fatigue and Stochastic Loadings", Ph.D. Thesis, Delft Univ., (1973).

24. Shah, R. C., "Mixed Mode Fracture and Fatigue Crack Propagation in Rail Steels", Final Report to appear Dec. 1977.

25. Anon., "Annual Accident Bulletins, Summary and Analysis of Accidents on Railroads in the U.S.", Dept. of Transportation, Federal Railroad Administration.

26. Cannon, D. F., and Allen, R. J., "The Application of Fracture Mechanics to Railway Failures", Paper to Institution of Mechanical Engineering, London, (1974).

27. Evans, P. R. V., Owen, N. B., and Hopkins, B. E., "Fatigue Crack Growth and Sudden Fast Fracture in a Rail Steel", J. Iron and Steel Institute, (1970), pp 560-568.

28. Hyzak, J. M., and Bernstein, I. M., "The Effects of Microstructural Variations on the Strength and Toughness of Rail Steel", Processing Res. Institute, Carnegie-Mellon Univ., PRI Report 75-127, (1975).

# APPENDIX A

## FRACTURE TOUGHNESS OF RAIL SAMPLES

Apparent fracture toughness data were obtained from all fatigue crack propagation tests. These data were reported in a previous report[1]. A number of specimens were subjected to formal fracture toughness tests, the results of which are presented in Table A-1.

It turned out that the 0.5-inch thick specimen had insufficient thickness for valid $K_{Ic}$ tests. The $K_Q$ values obtained varied from 31.8 to 58.8 ksi$\sqrt{in}$. The last two columns in Table A-1 present values for $K_{Ic_{min}}$ and $K_{app}$. Using the ASTM thickness requirement, $K_{Ic_{min}}$ is the maximum toughness that could be measured with a 0.5 inch specimen of a material of the given yield strength; thus, it is the minimum toughness of the rail material concerned. (If the toughness would have been lower than $K_{Ic_{min}}$, the test would have been valid.)

If the $K_{Ic_{min}}$ values are compared with the $K_Q$ values, it can be concluded that the differences are small enough to indicate that the $K_Q$ values must be very close to the actual $K_{Ic}$ values. This can also be concluded from a comparison with the $K_{app}$ values.

$K_{Ic}$ values for rails steels are reported at various places in the literature (e.g., References 27, 28, 29). Typical data are of the order of 30 - 40 ksi$\sqrt{in}$. at room temperature. At -40 F, values as low as 25 ksi$\sqrt{in}$. can be obtained[27]. The effect of loading rate or strain rate appears to be small, below the transition temperature, which is considerably above room temperature for the present rail steels.[1] The literature data indicate that the results in Table A-1 represent a reasonable indication of the magnitude and variability of the fracture toughness of the rail steels used in in this investigation.

TABLE A-1.  FRACTURE TOUGHNESS TEST RESULTS FOR $\frac{1}{2}$-INCH THICK COMPACT-TENSION RAIL SPECIMEN

| Specimen | TYS, ksi | $P_{max}/P_Q$ | $K_Q$, ksi$\sqrt{\text{In.}}$ | $2.5\left(\dfrac{K_Q}{\sigma_y}\right)^2$ | $K_{app}$ (Fatigue Tests), ksi$\sqrt{\text{In.}}$ | $K_{Ic_{min}}$ ksi$\sqrt{\text{In.}}$ |
|---|---|---|---|---|---|---|
| LT009-1 | 81.8 | 1.075(a) | 39.0 | 0.57 | 41.1 | 36.6 |
| LT016-1 | 75.6 | 1.180 | 40.6 | 0.72 | 42.3 | 33.8 |
| LT021-4 | 77.2 | 1.151 | 44.2 | 0.82 | 54.2 | 34.2 |
| LT022-1 | 76.0 | 1.036(a) | 56.9 | 1.40 | 56.8 | 34.1 |
| LT025-4 | 75.7 | 1.258 | 42.6 | 0.79 | 55.0 | 27.8 |
| TL029-1 | 61.7 | 1.454 | 39.2 | 1.01 | | 34.6 |
| TL030-1 | 76.8 | 1.000(a) | 58.8 | 1.47 | | 34.0 |
| TL031-1 | 75.6 | 1.449 | 31.8 | 0.44(b) | | 33.0 |
| LT065-4 | 73.3 | 1.307 | 38.2 | 0.68 | 48.9 | |
| | | Mean – | 43.5 | | | |
| | | Standard Deviation – | 8.85 | | | |

(a)  Passed $P_{max}/P_Q$ requirement.

(b)  Passed $2.5 \left(K_Q/\sigma_y\right)^2$ requirement.

## PROGRAM RAILIF

This program was developed to do block-by-block crack growth life summations for laboratory specimens and simulated rail flaws. A detailed description of the background and purpose of the program is contained in the final report. Details on spectrum representation and resulting train block can be found there. The computer language is FORTRAN and the computer system used in this program was a CDC 6500. The following list of control cards may be used (with the CDC 6500 computer) to load and execute the RAILIF program.

RCR, T100, CM50000, AC = G6265-0001.

    Job card - specifies programmer ID, maximum core processor time, core memory and project number.

RUN(S,,,,,, 100000,, CRT)

    Use the RUN compiler to load the program, limit output to 100000 records, and include a cross reference map of program.

SWITCH, 1.

    An optional card which, if included, indicates that a rail flaw is being simulated and K-crack length inputs are required.

LOAD, LGO.

    Load the program.

EXECUTE.

    Execute the program.

A listing of the program is included in Figure 1. The input card requirements are listed in Table 1.

```
          PROGRAM RAILIF(INPUT,OUTPUT,TAPE5=INPUT,TAPE99=OUTPUT)
     C
     C    THIS PROGRAM IS DESIGNED TO DO BLOCK BY BLOCK CRACK GROWTH LIFE
     C    SUMMATIONS FOR LABORATORY SPECIMENS AND SIMULATED RAIL FLAWS
     C
          DIMENSION SEQ(100),TRAIN(10),STR(10,20),REP(10,20),JI(10),MIN(10,2
         10),SUM(20,20),T(100),KMIN(6),KMAX(6),KRES(6),AK(3),WL(10,20),CRKTY
         2P(4)
          REAL M,INC,KMX,MIN,KTH,KC,MGT,KMIN,KMAX,KRES,KMX1,KMX2,KMN1,KMN2,K
         1RS1,KRS2,INC1,INC2
          INTEGER SEQ,REP,C2,TOT,BLOC
     2    FORMAT(A10,I5,2F5.3,1X,I3,6X,F5.3,A3,F7.3,2F5.2,F5.3,2F5.1)
     4    FORMAT(40I2)
     6    FORMAT(9X,*SPECTRUM NAME *,5X,A10/9X,*NO. OF TRAINS *I7 /9X,*INITI
         1AL CRACK *,F10.3/9X,*DADN INTERCEPT *,E15.5/9X,*DADN SLOPE     *,
         2F9.3/9X,*SPECIMEN TYPE*,6X,A8/9X,*MAXIMUM LOAD *,F11.3 /9X,*SPECIM
         3EN WIDTH *,F8.2/9X,*RESIDUAL STRESS *,F7.2 /9X,*STRESS TO LOAD
         4 *,F5.3/9X,*K-THRESHOLD *,F11.1/9X,*CRITICAL K *,F12.1///)
     8    FORMAT(A5)
     10   FORMAT(F10.2,I10)
     12   FORMAT(                        ///5X,*TRAIN NO.*,3X,*TRAIN ID*,5
         1X,*KMAX*,3X,*INCREMENTAL A*,3X,*EXTENDED CRACK*//)
     14   FORMAT(7X,I5,6X,I3,7X,F6.2,7X,F7.4,10X,F6.3)
     16   FORMAT(5X,F14.3,4X,F10.3,3X,I8)
     18   FORMAT(///40X,*TRAINS PER BLOCK OF EACH SEQUENCE*/)
     20   FORMAT(/20X,*SEQUENCE NO. *,I5/)
     22   FORMAT(/2X,*TRAIN*,A5)
     24   FORMAT(/2X,*BLOCK NO. *,I2,10X,20A5)
     26   FORMAT(////20X,*TOTAL TRAINS SURVIVED= *,I5/20X,*GROSS TONS TRAFFI
         1C= *,F8.2/1H1)
     28   FORMAT(1H1)
     30   FORMAT(10F8.2)
     32   FORMAT(5X,*NO CRACK GROWTH, STRESS INTENSITIES BELOW THRESHOLD*/1H
         11)
     34   FORMAT(///10X,*STRESS RANGE*,3X,*WHEEL LOAD*,3X,*OCCURENCES*//)
     36   FORMAT(5X,F8.3,7X,3F10.2, 9X,3F10.2/)
     38   FORMAT(//30X,*K-CRACK LENGTH DATA FOR *,4A10///
         1                                34X,*THETA=  0*,30X,*THETA=180
         1*//5X,*CRACK LENGTH*,9X,*KMAX*, 6X,*KMIN*, 6X,*KRES*,15X,*KMAX*, 6
         2X,*KMIN*, 6X,*KRES*//)
     40   FORMAT(4A10)
     42   FORMAT(7X,I5,6X,I3,7X,2F9.2,5X,2F9.3,5X,2F9.4,5X,2F9.3,5X,F9.3)
     44   FORMAT(///5X,*TRAIN NO.*,3X,*TRAIN ID*,8X,*KMX1*,5X,*KMX2*,10X,*R1
         1*,7X,*R2*,11X,*INC1*,5X,*INC2*,12X,*A1*,7X,*A2*, 9X,*TOTAL A*//)
     46   FORMAT(//5X,*TEST DISCONTINUED, CRACK LENGTH GREATER THAN 1.5 INCH
         1ES*//)
     C
     C    READ IN SPECTRUM INFORMATION- A COMPLETE SEQUENCE EQUALS 1/2 MGT
     C    ALSO READ IN INITIAL CRACK LENGTH AND CRACK GROWTH PARAMETERS
     C
          CALL SSWTCH(1,JJ)
     C
     C    JJ IS AN INDICATOR, IF JJ=1,K-CRACK LENGTH DATA ARE INPUT AND ANALYZED
     C                        IF JJ=2, A CT OR CC TYPE LABORATORY SPECIMEN IS USE(
     C
```

FIGURE B-1.

B-2

```
000005      50    I=1
000006            MX=12
000007            II=17
000010            READ 2,SPCTRM,NSEQ,A0,C1,C2,M,TYP,PMX,W,RESID,CONV,KTH,KC
000046            IF(EOF,5)110,55
000051      55    READ 4,(SEQ(I),I=1,NSEQ)
000064            I=1
000065            A=A0
000067            A1=A0
000070            A2=A0
000071            IF(JJ.EQ.1)A0=2.0*A0
000074            C=C1*10.0**C2
        C         IF JJ EQUAL 1 (CONTROL CARD IN PLACE) READ K-CRACK LENGTHS
000101            PRINT 6,SPCTRM,NSEQ,A0,C,M,TYP,PMX,W,RESID,CONV,KTH,KC
000134            IF(JJ.EQ.2)GO TO 60
000136            READ 40,CRKTYP
000144            READ 30,(KMAX(I),I=1,6),(KMIN(I),I=1,6),(KRES(I),I=1,6)
000172            READ 30,(AK(I),I=1,3)
000204            PRINT 38,CRKTYP
000212            DO 58 I=1,3
000214      58    PRINT 36,AK(I),KMAX(I),KMIN(I),KRES(I),KMAX(I+3),KMIN(I+3),KRES(I+
                  13)
000237            I=1
        C
        C         READ IN STRESS DATA FOR EACH TRAIN OF CYCLES
        C
000240      60    READ 8,TRAIN(I)
000246            IF(EOF,5)80,65
000251      65    J=1
000252      70    READ 10,STR(I,J),REP(I,J)
000266            IF(STR(I,J).LE.0.00)GO TO 75
000272            J=J+1
000274            GO TO 70
000274      75    JI(I)=J-1
000277            I=I+1
000300            GO TO 60
000300      80    N=I-1
000302            PRINT 34
000306            DO 82 I=1,N
000310            M1=JI(I)
000312            PRINT 22,TRAIN(I)
000317            DO 81 J=1,M1
000321            MIN(I,J)=RESID-CONV*STR(I,J)
000330            WL(I,J)=STR(I,J)*1.724
000332      81    PRINT 16,STR(I,J), WL(I,J),REP(I,J)
000352      82    CONTINUE
000354            PRINT 18
000360            NP=NSEQ/II
000363            DO 160 I=1,NSEQ
000365            N1=SEQ(I)
000367      160   T(I)=TRAIN(N1)
000373            DO 170 I=1,NP
000374            NA=(I-1)*II+1
000400            NB=II*I
000402      170   PRINT 24,I,(T(J),J=NA,NB)
000421            PRINT 28
```

```
C
C          START NUMERICAL INTEGRATION PROCESS
C
000424          MM=1
000425          DO 155 IK=1,NP
000427          DO 155 IJ=1,MX
000430          MIN(IK,IJ)=RESID
000434    155   SUM(IK,IJ)=0.00
000443          DO 150 I=1,NSEQ
000445          N1=SEQ(I)
000447          M1=JI(N1)
000451          NN=1+(I-1)/II
000456          DO 150 J=1,M1
000460          DO 150 K=1,MX
000461          IF(STR(N1,J).NE.STR(1,K))GO TO 150
000467          SUM(NN,K)=SUM(NN,K)+REP(N1,J)
000475          MIN(NN,K)=RESID-CONV*STR(N1,J)
000505          WL(NN,K)=STR(N1,J)*1.724
000514    150   CONTINUE
000524          IF(JJ.GT.1)PRINT 12
000532          IF(JJ.EQ.1)PRINT 44
000540          TOT=0
000541          TN=NN
000543          TP=1.0
000544          AI=A0
000546          AI1=A0/2.0
000550          AI2=A0/2.0
000551    84    TT=0.0
000552    85    IF(TP.GT.0.0.OR.TT.EQ.0.0) PRINT 20,MM
000570          BLOC=0
000571          DO 105 I=1,NN
000573          INC=0.0
000574          INC1=0.0
000575          INC2=0.0
000576          KK=0
000577          DO 100 J=1,MX
000600          AW=A/W
000602          R=MIN(I,J)/RESID
000606          IF(R.LT.0.00)R=0.00
000610          IF(R.GT.0.90)GO TO 100
000614          IF(JJ.EQ.1)GO TO 96
000616          IF(TYP.EQ.3HSEN)GO TO 90
000620          KMX=PMX/0.50/W**0.50*(29.6*AW**0.5-185.5*AW**1.5+655.7*AW**2.5-101
                17.*AW**3.5+638.9*AW**4.5)
000657          GO TO 95
000657    90    KMX=PMX*SQRT(AW*W)/0.50/W*(1.99-0.41*AW+18.7*AW**2.0-38.48*AW**3.0
                1+53.85*AW**4.0)
000712    95    IF(KMX.GE.KC)GO TO 100
000715          GO TO 97
C
C          COMPUTE STRESS INTENSITIES FROM K-CRACK LENGTH DATA
C
000715    96    IF(A1.LT.AK(2))K=1
000721          IF(A2.LT.AK(2))L=1
000725          IF(A1.GE.AK(2))K=2
000731          IF(A2.GE.AK(2))L=2
```

```
000734          KMX1=(KMAX(K+1)-KMAX(K))*(A1-AK(K))/(AK(K+1)-AK(K))+KMAX(K)
000745          KMX2=(KMAX(L+4)-KMAX(L+3))*(A2-AK(L))/(AK(L+1)-AK(L))+KMAX(L+3)
000755          KMN1=(KMIN(K+1)-KMIN(K))*(A1-AK(K))/(AK(K+1)-AK(K))+KMIN(K)
000765          KMN2=(KMIN(L+4)-KMIN(L+3))*(A2-AK(L))/(AK(L+1)-AK(L))+KMIN(L+3)
000775          KRS1=(KRES(K+1)-KRES(K))*(A1-AK(K))/(AK(K+1)-AK(K))+KRES(K)
001005          KRS2=(KRES(L+4)-KRES(L+3))*(A2-AK(L))/(AK(L+1)-AK(L))+KRES(L+3)
001015          KMX1=KMX1*WL(I,J)/19.0+KRS1
001023          KMX2=KMX2*WL(I,J)/19.0+KRS2
001031          R1=(KMN1*WL(I,J)/19.0+KRS1)/KMX1
001040          R2=(KMN2*WL(I,J)/19.0+KRS2)/KMX2
001046          KK=KK+1
001050          IF(KK.GT.1)GO TO 98
001052          STOR1=KMX1
001053          STOR2=KMX2
001054          STOR3=R1
001055          STOR4=R2
001057      98  IF(R1.LT.0.00)R1=0.00
001061          IF(R2.LT.0.00)R2=0.00
001063          IF(KMX1.LT.KTH)KMX1=KTH
001066          IF(KMX2.LT.KTH)KMX2=KTH
001071          IF(KMX1.GT.KC.OR.KMX2.GT.KC)GO TO 100
001102          RATE1=C*(1.0-R1)**2.0*(KMX1**2.0-KTH**2.0)*KMX1**(M-1.0)/(KC-KMX1)
001130          RATE2=C*(1.0-R2)**2.0*(KMX2**2.0-KTH**2.0)*KMX2**(M-1.0)/(KC-KMX2)
001157          INC1=INC1+RATE1*SUM(I,J)
001165          INC2=INC2+RATE2*SUM(I,J)
001171          GO TO 100
001172      97  RATE=C*(1.0-R)**2.0*(KMX**2.0-KTH**2.0)*KMX**(M-1.0)/(KC-KMX)
001221          INC=INC+RATE*SUM(I,J)
001226     100  CONTINUE
001231          A=A+INC
001233          IF(JJ.GT.1)GO TO 103
001236          A1=A1+INC1
001240          A2=A2+INC2
001242          A=A1+A2
001243          KMX=1.0
001245     103  TOT=TOT+II
001247          BLOC=BLOC+1
001250          IF(TT.EQ.1.0.AND.TP.EQ.0.0) GO TO 105
001260          IF(JJ.EQ.1)GO TO 104
001262          PRINT 14,TOT,BLOC,KMX,INC,A
001300          GO TO 105
001301     104  PRINT 42,TOT,BLOC,STOR1,STOR2,STOR3,STOR4,INC1,INC2,A1,A2,A
001333          IF(STOR1.GE.KC.OR.STOR2.GE.KC)NN=I
001347     105  IF(KMX.GE.KC)NN=I
001357          IF(KMX.GE.KC)GO TO 115
001361          IF(STOR1.GE.KC.OR.STOR2.GE.KC)GO TO 115
001372          IF(A.GT.1.50)GO TO 111
001376          MM=MM+1
           C
           C    EVALUATE CRACK GROWTH AND USE AN AVERAGE GROWTH RATE TO EXTEND CRACK
           C    AT LEAST 5 PERCENT OF INITIAL CRACK LENGTH IF SUCH GROWTH HAS NOT
           C    OCCURRED IN THE PAST SEQUENCE
           C
001377          IF(A.EQ.A0)GO TO 120
001401          AD=A-AI
001403          AD1=A1-AI1
```

```
001405      AD2=A2-AI2
001407      AB=0.05*A
001411      AI=A
001412      AI1=A1
001413      AI2=A2
001414      RR1=AD1/(AD1+AD2)
001417      RR2=1.0-RR1
001421      IF(MM.GT.1.AND.TT.GT.0.0) GO TO 106
001434      TP=0.0
001435  107 AC=AD
001437      IF(AD.GT.AB)GO TO 84
001442      FRAC=AB/AD
001443      NINC=FRAC
001445      MM=MM+NINC
001446      A=A+NINC*AD
001451      IF(JJ.GT.1)GO TO 108
001455      A1=A1+NINC*AD*RR1
001460      A2=A2+NINC*AD*RR2
001464  108 ADD=NINC*AD
001467      TT=1.0
001470      AI=A
001472      AI1=A1
001473      AI2=A2
001475      TOT = TOT+B5*NINC
001500      GO TO 85
001501  106 A=A+NINC*(AD+AC)/2.0-ADD
001507      IF(JJ.GT.1)GO TO 109
001513      A1=A1+(NINC*(AD+AC)/2.0-ADD)*RR1
001522      A2=A2+(NINC*(AD+AC)/2.0-ADD)*RR2
001531  109 TP=1.0
001533      GO TO 107
001533  111 PRINT 46
001537  115 AA=MM-1
001542      BB=NN
001543      MGT=AA/2.0+BB/(TN*2.0)
001551      PRINT 26,TOT,MGT
001561      GO TO 50
001562  120 PRINT 32
001566      GO TO 50
001567  110 CALL EXIT
001570      END
```

## TABLE B-1. INPUT CARD REQUIREMENTS

| Card Description | Variable Name | Columns | Field | Variable Description |
|---|---|---|---|---|
| **Parameters Card** | SPCTRM | 1-10 | A10 | Spectrum name |
| | NSEQ | 11-15 | I5 | Number of trains per sequence |
| | AO | 16-20 | F5.3 | Initial crack length |
| | C1 | 21-25 | F5.3 | Crack growth intercept mantissa |
| | C2 | 27-29 | I3 | Crack growth intercept exponent |
| | M | 36-40 | F5.3 | Crack growth exponent |
| | TYP | 41-43 | A3 | Specimen type, CT = compact tension; CC = center cracked panel |
| | PMX | 44-50 | F7.3 | Maximum load on specimen (kips) |
| | W | 51-55 | F5.2 | Specimen width (in.) |
| | RESID | 56-60 | F5.2 | Residual stress (ksi) |
| | CONV | 61-65 | F5.3 | Load to stress conversion factor |
| | KTH | 66-70 | F5.1 | Threshold stress intensity (ksi/$\overline{\text{in}}$.) |
| | KC | 71-75 | F5.1 | Fracture toughness level (ksi/$\overline{\text{in}}$.) |
| **Train Sequence Card** | SEQ(I) I = 1,NSEQ | 1-80 | 40 I2 | The pattern of trains within an overall sequence is defined as 1 sequence = ½ MGT |
| **Crack-Type Card**[a] | CRKTYP | 1-40 | 4A10 | Crack type description |
| **K-Crack Length Card**[a] | KMAX(I) I = 1,6 | 1-80 | 10F8.2 | Maximum stress intensities, 3 crack lengths, 2 sides of crack |
| | KMIN(I) I = 1,6 | | | Minimum stress intensities, 3 crack lengths, 2 sides of crack |
| | KRES(I) I = 1,6 | | | Residual stress intensity levels, 3 crack lengths, 2 sides of crack |
| **Crack Lengths Card**[a] | AK(I) I = 1,3 | 1-24 | 3F8.2 | 3 crack lengths for stress intensity values |
| **Train Card**[b] | TRAIN(I) | 1-5 | A5 | Train identification |
| **Stress and Repetition Card**[c] | STRESS(I,J) | 1-10 | F10.2 | Maximum stress for Ith train at level J |
| | REP(I,J) | 2-10 | I10 | Number of stress repetitions for Ith train at level J |

(a)  Included if SWITCH,1 included.

(b)  Repeated at beginning of each series of stress and cycle repetition cards.

(c)  The number of cards correspond to the number of stress levels within each train.

A sample of the program output is given in Figure 2. The output includes 4 or 5 major segments of information. First, the basic input parameters are printed for reference purposes. Second, the K-crack length data are tabulated if that type of analysis is being performed. Stress-intensity levels are given for 3 crack length and for both sides of the simulated rail flaw ($\theta$ = 0 and 180 degrees). Third, the stress ranges, maximum wheel loads and number of occurrences per train are tabulated. Fourth, the type and sequence of trains in each 17-car block are shown, 5 blocks constituting 1 sequence or ½ million gross tons (MGT) of rail traffic. Fifth, and most important, the computed stress intensities, stress ratios, incremental crack extensions and total crack growth are given for an increasing number of trains until one of two conditions is met, either the crack grows to 1.5 inches in length or the crack tip stress intensities on one side of the flaw reach the critical stress intensity. At this point, the total trains and million gross tons of traffic are tabulated and the run is completed.

| SPECTRUM NAME | FEC+UP RAN |
|---|---|
| NO. OF TRAINS | 85 |
| INITIAL CRACK | 0.380 |
| DADN INTERCEPT | 0.42700E-08 |
| DADN SLOPE | 2.130 |
| SPECIMEN TYPE | SEN |
| MAXIMUM LOAD | 9.000 |
| SPECIMEN WIDTH | 3.00 |
| RESIDUAL STRESS | 9.00 |
| STRESS TO LOAD | 0.362 |
| K-THRESHOLD | 13.5 |
| CRITICAL K | 55.0 |

### K-CRACK LENGTH DATA FOR TRANSVERSE FISSURE (HARD ROAD BED)

| | THETA= 0 | | | | THETA=180 | | |
|---|---|---|---|---|---|---|---|
| CRACK LENGTH | KMAX | KMIN | KRES | | KMAX | KMIN | KRES |
| 0.150 | 1.00 | -8.00 | 13.00 | | 1.00 | -6.00 | 13.00 |
| 0.400 | 1.00 | -13.00 | 22.80 | | 2.00 | -8.00 | 13.00 |
| 0.600 | 1.00 | -17.00 | 19.50 | | 1.00 | -8.00 | 13.00 |

| STRESS RANGE | WHEEL LOAD | OCCURENCES |
|---|---|---|

TRAIN    A1

| STRESS RANGE | WHEEL LOAD | OCCURENCES |
|---|---|---|
| 35.000 | 60.340 | 1 |
| 32.800 | 56.547 | 1 |
| 30.400 | 52.410 | 5 |
| 28.000 | 48.272 | 15 |
| 25.000 | 43.100 | 40 |
| 22.900 | 39.480 | 40 |
| 20.500 | 35.342 | 100 |
| 17.500 | 30.170 | 100 |
| 14.000 | 24.136 | 50 |
| 10.500 | 18.102 | 27 |
| 7.200 | 12.413 | 21 |

TRAIN    A2

| STRESS RANGE | WHEEL LOAD | OCCURENCES |
|---|---|---|
| 32.800 | 56.547 | 1 |
| 30.400 | 52.410 | 3 |
| 28.000 | 48.272 | 10 |
| 25.000 | 43.100 | 30 |
| 22.900 | 39.480 | 20 |

FIGURE B-2.

B 9

|         |         |     |
|---------|---------|-----|
| 20.500  | 35.342  | 50  |
| 17.500  | 30.170  | 50  |
| 14.000  | 24.136  | 25  |
| 10.500  | 18.102  | 6   |
| 7.200   | 12.413  | 5   |

**TRAIN    A3**

|         |         |     |
|---------|---------|-----|
| 30.400  | 52.410  | 1   |
| 28.000  | 48.272  | 5   |
| 25.000  | 43.100  | 20  |
| 22.900  | 39.480  | 25  |
| 20.500  | 35.342  | 50  |
| 17.500  | 30.170  | 100 |
| 14.000  | 24.136  | 100 |
| 10.500  | 18.102  | 50  |
| 7.200   | 12.413  | 49  |

**TRAIN    B**

|         |         |     |
|---------|---------|-----|
| 25.000  | 43.100  | 2   |
| 22.900  | 39.480  | 3   |
| 20.500  | 35.342  | 13  |
| 17.500  | 30.170  | 23  |
| 14.000  | 24.136  | 50  |
| 10.500  | 18.102  | 50  |
| 7.200   | 12.413  | 127 |

**TRAIN    C**

|         |         |     |
|---------|---------|-----|
| 25.000  | 43.100  | 3   |
| 22.900  | 39.480  | 7   |
| 20.500  | 35.342  | 16  |
| 17.500  | 30.170  | 25  |
| 14.000  | 24.136  | 110 |
| 10.500  | 18.102  | 150 |
| 7.200   | 12.413  | 169 |

**TRAIN    D**

|         |         |     |
|---------|---------|-----|
| 20.500  | 35.342  | 2   |
| 17.500  | 30.170  | 4   |
| 14.000  | 24.136  | 35  |
| 10.500  | 18.102  | 31  |
| 7.200   | 12.413  | 72  |

### TRAINS PER BLOCK OF EACH SEQUENCE

| BLOCK NO. 1 | B | B | B  | B | B | B | B  | A3 | B | B | D  | B  | B | B | A3 |
|-------------|---|---|----|---|---|---|----|----|---|---|----|----|---|---|----|
| BLOCK NO. 2 | B | B | A1 | B | B | B | A3 | A2 | C | C | A3 | B  | B | C | B  |
| BLOCK NO. 3 | D | C | A2 | B | C | B | B  | B  | D | B | B  | C  | B | B | C  |
| BLOCK NO. 4 | B | B | B  | B | C | B | B  | B  | B | A3| B  | A2 | B | B | C  |
| BLOCK NO. 5 | B | D | B  | B | C | B | B  | B  | B | B | B  | B  | B | B | B  |

| TRAIN NO. | TRAIN ID | KHX1 | KMX2 | R1 | R2 | INC1 | INC2 | A1 | A2 | TOTAL A |
|---|---|---|---|---|---|---|---|---|---|---|
| | | SEQUENCE NO. 1 | | | | | | | | |
| 17 | 1 | 15.76 | 15.76 | -0.575 | -0.225 | 0.0001 | 0.0001 | 0.150 | 0.150 | 0.300 |
| 34 | 2 | 16.18 | 16.18 | -0.767 | -0.374 | 0.0002 | 0.0001 | 3.150 | 0.150 | 0.300 |
| 51 | 3 | 15.99 | 15.98 | -0.676 | -0.304 | 0.0001 | 0.0001 | 0.150 | 0.150 | 0.301 |
| 68 | 4 | 15.99 | 15.98 | -0.676 | -0.304 | 0.0001 | 0.0001 | 0.151 | 0.150 | 0.301 |
| 85 | 5 | 15.78 | 15.76 | -0.575 | -0.226 | 0.0001 | 0.0001 | 0.151 | 0.150 | 0.301 |
| | | SEQUENCE NO. 28 | | | | | | | | |
| 2312 | 1 | 16.62 | 15.90 | -0.567 | -0.241 | 0.0003 | 0.0001 | 0.172 | 0.163 | 0.335 |
| 2329 | 2 | 17.04 | 16.34 | -0.760 | -0.391 | 0.0003 | 0.0001 | 0.172 | 0.163 | 0.335 |
| 2346 | 3 | 16.86 | 16.13 | -0.668 | -0.320 | 0.0003 | 0.0001 | 0.173 | 0.163 | 0.336 |
| 2363 | 4 | 16.87 | 16.13 | -0.668 | -0.320 | 0.0003 | 0.0001 | 0.173 | 0.163 | 0.336 |
| 2380 | 5 | 16.66 | 15.90 | -0.566 | -0.242 | 0.0002 | 0.0001 | 0.173 | 0.163 | 0.337 |
| | | SEQUENCE NO. 38 | | | | | | | | |
| 3162 | 1 | 17.23 | 15.96 | -0.561 | -0.248 | 0.0004 | 0.0001 | 0.168 | 0.168 | 0.356 |
| 3179 | 2 | 17.66 | 16.41 | -0.755 | -0.398 | 0.0005 | 0.0001 | 0.188 | 0.169 | 0.357 |
| 3196 | 3 | 17.48 | 16.20 | -0.663 | -0.327 | 0.0004 | 0.0001 | 0.189 | 0.169 | 0.357 |
| 3213 | 4 | 17.49 | 16.20 | -0.663 | -0.327 | 0.0004 | 0.0001 | 0.189 | 0.169 | 0.358 |
| 3230 | 5 | 17.29 | 15.97 | -0.561 | -0.248 | 0.0004 | 0.0001 | 0.189 | 0.169 | 0.358 |
| | | SEQUENCE NO. 46 | | | | | | | | |
| 3842 | 1 | 17.94 | 16.01 | -0.555 | -0.253 | 0.0005 | 0.0001 | 0.206 | 0.173 | 0.379 |
| 3859 | 2 | 18.38 | 16.47 | -0.749 | -0.403 | 0.0007 | 0.0001 | 0.207 | 0.173 | 0.380 |
| 3876 | 3 | 18.20 | 16.25 | -0.657 | -0.333 | 0.0005 | 0.0001 | 0.207 | 0.173 | 0.381 |
| 3893 | 4 | 18.23 | 16.25 | -0.657 | -0.333 | 0.0006 | 0.0001 | 0.208 | 0.173 | 0.381 |
| 3910 | 5 | 18.03 | 16.02 | -0.554 | -0.254 | 0.0005 | 0.0001 | 0.208 | 0.174 | 0.382 |
| | | SEQUENCE NO. 52 | | | | | | | | |
| 4352 | 1 | 18.70 | 16.05 | -0.549 | -0.258 | 0.0007 | 0.0001 | 0.226 | 0.177 | 0.403 |
| 4369 | 2 | 19.14 | 16.52 | -0.744 | -0.408 | 0.0009 | 0.0002 | 0.227 | 0.177 | 0.404 |
| 4386 | 3 | 18.98 | 16.30 | -0.652 | -0.337 | 0.0007 | 0.0001 | 0.227 | 0.177 | 0.404 |
| 4403 | 4 | 19.01 | 16.30 | -0.651 | -0.338 | 0.0008 | 0.0001 | 0.228 | 0.177 | 0.405 |
| 4420 | 5 | 18.82 | 16.06 | -0.548 | -0.258 | 0.0007 | 0.0001 | 0.229 | 0.177 | 0.406 |
| | | SEQUENCE NO. 57 | | | | | | | | |
| 4777 | 1 | 19.54 | 16.09 | -0.543 | -0.262 | 0.0009 | 0.0001 | 0.247 | 0.180 | 0.427 |
| 4794 | 2 | 19.99 | 16.56 | -0.739 | -0.412 | 0.0012 | 0.0002 | 0.249 | 0.180 | 0.429 |
| 4811 | 3 | 19.84 | 16.33 | -0.646 | -0.341 | 0.0010 | 0.0001 | 0.250 | 0.180 | 0.430 |
| 4828 | 4 | 19.88 | 16.33 | -0.646 | -0.341 | 0.0010 | 0.0001 | 0.251 | 0.180 | 0.431 |
| 4845 | 5 | 19.71 | 16.09 | -0.542 | -0.262 | 0.0009 | 0.0001 | 0.252 | 0.180 | 0.432 |

B-11

SEQUENCE NO. 61

| | | | | | | | | | |
|---|---|---|---|---|---|---|---|---|---|
| 5117 | 1 | 20.44 | 16.11 | -0.537 | -0.265 | 0.0012 | 0.0001 | 0.271 | 0.182 | 0.453 |
| 5134 | 2 | 20.91 | 16.59 | -0.734 | -0.415 | 0.0016 | 0.0002 | 0.272 | 0.183 | 0.455 |
| 5151 | 3 | 20.77 | 16.36 | -0.640 | -0.344 | 0.0013 | 0.0001 | 0.274 | 0.183 | 0.456 |
| 5168 | 4 | 20.82 | 16.36 | -0.640 | -0.344 | 0.0014 | 0.0001 | 0.275 | 0.183 | 0.458 |
| 5185 | 5 | 20.66 | 16.12 | -0.536 | -0.265 | 0.0013 | 0.0001 | 0.276 | 0.183 | 0.459 |

SEQUENCE NO. 65

| | | | | | | | | | |
|---|---|---|---|---|---|---|---|---|---|
| 5457 | 1 | 21.60 | 16.14 | -0.530 | -0.267 | 0.0017 | 0.0001 | 0.301 | 0.185 | 0.485 |
| 5474 | 2 | 22.08 | 16.62 | -0.728 | -0.418 | 0.0022 | 0.0002 | 0.303 | 0.185 | 0.488 |
| 5491 | 3 | 21.97 | 16.39 | -0.633 | -0.347 | 0.0017 | 0.0001 | 0.305 | 0.185 | 0.490 |
| 5508 | 4 | 22.04 | 16.39 | -0.633 | -0.347 | 0.0019 | 0.0001 | 0.306 | 0.185 | 0.492 |
| 5525 | 5 | 21.89 | 16.15 | -0.528 | -0.268 | 0.0017 | 0.0001 | 0.308 | 0.185 | 0.494 |

SEQUENCE NO. 68

| | | | | | | | | | |
|---|---|---|---|---|---|---|---|---|---|
| 5712 | 1 | 22.83 | 16.16 | -0.523 | -0.270 | 0.0023 | 0.0001 | 0.333 | 0.187 | 0.520 |
| 5729 | 2 | 23.34 | 16.64 | -0.722 | -0.420 | 0.0030 | 0.0002 | 0.336 | 0.187 | 0.523 |
| 5746 | 3 | 23.26 | 16.42 | -0.627 | -0.350 | 0.0024 | 0.0001 | 0.338 | 0.187 | 0.525 |
| 5763 | 4 | 23.35 | 16.42 | -0.627 | -0.350 | 0.0026 | 0.0001 | 0.341 | 0.187 | 0.528 |
| 5780 | 5 | 23.23 | 16.17 | -0.521 | -0.270 | 0.0024 | 0.0001 | 0.343 | 0.187 | 0.530 |

SEQUENCE NO. 71

| | | | | | | | | | |
|---|---|---|---|---|---|---|---|---|---|
| 5967 | 1 | 24.44 | 16.19 | -0.516 | -0.272 | 0.0032 | 0.0001 | 0.375 | 0.189 | 0.563 |
| 5984 | 2 | 24.98 | 16.67 | -0.715 | -0.422 | 0.0043 | 0.0002 | 0.379 | 0.189 | 0.568 |
| 6001 | 3 | 24.95 | 16.44 | -0.620 | -0.352 | 0.0034 | 0.0001 | 0.382 | 0.189 | 0.571 |
| 6018 | 4 | 25.08 | 16.44 | -0.619 | -0.352 | 0.0037 | 0.0001 | 0.386 | 0.189 | 0.575 |
| 6035 | 5 | 25.01 | 16.19 | -0.513 | -0.273 | 0.0034 | 0.0001 | 0.389 | 0.189 | 0.579 |

SEQUENCE NO. 73

| | | | | | | | | | |
|---|---|---|---|---|---|---|---|---|---|
| 6137 | 1 | 25.35 | 16.20 | -0.551 | -0.274 | 0.0040 | 0.0001 | 0.417 | 0.190 | 0.607 |
| 6154 | 2 | 25.70 | 16.69 | -0.771 | -0.424 | 0.0052 | 0.0002 | 0.422 | 0.190 | 0.612 |
| 6171 | 3 | 25.42 | 16.46 | -0.690 | -0.354 | 0.0040 | 0.0001 | 0.426 | 0.190 | 0.616 |
| 6188 | 4 | 25.35 | 16.46 | -0.704 | -0.354 | 0.0042 | 0.0001 | 0.430 | 0.191 | 0.621 |
| 6205 | 5 | 25.06 | 16.21 | -0.607 | -0.274 | 0.0038 | 0.0001 | 0.434 | 0.191 | 0.624 |

SEQUENCE NO. 75

| | | | | | | | | | |
|---|---|---|---|---|---|---|---|---|---|
| 6307 | 1 | 24.63 | 16.21 | -0.695 | -0.275 | 0.0039 | 0.0001 | 0.460 | 0.191 | 0.652 |
| 6324 | 2 | 24.98 | 16.70 | -0.933 | -0.426 | 0.0050 | 0.0002 | 0.465 | 0.192 | 0.657 |
| 6341 | 3 | 24.70 | 16.47 | -0.844 | -0.355 | 0.0039 | 0.0001 | 0.469 | 0.192 | 0.661 |
| 6358 | 4 | 24.63 | 16.47 | -0.859 | -0.355 | 0.0041 | 0.0001 | 0.473 | 0.192 | 0.665 |
| 6375 | 5 | 24.35 | 16.22 | -0.752 | -0.276 | 0.0037 | 0.0001 | 0.477 | 0.192 | 0.669 |

SEQUENCE NO. 77

| | | | | | | | | | |
|---|---|---|---|---|---|---|---|---|---|
| 6477 | 1 | 23.95 | 16.23 | -0.836 | -0.277 | 0.0037 | 0.0001 | 0.501 | 0.193 | 0.694 |
| 6494 | 2 | 24.31 | 16.72 | -1.093 | -0.427 | 0.0047 | 0.0002 | 0.506 | 0.193 | 0.698 |
| 6511 | 3 | 24.03 | 16.49 | -0.995 | -0.356 | 0.0037 | 0.0001 | 0.509 | 0.193 | 0.702 |
| 6528 | 4 | 23.97 | 16.49 | -1.010 | -0.357 | 0.0039 | 0.0001 | 0.513 | 0.193 | 0.706 |
| | | | | | | | | 0.547 | 0.192 | 0.710 |

**SEQUENCE NO. 79**

| ID | Row | | | | | | | | |
|---|---|---|---|---|---|---|---|---|---|
| 6647 | 1 | 23.32 | 16.24 | -0.978 | -0.278 | 0.0035 | 0.0001 | 0.539 | 0.194 | 0.733 |
| 6664 | 2 | 23.68 | 16.73 | -1.252 | -0.428 | 0.0044 | 0.0002 | 0.544 | 0.194 | 0.738 |
| 6681 | 3 | 23.40 | 16.50 | -1.146 | -0.358 | 0.0036 | 0.0001 | 0.547 | 0.194 | 0.742 |
| 6698 | 4 | 23.34 | 16.50 | -1.161 | -0.358 | 0.0037 | 0.0001 | 0.551 | 0.194 | 0.745 |
| 6715 | 5 | 23.07 | 16.25 | -1.036 | -0.279 | 0.0034 | 0.0001 | 0.554 | 0.194 | 0.749 |

**SEQUENCE NO. 81**

| ID | Row | | | | | | | | |
|---|---|---|---|---|---|---|---|---|---|
| 6817 | 1 | 22.71 | 16.26 | -1.120 | -0.280 | 0.0033 | 0.0001 | 0.576 | 0.195 | 0.771 |
| 6834 | 2 | 23.08 | 16.75 | -1.411 | -0.430 | 0.0040 | 0.0002 | 0.580 | 0.195 | 0.775 |
| 6851 | 3 | 22.81 | 16.52 | -1.296 | -0.359 | 0.0033 | 0.0001 | 0.583 | 0.195 | 0.779 |
| 6868 | 4 | 22.75 | 16.52 | -1.310 | -0.360 | 0.0034 | 0.0001 | 0.587 | 0.196 | 0.782 |
| 6885 | 5 | 22.48 | 16.26 | -1.176 | -0.280 | 0.0031 | 0.0001 | 0.590 | 0.196 | 0.785 |

**SEQUENCE NO. 84**

| ID | Row | | | | | | | | |
|---|---|---|---|---|---|---|---|---|---|
| 7072 | 1 | 21.88 | 16.28 | -1.327 | -0.282 | 0.0028 | 0.0001 | 0.626 | 0.197 | 0.823 |
| 7089 | 2 | 22.25 | 16.77 | -1.643 | -0.432 | 0.0035 | 0.0002 | 0.629 | 0.197 | 0.826 |
| 7106 | 3 | 21.99 | 16.54 | -1.515 | -0.362 | 0.0029 | 0.0001 | 0.632 | 0.197 | 0.829 |
| 7123 | 4 | 21.94 | 16.54 | -1.529 | -0.362 | 0.0030 | 0.0001 | 0.635 | 0.197 | 0.833 |
| 7140 | 5 | 21.68 | 16.28 | -1.380 | -0.282 | 0.0027 | 0.0001 | 0.638 | 0.198 | 0.835 |

**SEQUENCE NO. 87**

| ID | Row | | | | | | | | |
|---|---|---|---|---|---|---|---|---|---|
| 7327 | 1 | 21.18 | 16.30 | -1.515 | -0.284 | 0.0025 | 0.0001 | 0.668 | 0.199 | 0.867 |
| 7344 | 2 | 21.55 | 16.80 | -1.853 | -0.434 | 0.0031 | 0.0002 | 0.671 | 0.199 | 0.870 |
| 7361 | 3 | 21.30 | 16.56 | -1.713 | -0.364 | 0.0026 | 0.0001 | 0.674 | 0.199 | 0.873 |
| 7378 | 4 | 21.26 | 16.56 | -1.726 | -0.364 | 0.0026 | 0.0001 | 0.676 | 0.199 | 0.876 |
| 7395 | 5 | 21.00 | 16.30 | -1.565 | -0.284 | 0.0024 | 0.0001 | 0.679 | 0.199 | 0.878 |

**SEQUENCE NO. 91**

| ID | Row | | | | | | | | |
|---|---|---|---|---|---|---|---|---|---|
| 7667 | 1 | 20.34 | 16.32 | -1.758 | -0.287 | 0.0021 | 0.0001 | 0.719 | 0.201 | 0.920 |
| 7684 | 2 | 20.72 | 16.83 | -2.123 | -0.437 | 0.0025 | 0.0002 | 0.721 | 0.202 | 0.923 |
| 7701 | 3 | 20.48 | 16.59 | -1.968 | -0.367 | 0.0022 | 0.0001 | 0.723 | 0.202 | 0.925 |
| 7718 | 4 | 20.44 | 16.59 | -1.980 | -0.367 | 0.0022 | 0.0001 | 0.725 | 0.202 | 0.927 |
| 7735 | 5 | 20.19 | 16.33 | -1.802 | -0.287 | 0.0020 | 0.0001 | 0.727 | 0.202 | 0.929 |

**SEQUENCE NO. 96**

| ID | Row | | | | | | | | |
|---|---|---|---|---|---|---|---|---|---|
| 8092 | 1 | 19.49 | 16.36 | -2.024 | -0.290 | 0.0016 | 0.0001 | 0.770 | 0.205 | 0.974 |
| 8109 | 2 | 19.88 | 16.87 | -2.418 | -0.441 | 0.0020 | 0.0002 | 0.772 | 0.205 | 0.976 |
| 8126 | 3 | 19.64 | 16.63 | -2.247 | -0.370 | 0.0017 | 0.0001 | 0.773 | 0.205 | 0.978 |
| 8143 | 4 | 19.62 | 16.63 | -2.257 | -0.371 | 0.0017 | 0.0001 | 0.775 | 0.205 | 0.980 |
| 8160 | 5 | 19.37 | 16.36 | -2.062 | -0.291 | 0.0016 | 0.0001 | 0.777 | 0.205 | 0.982 |

**SEQUENCE NO. 102**

| ID | Row | | | | | | | | |
|---|---|---|---|---|---|---|---|---|---|
| 8602 | 1 | 18.70 | 16.40 | -2.293 | -0.295 | 0.0013 | 0.0001 | 0.817 | 0.208 | 1.025 |
| 8619 | 2 | 19.09 | 16.92 | -2.717 | -0.445 | 0.0015 | 0.0002 | 0.819 | 0.208 | 1.027 |
| 8636 | 3 | 18.87 | 16.67 | -2.529 | -0.375 | 0.0013 | 0.0001 | 0.820 | 0.209 | 1.029 |
| 8653 | 4 | 18.84 | 16.67 | -2.538 | -0.375 | 0.0014 | 0.0001 | 0.821 | 0.209 | 1.030 |
| 8670 | 5 | 18.60 | 16.41 | -2.325 | -0.295 | 0.0012 | 0.0001 | 0.823 | 0.209 | 1.031 |

SEQUENCE NO. 313

| 26537 | 1 | 14.86 | 18.00 | -4.005 | -0.504 | 0.0000 | 0.0003 | 1.048 | 0.438 | 1.486 |
| 26554 | 2 | 15.28 | 18.75 | -4.605 | -0.662 | 0.0000 | 0.0004 | 1.048 | 0.439 | 1.487 |
| 26571 | 3 | 15.08 | 18.38 | -4.323 | -0.588 | 0.0000 | 0.0003 | 1.048 | 0.439 | 1.487 |
| 26588 | 4 | 15.08 | 18.37 | -4.323 | -0.588 | 0.0000 | 0.0003 | 1.048 | 0.439 | 1.488 |
| 26605 | 5 | 14.86 | 17.98 | -4.006 | -0.504 | 0.0000 | 0.0003 | 1.048 | 0.439 | 1.488 |

SEQUENCE NO. 355

| 30107 | 1 | 14.78 | 17.04 | -4.049 | -0.532 | 0.0000 | 0.0002 | 1.053 | 0.508 | 1.561 |
| 30124 | 2 | 15.20 | 17.64 | -4.653 | -0.703 | 0.0000 | 0.0003 | 1.053 | 0.508 | 1.561 |
| 30141 | 3 | 15.00 | 17.35 | -4.369 | -0.623 | 0.0000 | 0.0002 | 1.053 | 0.508 | 1.561 |
| 30158 | 4 | 15.00 | 17.34 | -4.369 | -0.623 | 0.0000 | 0.0002 | 1.053 | 0.508 | 1.561 |
| 30175 | 5 | 14.78 | 17.02 | -4.049 | -0.533 | 0.0000 | 0.0002 | 1.053 | 0.508 | 1.562 |

TEST DISCONTINUED. CRACK LENGTH GREATER THAN 1.5 INCHES

TOTAL TRAINS SURVIVED= 30175
GROSS TONS TRAFFIC=   177.50

B-14

| ID | No. | | | | | | | | | |
|---|---|---|---|---|---|---|---|---|---|---|
| 9197 | 1 | 17.98 | 16.45 | -2.555 | -0.300 | 0.0010 | 0.0001 | 0.860 | 0.213 | 1.073 |
| 9214 | 2 | 18.39 | 16.97 | -3.067 | -0.451 | 0.0012 | 0.0002 | 0.861 | 0.213 | 1.074 |
| 9231 | 3 | 18.17 | 16.72 | -2.805 | -0.380 | 0.0010 | 0.0001 | 0.862 | 0.213 | 1.075 |
| 9248 | 4 | 18.15 | 16.73 | -2.812 | -0.380 | 0.0010 | 0.0001 | 0.863 | 0.213 | 1.076 |
| 9265 | 5 | 17.91 | 16.46 | -2.582 | -0.300 | 0.0010 | 0.0001 | 0.864 | 0.213 | 1.078 |

SEQUENCE NO. 119

| ID | No. | | | | | | | | | |
|---|---|---|---|---|---|---|---|---|---|---|
| 10047 | 1 | 17.20 | 16.52 | -2.872 | -0.307 | 0.0007 | 0.0001 | 0.908 | 0.219 | 1.127 |
| 10064 | 2 | 17.60 | 17.06 | -3.357 | -0.458 | 0.0008 | 0.0002 | 0.908 | 0.220 | 1.128 |
| 10081 | 3 | 17.39 | 16.80 | -3.136 | -0.388 | 0.0007 | 0.0001 | 0.909 | 0.220 | 1.129 |
| 10098 | 4 | 17.38 | 16.81 | -3.141 | -0.388 | 0.0007 | 0.0002 | 0.910 | 0.220 | 1.130 |
| 10115 | 5 | 17.15 | 16.53 | -2.892 | -0.308 | 0.0006 | 0.0001 | 0.910 | 0.220 | 1.130 |

SEQUENCE NO. 133

| ID | No. | | | | | | | | | |
|---|---|---|---|---|---|---|---|---|---|---|
| 11237 | 1 | 16.50 | 16.62 | -3.178 | -0.318 | 0.0004 | 0.0002 | 0.950 | 0.229 | 1.178 |
| 11254 | 2 | 16.91 | 17.17 | -3.695 | -0.469 | 0.0005 | 0.0002 | 0.950 | 0.229 | 1.179 |
| 11271 | 3 | 16.70 | 16.91 | -3.456 | -0.398 | 0.0004 | 0.0001 | 0.951 | 0.229 | 1.179 |
| 11288 | 4 | 16.69 | 16.92 | -3.459 | -0.398 | 0.0004 | 0.0002 | 0.951 | 0.229 | 1.180 |
| 11305 | 5 | 16.47 | 16.63 | -3.191 | -0.318 | 0.0004 | 0.0001 | 0.951 | 0.229 | 1.181 |

SEQUENCE NO. 154

| ID | No. | | | | | | | | | |
|---|---|---|---|---|---|---|---|---|---|---|
| 13022 | 1 | 15.88 | 16.78 | -3.469 | -0.334 | 0.0002 | 0.0002 | 0.987 | 0.243 | 1.230 |
| 13039 | 2 | 16.29 | 17.36 | -4.016 | -0.485 | 0.0003 | 0.0002 | 0.987 | 0.243 | 1.230 |
| 13056 | 3 | 16.09 | 17.09 | -3.761 | -0.414 | 0.0002 | 0.0002 | 0.987 | 0.243 | 1.231 |
| 13073 | 4 | 16.09 | 17.09 | -3.762 | -0.414 | 0.0002 | 0.0002 | 0.987 | 0.244 | 1.231 |
| 13090 | 5 | 15.87 | 16.79 | -3.476 | -0.334 | 0.0002 | 0.0002 | 0.988 | 0.244 | 1.231 |

SEQUENCE NO. 187

| ID | No. | | | | | | | | | |
|---|---|---|---|---|---|---|---|---|---|---|
| 15827 | 1 | 15.41 | 17.06 | -3.709 | -0.360 | 0.0001 | 0.0002 | 1.015 | 0.268 | 1.283 |
| 15844 | 2 | 15.82 | 17.67 | -4.280 | -0.512 | 0.0001 | 0.0003 | 1.015 | 0.268 | 1.284 |
| 15861 | 3 | 15.62 | 17.38 | -4.012 | -0.441 | 0.0001 | 0.0002 | 1.016 | 0.268 | 1.284 |
| 15878 | 4 | 15.62 | 17.38 | -4.013 | -0.441 | 0.0001 | 0.0002 | 1.016 | 0.268 | 1.284 |
| 15895 | 5 | 15.40 | 17.07 | -3.713 | -0.361 | 0.0001 | 0.0002 | 1.016 | 0.269 | 1.284 |

SEQUENCE NO. 231

| ID | No. | | | | | | | | | |
|---|---|---|---|---|---|---|---|---|---|---|
| 19567 | 1 | 15.13 | 17.50 | -3.856 | -0.402 | 0.0000 | 0.0002 | 1.032 | 0.308 | 1.340 |
| 19584 | 2 | 15.55 | 18.19 | -4.441 | -0.554 | 0.0001 | 0.0003 | 1.032 | 0.309 | 1.341 |
| 19601 | 3 | 15.35 | 17.87 | -4.166 | -0.483 | 0.0000 | 0.0002 | 1.032 | 0.309 | 1.341 |
| 19618 | 4 | 15.35 | 17.87 | -4.167 | -0.484 | 0.0000 | 0.0003 | 1.032 | 0.309 | 1.341 |
| 19635 | 5 | 15.13 | 17.51 | -3.858 | -0.403 | 0.0000 | 0.0002 | 1.032 | 0.309 | 1.342 |

SEQUENCE NO. 275

| ID | No. | | | | | | | | | |
|---|---|---|---|---|---|---|---|---|---|---|
| 23307 | 1 | 14.96 | 18.14 | -3.951 | -0.459 | 0.0000 | 0.0003 | 1.042 | 0.366 | 1.409 |
| 23324 | 2 | 15.38 | 18.92 | -4.545 | -0.610 | 0.0000 | 0.0004 | 1.042 | 0.367 | 1.409 |
| 23341 | 3 | 15.18 | 18.56 | -4.266 | -0.540 | 0.0000 | 0.0003 | 1.042 | 0.367 | 1.410 |
| 23358 | 4 | 15.18 | 18.56 | -4.266 | -0.540 | 0.0000 | 0.0003 | 1.043 | 0.367 | 1.410 |
| 23375 | 5 | 14.96 | 18.16 | -3.952 | -0.460 | 0.0000 | 0.0003 | 1.043 | 0.368 | 1.410 |

APPENDIX C

<u>REPORT OF NEW TECHNOLOGY</u>

This report contains experimental data on fatigue crack propagation in specimens cut from rails. The specimens were subjected to a cyclic load history simulating actual rail service loading. The results of the experiments could be predicted reasonably well on the basis of constant amplitude crack growth data generated previously.

After diligent review of the work performed to establish the data base and the predictive scheme, it is believed that no patentable innovation, improvement, or invention was made.